MINISTRY OF NATIONAL EDUCATION
AND SCIENTIFIC RESEARCH

THE ANNALS OF "DUNAREA DE JOS" UNIVERSITY OF GALATI

Fascicle IX
METALLURGY AND MATERIALS SCIENCE

YEAR XXXIV (XXXIX)
December 2016, no. 4

ISSN 1453-083X

2016
GALATI UNIVERSITY PRESS

EDITORIAL BOARD

Table of Contents

THE ANNALS OF "DUNAREA DE JOS" UNIVERSITY OF GALATI
FASCICLE IX. METALLURGY AND MATERIALS SCIENCE
Nº. 4 - 2016, ISSN 1453-083X

INFLUENCE OF REDUCTION SCHEME ON HARDNESS COLD ROLLED STRIP MARK STEEL ST 12

Marian-Iulian NEACȘU, Viorel DRAGAN
"Dunarea de Jos" University of Galati
e-mail: uscaeni@yahoo.com

ABSTRACT

The paper presents the results of the research on the influence of the evolution hardness scheme rolled steel, for the cold-rolled strip steel St 12. St 12 is intended for the manufacture of cold rolled strip stamping properties environments

We studied three variants of rolling with the same degree of deformation. The total = 60% of the samples submitted to the research were divided into 3 groups. Samples from the first group were rolled with uniform reduction coefficient increased from the first to the last pass. Samples from the second group were rolled with constant coefficients decreased from the first to the last pass. Samples of the third group were rolled with uniform reduction coefficient decreased from the first to the last pass.

By statistical processing of the experimental data was done correlation HRB = f (ε) using an equation like: $HRB = HRB_0 + a \times \varepsilon^b$ from which the mathematical calculations specific led to obtain equations curves hardening for the three kinds of rolling schemes.

Following research consisting in observing as steel hardening analyzed has a very high speed we can say that the limit of plasticity of the material cold rolling is more than 60% where cracks are observed.

KEYWORDS: rolling, roll, drawing, rank reduction

1. Introduction

Lamination process by passing through the space between two metal cylinders rotating met successive improvements, achieving a quantum leap after 50 years with the expansion of large-scale electrical applications [1, 2].

Consequently, it could switch to complex constructions which have increased production capacity to meet the growing requirements of the user industries of steel sheets and strips [3].

Introduction of automation and computerized techniques in metallurgy meant also an important step in the direction of the processes of plastic deformation of steel [4].

Tables and cold rolled steel strips is a staple with multiple uses in various industrial fields, working to achieve different product categories, a diverse array. Thin steel sheet and strip of low-carbon killed or semi-killed are processed in the body parts of cars, equipment and household appliances and various parts or goods obtained by die-stamping or deep drawing [3, 4].

Packaging industry is another area of using sheet and cold rolled steel strips.

A considerable proportion of the production of sheet and strip is covered by various methods (zinc plating, tinning, lacquering, painting) and is designed to create the outer shell in the construction industry.

Steel strips nickel, chromium or copper is widely used for decorative purposes. The multitude in the areas of use and processability requirements for manufactured products of cold strip mills can have different embodiments.

The machine itself is a twisting rolling stand whose construction differs from case to case, depending on the type of mill and form part of the finished product.

Lamination means not only the machine itself used for plastic deformation, but a complex of operations and production lines which, aside preparing raw material for cold rolling, after rolling is conjuring various properties and characteristics of the material that make it suitable for further processing [2, 3].

The complexity of technological lines of the composition of a polling cold rolling largely depends on the assortment of production, its destination and the conditions of the material in terms of the appearance of the surface, the mechanical and technological final of employment in tolerances imposed.

2. Materials and methods of research

Steel St 12 is a carbon steel (C = 0.1%, N = 0.007%) of general purpose and is produced according to DIN 50014 [7]. It is intended for the manufacture of cold rolled strip stamping properties environments. Strips of this steel grade are produced by DIN 1623-1.

2.1. The research method

For conducting research on the influence on the development scheme of rolled strip cold-rolled hardness, were used 12 samples of hot rolled strip with dimensions of 4 × 30 × 200 mm steel St 12. The samples were divided into three groups (each with 4 samples in each group) and were cold rolled by the rolling according to the following scheme [2, 3]:

- samples of the first group were rolled with uniform reduction coefficient increased from the first to the last pass (ε_1 = 9.55%; ε_2 = 13.07%; ε_3 = 16.60%; ε_4 = 20.12%; ε_5 = 23.64%);
- samples from the second group were rolled with constant coefficients decreased from the first to the last pass (ε1 = ε2 ε4 = = = ε3 ε5 = 16.74%);
- samples of the third group were rolled with uniform reduction coefficient decreased from the first to the last pass (ε1 = 23.64%; ε2 = 20.12%; ε3 = 16.60%; ε4 = 13.07%; ε5 = 9.55 %);

In all three variants was performed the same total degree of deformation ε_{total} = 60%.

Rolling mill was made irreversible in an experimental type of lamination technology laboratory of the Department of Materials Processing and faculty Ecometallurgy SIM - UPB having the following characteristics [2]:

- diameter cylinders: 200 mm;
- rolling speed: 1 m/s;
- drive motor power: 40 kW.

Of the four samples in each group, the first sample was used to adjust the rolling stands while the other three were laminated under the same lamination as shown in the repeatability of results and for monitoring eventual elimination of disturbing factors. Before the first pass and after each pass, HRB hardness was measured under standard conditions (ball 1/16" and load 100 kg) device from the laboratory TDP. For each sample, determinations were made in May and was calculated arithmetic average of the three of these determinations eliminating outliers.

After each run was measured sample thickness (Hi) and calculated the relative reduction in that passage (ε_i) and total relative reduction to the passage in question (ε_{toti}) relations:

$$\varepsilon_i = \frac{\Delta h_i}{H_{i-1}} = \frac{H_{i-1} - H_i}{H_{i-1}} \times 100 \ [\%] \quad (1)$$

$$\varepsilon_{tot_i} = \frac{\Delta h_{tot_i}}{H_0} = \frac{H_0 - H_i}{H_0} \times 100 \ [\%] \quad (2)$$

In these relationships:

- H_{i-1} is the thickness of the sample before passage i;
- H_i is the thickness of the sample after passing;
- H_0 is the initial thickness of the sample (prior to the first pass).

3. Results obtained

After performing experiments, the results are summarized in Tables 1, 2, 3.

Table 1. *Get the HRB hardness as planned rolling with increasing relative reductions*

No. of pas.	ε_i proposed %	H_i proposed mm	Sample no.	H_{i-1} mm	H_i mm	Δh_i mm	ε_i realiz. %	Δh_{toti} mm	ε_{toti} realiz. %	HRB					
										1	2	3	4	5	Average
0	-	-	-	-	4.00	-	-	-	-	66.6	69.8	66.9	65	70.2	67.7
1	9.55	3.6	**1**	4.00	3.67	0.33	8.25	0.33	8.25	76.4	75.9	75.0	77.2	75.5	76.0
			2	4.00	3.73	0.27	6.75	0.27	6.75	70.9	72.3	72.5	69.1	69.5	70.9
			3	4.00	3.67	0.33	8.25	0.33	8.25	75.4	74.7	73.8	72.9	72.1	73.8
2	13.07	3.1	**1**	3.67	3.09	0.58	15.80	0.91	22.75	88.9	89.8	88.2	84.7	87.0	87.7
			2	3.73	3.10	0.63	16.89	0.90	22.50	87.2	87.4	85.5	84.8	85.2	86.0
			3	3.67	3.18	0.49	13.35	0.82	20.50	86.7	87.0	85.0	86.0	84.7	85.9
3	16.60	2.6	**1**	3.09	2.60	0.49	15.86	1.40	35.00	89.1	86.6	89.0	90.4	90.8	89.2
			2	3.10	2.59	0.51	16.45	1.41	35.25	90.0	88.3	89.0	89.2	89.5	89.2
			3	3.18	2.63	0.55	17.30	1.37	34.25	87.7	91.4	89.7	91.0	89.1	89.8
4	20.12	2.1	**1**	2.60	1.94	0.66	25.38	2.06	51.50	91.1	86.6	91.2	89.6	87.2	89.2

			2	2.59	2.16	0.43	16.60	1.84	46.00	86.8	85.5	89.8	88.7	88.5	87.9
			3	2.63	2.15	0.48	18.25	1.85	46.25	86.1	86.0	89.4	88.7	87.6	78.6
5	23.64	1.6	**1**	1.94	1.55	0.39	20.10	2.45	61.25	86.4	90.0	90.5	90.2	89.0	89.2
			2	2.16	1.63	0.53	24.54	2.37	59.25	87.7	87.5	90.0	86.5	85.0	87.3
			3	2.15	1.59	0.56	26.05	2.41	60.25	86.4	88.0	85.5	87.7	86.3	86.8

Table 2. *Get the HRB hardness as planned rolling with constant relative reduction*

No. of pas.	**ε_i proposed %**	**H_i proposed mm**	**Sample no.**	**H_{i-1} mm**	**H_i mm**	**Δh_i mm**	**ε_i realiz. %**	**Δh_{toti} mm**	**ε_{toti} realiz. %**	**HRB**					
										1	**2**	**3**	**4**	**5**	**Average**
0	-	-	-	-	4.00	-	-	-	-	66.6	69.8	66.9	65	70.2	67.7
1	16.74	3.3	**1**	4.00	3.31	0.69	17.25	0.69	17.25	83.9	82.3	85.8	86.3	79.9	83.6
			2	4.00	3.45	0.55	13.75	0.55	13.75	84.8	85.8	81.3	86.5	85.3	84.7
			3	4.00	3.35	0.65	16.25	0.65	16.25	84.7	85.3	85.7	86.8	86.4	85.8
2	16.74	2.8	**1**	3.31	2.82	0.49	14.80	1.18	29.50	88.5	89.3	88.8	89.9	87.5	88.8
			2	3.45	2.78	0.67	19.42	1.22	30.50	89.0	90.3	89.4	86.9	90.5	89.2
			3	3.35	2.75	0.60	17.91	1.25	31.25	87.5	86.4	86.1	87.3	87.2	86.9
3	16.74	2.3	**1**	2.82	2.36	0.46	16.31	1.64	41.00	87.5	87.1	86.7	90.5	90.5	88.5
			2	2.78	2.23	0.55	19.78	1.77	41.25	90.0	88.0	91.1	91.5	88.0	89.7
			3	2.75	2.28	0.47	17.09	1.72	43.00	88.5	89.7	88.2	87.8	89.0	88.6
4	16.74	1.9	**1**	2.36	1.84	0.52	22.03	2.16	54.00	90.4	89.4	91.3	91.8	90.0	90.6
			2	2.23	1.85	0.38	17.04	2.15	53.75	87.0	91.0	90.6	90.0	89.0	89.5
			3	2.28	1.87	0.41	17.98	2.13	53.25	85.0	85.0	86.3	89.3	89.5	87.0
5	16.74	1.6	**1**	1.84	1.58	0.26	14.13	2.42	60.60	86.1	90.4	88.3	84.0	88.0	87.4
			2	1.85	1.53	0.32	17.30	2.47	61.75	90.8	90.8	90.0	88.4	90.8	90.2
			3	1.87	1.57	0.31	16.04	2.43	60.75	88.2	88.8	84.5	83.4	87.2	86.4

Table 3. *Hardness HRB obtained as planned rolling with decreasing relative reductions*

No. of pas.	**ε_i proposed %**	**H_i proposed mm**	**Sample no.**	**H_{i-1} mm**	**H_i mm**	**Δh_i mm**	**ε_i realiz. %**	**Δh_{toti} mm**	**ε_{toti} realiz. %**	**HRB**					
										1	**2**	**3**	**4**	**5**	**Average**
0	-	-	-	-	4.00	-	-	-	-	66.6	69.8	66.9	65	70.2	67.7
1	23.64	3.1	**1**	4.00	3.14	0.86	21.50	0.86	21.50	84.6	88.0	87.6	87.7	90.4	87.7
			2	4.00	3.06	0.94	23.50	0.94	23.50	88.4	89.8	90.8	89.5	88.9	89.5
			3	4.00	3.15	0.85	21.25	0.85	21.25	88.0	88.5	88.0	88.8	88.0	88.3
2	20.12	2.4	**1**	3.14	2.55	0.59	18.79	1.45	36.25	88.6	90.8	92.5	90.4	91.3	90.7
			2	3.06	2.58	0.48	15.69	1.42	35.50	91.7	90.1	90.8	89.0	90.8	90.5
			3	3.15	2.45	0.70	22.22	1.55	38.75	90.3	85.9	89.4	90.2	89.3	89.0
3	16.60	2.0	**1**	2.55	2.05	0.50	19.61	1.95	48.75	88.6	85.8	86.0	89.5	88.7	87.7
			2	2.58	2.12	0.46	17.83	1.88	47.00	89.0	88.7	88.2	88.5	91.2	89.1
			3	2.45	2.13	0.32	13.06	1.87	46.75	89.2	86.1	87.4	88.2	87.0	87.6
4	13.07	1.8	**1**	2.05	1.77	0.28	13.66	2.23	55.75	86.7	91.5	89.5	91.6	87.0	89.3
			2	2.12	1.8	0.32	15.09	2.20	55.00	90.6	88.7	85.8	85.0	84.0	86.8
			3	2.13	1.75	0.38	17.84	2.25	56.25	89.5	89.5	91.5	88.0	91.3	90.0
5	9.55	1.6	**1**	1.77	1.60	0.17	9.60	2.40	60.00	86.0	86.4	85.0	86.3	86.2	86.0
			2	1.8	1.50	0.30	16.67	2.50	62.50	89.0	89.6	89.0	91.0	88.4	89.4
			3	1.75	1.65	0.10	5.71	2.35	58.75	88.5	84.8	86.8	90.0	87.3	87.5

Based on data in Table 1 was built variation diagram (Fig. 1) depending on the degree of hardness reduction.

Figure 2 shows the variation HRB hardness depending on the degree of reduction in total under the scheme rolling with constant relative reduction.

Figure 3 shows the variation in hardness depending on the degree of reduction based on the data in Table 3.

The correlation HRB = f (ε) was obtained by statistical processing of the experimental data using an equation of the type [5, 6]:

$$HRB = HRB_0 + a \cdot \varepsilon^b \quad (3)$$

The equation was linearized as follows:

$$HRB - HRB_0 = a \cdot \varepsilon^b \quad (4)$$

$$\log(HRB - HRB_0) = \log a + b \cdot \log \varepsilon \quad (5)$$

The change of variables was made:

$$Y = \log(HRB - HRB_0) \quad (6)$$

$$X = \log \varepsilon \quad (7)$$

$$A = b \quad (8)$$

$$B = \log a \, a \quad (9)$$

and there was obtained a linear equation of the type:

$$Y = A \cdot X + B \tag{10}$$

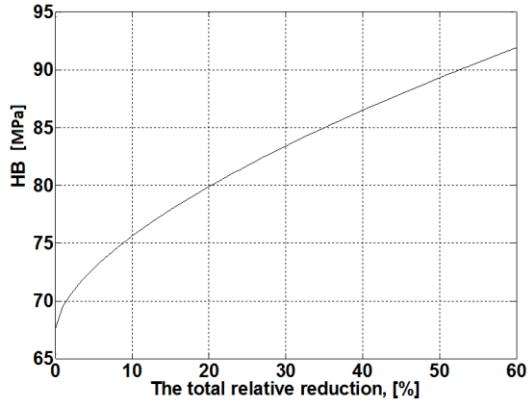

Fig. 1. *HRB hardness grade 1 for total variation reduction as planned rolling with increasing relative reductions*

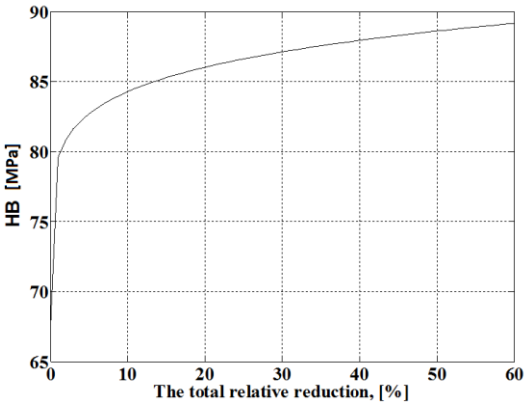

Fig. 2. *HRB hardness grade 2 for total variation reduction as planned rolling with constant relative reduction*

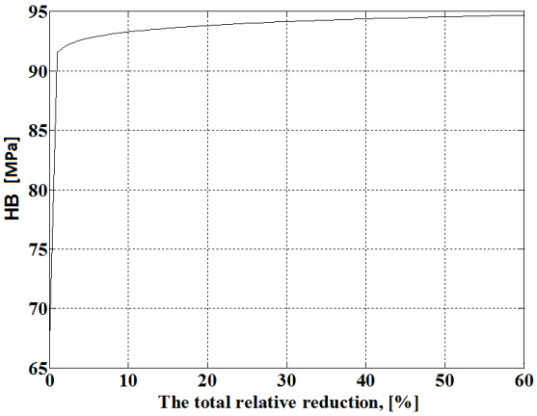

Fig. 3. *HRB hardness variation with the total degree reduction as planned rolling with decreasing relative reductions*

The coefficients A and B are determined by the relationship:

$$A = \frac{n \cdot \sum_{i=1}^{n} X_i \cdot Y_i - \sum_{i=1}^{n} X_i \cdot \sum_{i=1}^{n} Y_i}{n \cdot \sum_{i=1}^{n} X_i^2 - \left(\sum_{i=1}^{n} X_i\right)^2} \tag{11}$$

$$B = \frac{\sum_{i=1}^{n} Y_i \cdot \sum_{i=1}^{n} X_i^2 - \sum_{i=1}^{n} X_i \cdot Y_i \cdot \sum_{i=1}^{n} X_i}{n \cdot \sum_{i=1}^{n} X_i^2 - \left(\sum_{i=1}^{n} X_i\right)^2} \tag{12}$$

After calculating the coefficients, it returns to initial variables:

$$a = 10^B \tag{13}$$

$$b = A \tag{14}$$

After the calculations, there result specific equations hardening curves (15, 16, 17) for the three kinds of rolling regimens studied.

For the scheme rolling, coefficient reduction breeders:

$$HRB = 66.7 + 1.8757 \times \varepsilon^{0.623} \tag{15}$$

For the scheme in order to reduce rolling with constant coefficients:

$$HRB = 67.7 + 11.8957 \times \varepsilon^{0.14} \tag{16}$$

For the scheme of rolling coefficient, it reduces to the lower value:

$$HRB = 67.7 + 23.85 \times \varepsilon^{0.03} \tag{17}$$

4. Conclusions

Analyzed steel has a very high work-hardening rate, the area of the gliding limited degree of deformation is up to about 15% and occurs after the linear sliding. Over 40% of the total grade material deformation from the zone where the speed of hardening is greatly decreasing is tending to zero.

For proper technological behavior in the cold rolling, rolling the most appropriate scheme is the scheme with coefficients relative reduction breeders. Since entry into the dish to this type of scheme rolling is done at a relative reduction of approximately 40%

it is recommended for the line rolling from MITTAL STEEL (lamination line with five stands arranged in tandem to work continuously) to use a rolling scheme with discounts increasing relative to the passage III after the reduction coefficients will be descending.

As the experimental tests were made to a total level of 60% relative reduction, no cracks were observed in the material, it can be appreciated that the plasticity limit of the material of cold rolling is 60%.

References

[1]. Banaba D., Dorr R. I., *Process modeling plastic deformation of sheet metal*, Press Publisher Transylvania, Cluj-Napoca, 1995.

[2]. Cazimirovici E., *Fundamentals of plastic deformation*, Editura Bren Bucharest, 1999.

[3]. Cananau N., Tănase D., *Plastic deformation technology*, Galati University Press, 2010.

[4]. Ciucă Dumitriu I. S., *Metallurgical Processes Modeling and Optimization of Plastic Deformation and Heat Treatment*, Didactic and Pedagogic Publishing, Bucharest, 1998.

[5]. Popescu D., Ionescu F., Dobrescu R., Stefanoiu D., *Modeling in industrial process engineering*, AGIR Publishing House, Bucharest, 2011.

[6]. Talo D., *Optimizing processes - applications in metallurgy*, Publishing House, Bucharest, 1987.

[7]. ***, DIN 50014 and DIN 1623-1.

THE ANNALS OF "DUNAREA DE JOS" UNIVERSITY OF GALATI
FASCICLE IX. METALLURGY AND MATERIALS SCIENCE
N°. 4 - 2016, ISSN 1453 – 083X

NEW MATERIALS AND PRACTICES FOR BRICKWORK TIP "TORPEDO" POT

Adrian VASILIU
"Dunarea de Jos" University of Galati
e-mail: avasiliu@ugal.ro

ABSTRACT

Nowadays, pots, besides transport operations and liquid metal desulphurization perform functions of dephosphorization. Intense refractory brickwork is required, and in such cases, it is recommended that the performance refractory materials are used. This paper presents a case analysis on modernizing transport ladles or "Torpedo" pot in order to increase service life.

KEYWORDS: iron pots, masonry degradation, new materials

1. Introduction

Steel industry is one of the industrial activities, consuming fuel, which had to reduce their consumption by streamlining the process flows. So, it occurred and it manifests currently worldwide trends towards implementing in production technologies, aggregates and machinery thermo, raw materials, characterized by efficiency and performance, with the ultimate aim of reducing specific consumption of fuels and reduce energy losses to the environment.

Integrated steel mills are used to transport iron to the steelworks blast furnace with pots of different shapes: pot with a spout, pot - type mixer and Torpedo ladles. Whatever form for transporting hot metal ladles, they are made of sheet steel riveted or welded and are lined with refractory brick.

Fig. 1. *Assembly wagon - Torpedo pot*

Of the various construction types, depending on the furnace capacity and transport distance, ArcelorMittal Galati, was chosen type Torpedo ladles 300-ton capacity. These pots are mounted on carriages C.F. special type of tread must withstand high loads.

Torpedo type pots are placed horizontally cylindrical shape with tapered ends. At the upper metal shell is provided with an opening for loading and unloading. The body of the pot rests on two platforms C.F. through two rotating axes that allow the pot to download. On one of the two platforms are mounted rotating devices. The body of the pot along with the two platforms, "wagon pot Torpedo" (Fig. 1).

Refractory materials used in building up the pot must withstand temperature liquid metal erosion mechanical abrasive action of the metal to flow into the pot and transport, chemical action of foam and temperature variations. Of liquid iron pots Torpedo download body by rotating the pan in a pot of transfer (transmission) sitting on a transfer car, where the bridge crane is downloaded directly into the inverter.

2. Objectives

This paper presents an analysis of the degradation and destruction builders liquid pig iron transport ladles type Torpedo. Based on this analysis and new functions met, this type of pot requires revision of classic refractory materials used so far and the use of new materials with specific properties superior.

Integrated steel torpedo cars are used for transporting molten metal from the furnace to the steelworks. Each car has a torpedo-shaped pot, which can carry up to 250 tons of liquid metal. The pot is lined with refractory brick to maintain the contents of the liquid and to protect the external steel casing.

Volatility and erosive nature of molten metal has to be monitored for the torpedo car, this maintenance function of the refractory lining being vital. Following a breakout is significant in terms of safety and cost.

Benefits of the system Torpedo measuring machines Land:

Avoiding Breakout and its consequences - time, materials, labor through:

- automated process - saves costs and time man;
- historic thermal image database on both sides of each car;

Analysis of the data over a long period of time can reduce the cost and:

- Improve safety;
- Improving confidence in refractory status and safety of cars by planned programs for refractory relining and maintenance.

3. Theoretical considerations

Transport of hot metal from blast furnaces to steel mills or M.T is made with iron pots. Sometimes these pots, in addition to the role of transport, have the sole of storage for short periods of liquid pig iron.

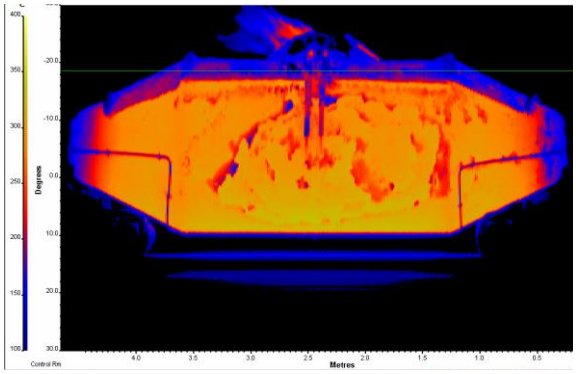

Fig. 2. *Infrared scanning Torpedo type pot*

Choosing the appropriate refractory linings execution iron pots, it is subject to a number of factors physicochemical nature of thermal and mechanical. Besides temperature of 1300-1350 °C, there are other applications which alone or together are more important.

Chemical corrosion to slag temperature drop (load pots), mechanical shocks due to load iron jet rotation, erosion and abrasion molten metal are essential to choosing refractory necessary.

The action of chemical corrosion is due to the chemical nature of hot metal and slag. Most blast-furnace slag is characterized by reports CaO/SiO_2 contained within 1.0-1.3 and $(CaO + MgO)/(SiO_2 + Al_2O_3)$ from 0.85-1.20. The attack is manifested by slag penetration and corrosion of masonry joints.

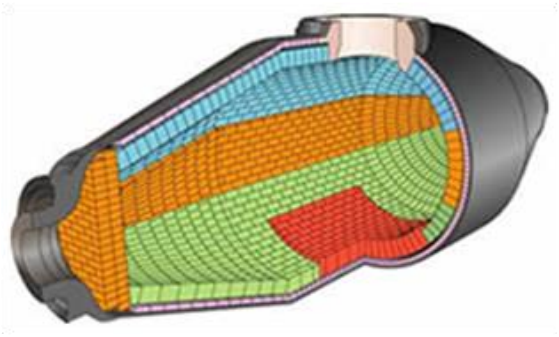

Fig. 3. *Infrared scanning Torpedo type pot*

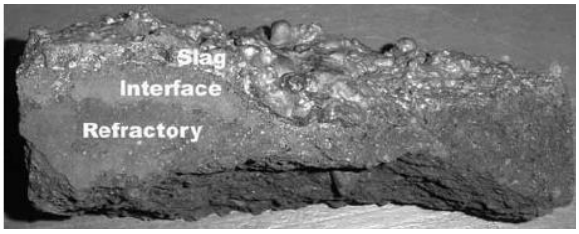

Fig. 4. *Chemical adhesion slag - refractory* [1]

Refractory corrosion is a very complex process and is described by three factors:

- *dissolution*, or diffusion, is a chemical process in which the refractory material is dissolved or goes slag.

- *penetration*; it is a physical-chemical process and is manifested by entering masonry slag and corrosion, especially on the joints causing mechanical stress in masonry.

- *abrasion* occurs due to movement of hot metal, loading and unloading, but especially to transport and produce phenomena of abrasion on refractories.

Dissolution of refractory material in liquid slag is usually expressed in terms of dissolution rate, which shows what percentage of saturation of the slag, the process is balanced and does not occur. It is known that the highest rate of the dissolution process is controlled by solid liquid mass transfer, given by equation (1):

$$-\frac{dr}{dt} = A_0 \cdot U^b \qquad (1)$$

where:

- r is the radius of the interior [m];
- t is the time [s];
- A_0 is a constant specific to conditions;
- U is the peripheral speed of rotation;
- b is a constant.

The rate of dissolution is given by the equation:

$$v = k \cdot (n_s - n_b) \quad (2)$$

where:

- ν is the rate of dissolution;
- k - coefficient of mass transfer;
- n_s, n_b - oxide interface slag / refractory.

Slag resistance of refractory bricks to be determined primarily by the equilibrium relationships. It is clear that a slag, which is already saturated with a solid phase still, cannot attack a refractory product.

The thermal shock that occurs when loading and unloading the pots causes destruction of the brickwork, the occurrence of cracks or dislocations bricks. The phenomenon is more serious as the temperature gradient is higher and the number of heating cycles is higher.

4. Torpedo ladles iron masonry

ArcelorMittal Galati iron pots of 300 tons, Torpedo type were lined with indigenous materials, silica-alumina FA85, D82, EC79, CA75, C71 (STAS 1580 / 3-81).

Table 1. *Features refractory*

Characteristics	STAS				
	270/81		1026	136/81	
	FA85	EC79	D82	CA75	C71
Content Al_2O_3 [%]	80	65	60	40	-
Content Fe_2O_3 [%]	1.0	1.5	2.1	2.5	-
Refractoriness [I.P]	185	179	182	175	171
Porosity apar. [%]	23	23	22	22	22
Thermal shock	10	10	-	20	15

To increase sustainability by about 30% silica alumina liners, they are impregnated with liquid tar. Heated to 1200 ºC it is absorbed by the pores of the pores of the brick and the free residual water by evaporation from the mortar of the connection between the bricks. By burning in a reducing atmosphere at ~700-800 ºC, tar is produced, and cracking is accompanied by a separation of carbon forming a carbon skeleton, resistant to high temperatures and mechanical wear.

Isolation pots run with pleasant I 79 having refractory capabilities, additional caps sit in the compressible layer of insulating concrete aluminous (BTIA) 78-79 mm thick. The discharge pots refractory concrete is made with hard super aluminous BR94.

Torpedo pot having the role of transport and storage for short periods of cast iron pot of operation is simple. The charge brings Torpedo ladle car port under the discharge spout of the furnace so that the jet of liquid iron pot to flow through the spout.

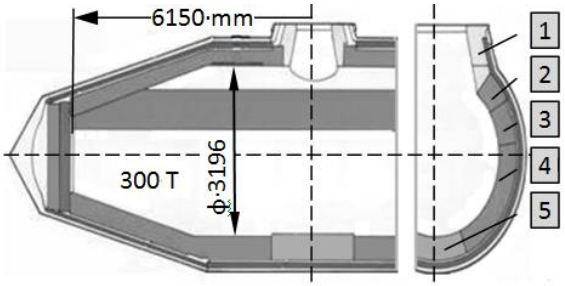

Fig. 5. *Masonry pot 300T (current situation) 1-BR94; 2-FA85; 3-D82; 4-EC79, 5-D82*

The torpedo liquid iron pots download their content by rotating the pan in a pot placed on a transfer car, from where, the content, will be downloaded directly into the inverter. The technical features are:

- Nominal Capacity: 300 tons;
- The distance the buffers 27500 mm;
- Total weight: 640 tons loaded;
- Ladle length: 12300 mm;
- Diameter: 3196 mm.

In order to increase the life of Torpedo, ladles of iron transport in the new operating conditions superior refractories must be used.

5. The causes of refractory linings wear

Given the role of transport and storage for short periods liquid pig iron, cast iron pot operation is simple. To make car charging port to download cast iron trough furnace, the flow of liquid iron in the pot is directed to flow through the spout. Avoiding falling jet of liquid iron directly on a metal sheath, the degradation and decommissioning of the pot is prevented.

Fig. 6. *Charging hole (mouth) 300T casting ladle after 1020*

In the loading-unloading mouth, where mechanical wear due to jet iron is high, the wear layer which is over a length of ~1 m on both sides of the mouth is made of FA85 PLS6 format bricks, PLS7 having a thickness of 300 mm.

At pots 300T Torpedo type change ring at the mouth of loading - unloading is done by loosening the cap and replacement piece shaped refractory (Fig. 7).

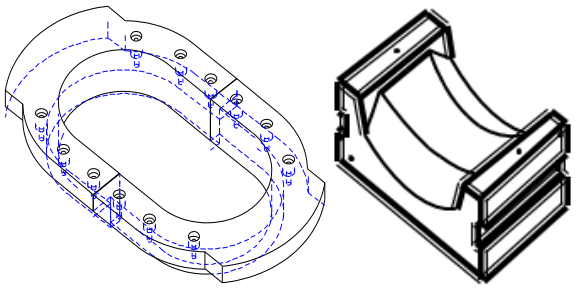

Fig. 7. *Fixing ring and lantern refractory*

The Torpedo liquid iron pots are downloaded by rotating the pan in a pot of transfer (transmission) sitting on a transfer car, where the bridge crane is discharged directly into the mixer or converter.

The movement of liquid pig iron in the charge inside the pot causes erosion and abrasion of refractory, leading to a decrease in the thickness of the refractory lining (Fig. 8).

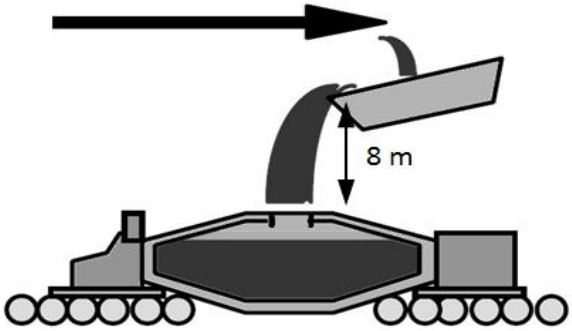

Fig. 8. *Download iron liquid in the pot*

Flushing phenomenon can be avoided by filling the pot at normal capacity and by draining of iron. Gradients in temperature are induced in the resistant during filling and emptying the pot, ring masonry destroyed by thermal shock when the brick refractory was exposed to the hot iron casting in the pot, due to the phenomenon of thermal expansion (Fig. 3).

The crack at the ends of the horizontal surface of bricks induced sudden contraction as a result of contact with ambient air, after emptying the pot.

In many cases, the various slagging and deposits (bears), chemically or mechanically adhering the refractory lining, the cleaning and detachment causes degradation or destruction of masonry.

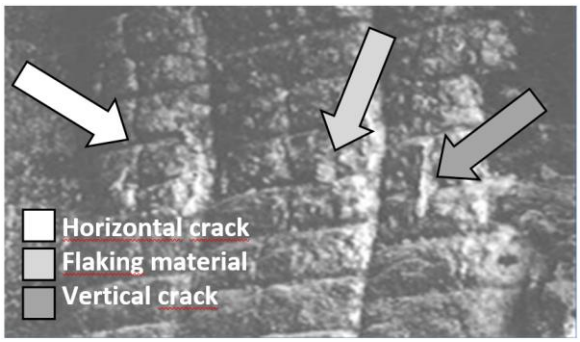

Fig. 9. *Masonry degradation - thermal shock*

6. Refractory news

Modern technology provides a number of metallurgical operations to be performed on the discharge spout cast iron pot or transport. Therefore, torpedo containers are used no longer just for transport but also to perform functions for the treatment of hot metal, such as desulfurization or dephosphorising (Fig. 10).

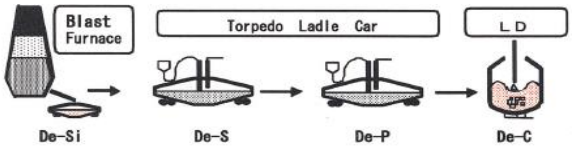

Fig. 10. *Treatment of hot metal pot*

These practices involve high temperature, turbulence of the bath metal/slag by the injection of the reactive streams and a high chemical attack by the slag on the refractory lining. Therefore, the life of the solutions listed above like "bricks impregnated with tar" is outdated, alumina being reduced dramatically.

In order to increase the life of Torpedo ladles of iron transport in the new operating conditions, there must be used superior refractory and differentiated embedding pot on demand.

Thus, refractory products recommended to be used for Torpedo type cast iron pots are:

- Silica-alumina;
- Alumina (Al_2O_3 65%, 50% Al_2O_3);
- ASC (aluminum - silicon - carbon);
- AMC (aluminum-magnesium-carbon);
- Mortars and concretes, inclusive.

The experimental results have shown that the resistance to molten slag of Al_2O_3, spinel, depends mainly on the amount of converted spinel containing 75% Al_2O_3 by weight [3].

As apparent from the graph in Figure 11, Al_2O_3-MgO cast is able to resist much better to attack slag

(penetration and corrosion) compared with Al_2O_3-spinel.

Worldwide there were made a series of tests with good insulation refractory fiber pots with 45% Al_2O_3 in thickness of 10 to 30 mm.

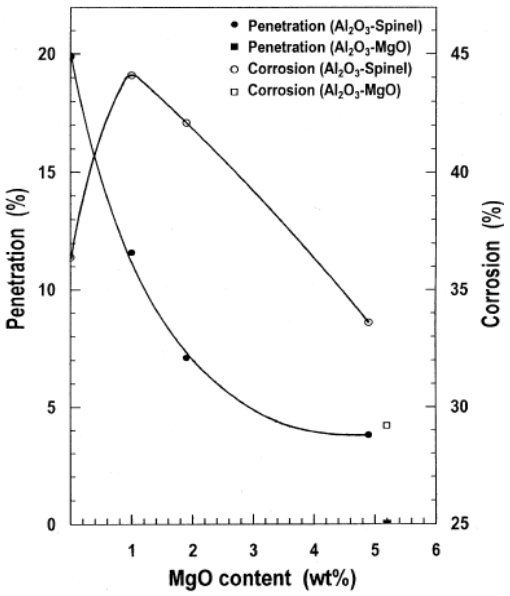

Fig. 11. *Resistance to slag attack* [3]

Refractory lining of Torpedo ladles type consists of a layer of insulation, a layer of duration and a wear layer (Table 2, Table 3).

Table 2.

Refractory material	Zone	
	slag	impact
	[mm]	[mm]
Bricks ASC (5/10%SiC+10/15%C)	275	382
Poured concrete (65%Al_2O_3)	20	20
Bricks (50%Al_2O_3)	70	70

Table 3.

Refractory material	Zone	
	cylindrical	conic
	[mm]	[mm]
Bricks (75%Al_2O_3+22%SiC+%C)	275	382
Poured concrete (65%Al_2O_3)	20	20
Bricks (50%Al_2O_3)	70	70

The discharge pots are made of alumina-carbon Al_2O_3 + 22% SiC (Figure 12).

For the loading mouth, a method was adopted for work implementing by shotcrete material. Alumina-carbon which is based on silicon carbide and bauxite as main raw material was used, which is bound with cement or micro-dust, and non-adhesive slag with high strength and resistance corrosion.

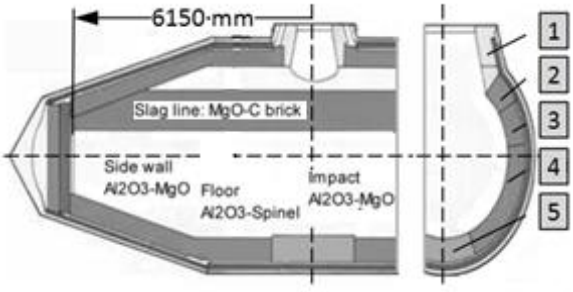

Fig. 12. *Laying pot 300T (proposed situation) 1-Al_2O_3-SiC; 2-MgO-C; 3-5/10%SiC+10/15%C; 4-75%Al_2O_3+22%SiC+%C; 5- Al_2O_3 -MgO*

Fig. 13. *Loading mouth area*

Cast iron pots can be removed from circulation before performing the normal operating cycle, only with the recipient section in the following situations:

- the occurrence of uneven wear and delivered to a depth of more than half the thickness of wear;
- bricks dislocation in certain areas;
- it finds the broken bricks, with deep cracks wider than 2 mm;
- when joints between bricks are weathered and appear exaggerated due coking iron and slag area.

In refractory brickwork iron pots not leave an expansion joint, which is taken from the metal sheath of insulating layers and plastics.

7. Conclusions

Increasing availability of transport iron pot Torpedo wagon can be achieved by:

- Reducing heat loss through the walls of the pot, using as insulating refractory ceramic fiber (45% Al_2O_3 10 to 30 mm);
- Resistant to thermal shock lasting refractory layer type ASC (Al_2O_3-SiC-C);

- The decrease of penetration and corrosion- $MgOAl_2O_3$ brick type;
- Reduce slagging and crusts, adhering mechanically or chemically on the refractory lining.

Reduce the number of stops for repairs in the outlet by using a removable ring - shaped as a ceramic piece.

References

[1]. Hady Efendy *et al.*, *Molten Metal-Slag-Refractory Reactions During Converting Process*, International Journal of Engineering & Technology, IJET-IJENS, vol. 10, no, 3, p. 52-54.

[2]. Chen Y., *Slag Line Dissolution of MgO Refractory*, Canadian Metalurgical, vol. 44, p. 323-330, 2005.

[3]. Deică N., *Utilizarea rațională a produselor refractare*, Editura Tehnică, București, 1982.

[4]. Kronthaler A., *Raw materials for refractories – a strategic challenge*, Interceram – Refractories, Special Edition, 2009.

[5]. Rău Al., Tripșa I., *Metalurgia oțelului*, Editura Didactică și Pedagogică, București, 1973.

[6]. Avram C., Bob C., *Noi tipuri de betoane speciale*, Editura Tehnică, București, 1980.

THE ANNALS OF "DUNAREA DE JOS" UNIVERSITY OF GALATI
FASCICLE IX. METALLURGY AND MATERIALS SCIENCE
N°. 4 - 2016, ISSN 1453 – 083X

CHARGERS FOR BLAST FURNACES DOUBLE BELL VS. ROTARY CHUTE

Adrian VASILIU
"Dunarea de Jos" University of Galati
e-mail: avasiliu@ugal.ro

ABSTRACT

The distribution of materials at the mouth of the loading of a furnace is decisive for its operation at optimal efficiency. For this operation using charging devices that can be of several types is useful. The paper presents a case study from ArcelorMittal Galati, the blast furnace no. 5, where a double bell charging device was changed with a type of rotating Paul Wurth channel, thereby achieving improved productivity.

KEYWORDS: blast furnaces charging device, double bell vs. rotating chute

1. Introduction

Developing a continuous process of pig iron is done by suppling the furnace with raw materials and coke achieving a rhythmic descent of material column, due to the combustion of coke, smelting and periodic evacuation products.

The furnace charge is done with the goal to alternate ore and coke. Load size is determined by the volume of the furnace, installation of transmission and distribution of load module at the mouth of the furnace. Establishing the optimal size of the load and charging system is made for each furnace gas after analyzing traffic, maintaining ratios between the gas temperature in the central and the peripheral.

The types of charging systems may be different, the most famous being the dual locking hopper and cone (Fig. 1), or loading facilities without Paul Wurth bell-type (Fig. 2).

Lately there have been proposed solutions that are dropped cones, using closure flaps for symmetrical distribution of material in the furnace.

Closing the furnace mouth funnel-con systems results in deficient gas pressure exceeding 1.5 atm. The large cone has the role of ensuring the settlement material in the furnace so that a uniform movement of gas could be obtained.

Unlike loading apparatus, bell charging devices with rotating chute is best suited to supply the furnace with tape, and portions of coke and ore are loaded into a separate furnace, the whole amount by a single movement of the trough rocker.

It is designed to distribute in a controlled manner into the furnace raw materials. This can print a rotational motion in both directions by 360° and move vertically from 0° to 50°. The vertical motion can be achieved in 11 preset position, rotation and tilting movements are independent.

To withstand, the wear side is covered with wear plates stacked circularly and in the area wear plates are mounted in a circular type ("honeycomb").

Functioning with rotating chute: Raw materials are brought and unloaded in bunkers supply of materials flowing into the bunker. The bunker material is provided at the top with two superior sealing flaps (keyboard tray).

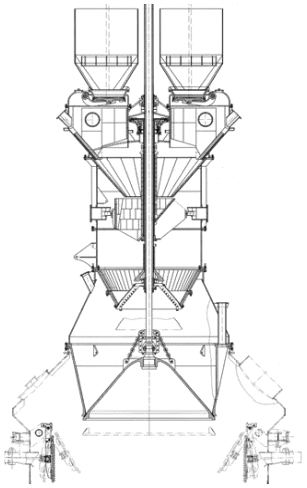

Fig. 1. *Device charging the cones* [1]

After downloading materials from the materials skip bunker, the upper sealing flap (flap plate) corresponding to the skip that transported raw

materials and the hopper closes with blast furnace gas and is pressurized by opening the flip equalization.

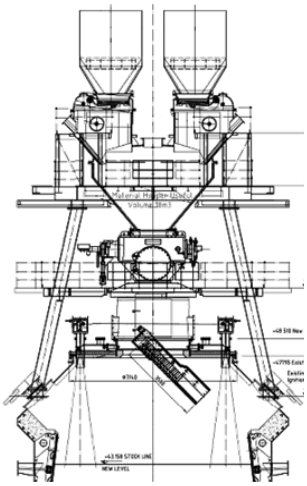

Fig. 2. *Device charging with cones* [1]

If the furnace is ready for loading (condition of furnace goal is met), it will start the sequence regulating the flow of material discharged into the furnace, by opening the bottom seal, followed by flap material that opens up in a certain given position which controls the flow rate of the various materials.

Raw material loaded into hopper material flow from the hopper through the flap of material, flap bottom sealing and operator trough rocker (box mechanisms pan and tilt trough distribution), which is protected against wear by a feeding tube central distribution chute during turning.

The raw materials can be loaded at any point desired trough distribution and can be performed simultaneously by a completely independent movement of rotation around the central axis of the furnace and a rolling movement, to the surface of the column materials.

The use of this device requires continuous control of the charging load level and composition of blast furnace gas. That charging with this type of machine offers the most opportunities for sharing materials at the loading mouth.

This type of apparatus has several technological advantages, including:

- weighing the material in the charging unit SAS sites;
- controlling the amount of material introduced into the furnace circumference;
- distributing the rings or spiral material loaded into the furnace;
- the possibility of surface loading cargo sectors;
- ordering and tracking computer charging schemes, the amounts entered;
- adjusting the speed and changing the angle for each of the 11 positions tipping.

2. Objective

Worldwide furnaces are equipped with Chargers bicameral bell or devices with rotating chute performance. Temperature protection action from the loading mouth is not strictly necessary since the furnaces have a stable and appliances bicameral upper chamber works with excess nitrogen [1-6].

Blast furnaces (F3, F5) from ArcelorMittal Steel Galati S.A. chargers are equipped with two bells and keyboards bicameral sealing. Charging devices are exposed to prolonged high temperatures and variable neck furnace against the background of deficiencies in operation [1].

In 1998 blast furnace no. 5 May 2700 m^3 was equipped with an upgraded battery charger, a Mannesmann - Germany, which has been provided with two working chambers (bicameral) and 2 sealing flaps that close to the upper chamber above the small bell. Furnace no. 5 may work from the beginning with batch consisting of two semi-loads of coke and ore each of three skips. Ferrous load weight ranged from 70-86 t.

From the start, after the explosion in November 2011, the furnace operates with high thermal losses and instability. One reason is implicit by the conceptual design of loading equipment: the large bell is too small in diameter at the mouth of charge and it is not possible to upload material to the periphery (wall).

The current load device with the second upper flap of the sealing bell is not able to distribute the charge material near the furnace wall and the gas distribution in the stack that is preferential to the wall. Heat losses are controlled.

The current loading device with the second upper flap of the sealing bell is not able to distribute the charge material near the furnace wall and the gas distribution in the stack is preferential to the wall. This promotes peripheral circulation inside the furnace, so a poor thermal condition with frequent reduction/burn can stop and cool the element. Heat losses are controlled.

Blast furnace productivity and low fuel consumption remain high.

It was decided to continue furnace operation following losses related to the replacement of the charging unit, with one powerful channel rotating outages to 04/27/2014.

This change aims:

- productivity: 5,600 tons iron / day;
- equivalent comb. Total 490 kg/t HM;
- report of use: 96%;
- increased life of the furnace;

- facilitate maintenance work.

3. Theoretical considerations

Material coating the entire section of the mouth of the opening bell loading requires maintaining high correlation between neck diameter and the diameter of the large bell furnace.

The differences between these two dimensions report the blast from various countries and from Furnaces 3 and 5 at ArcelorMittal Steel Galati S.A. They are shown in the table below:

Table 1. [1]

Difference Reports	CSI	SUA	Germany	ArcelorMittal Steel Galati	
				F3	F5
d_g - d_{CM}	<1.9	<1.7	<1.2	1.9	3.0
d_{CM} / d_g	0.55 - 0.76	0.65 - 0.81	0.7 - 0.8	0.72	0.65

where:

- d_g - furnace neck diameter, m;
- d_{CM} - great bell diameter, m.

The shape and dimensions of technological sub-assemblies are established on experimental basis. Thus, it was found that the volume of cargo storage space on the large bell to be approx. 2.5 to 3.0% of the volume of the furnace. At small furnaces (F3), the lower chamber volume is 54 m^3, which represents 3.16% of the useful space and for the furnace F-5 (90 m^3) this ratio is 3.3.

The great bell diameter d_{CM} of the charging unit is determined by the following two criteria:

- after d_1 - d_0 values:
  - 1.41 - small and medium furnaces (d_1 < 4.5 m);
  - 1.34...1.4, furnaces and large intercede (d_1 = 4...8 m);
  - 1.3 ... 1.35 - furnaces very large (d > 8 m);
- after values and the difference between the diameters d_1, d_0: $c = d_1 – d_0$

that, for d_1 = 5...8 m according to the equation:

$$c = 0.26\, d_1 + 0.1 \text{ [m]}$$

$$d_0 = d_1 – (0.26 \cdot d_1 + 0.1) \text{ [m]}$$

Heat loss is not evenly distributed on the circumference and height of the furnace. This occurs due to damage to the cooling element.

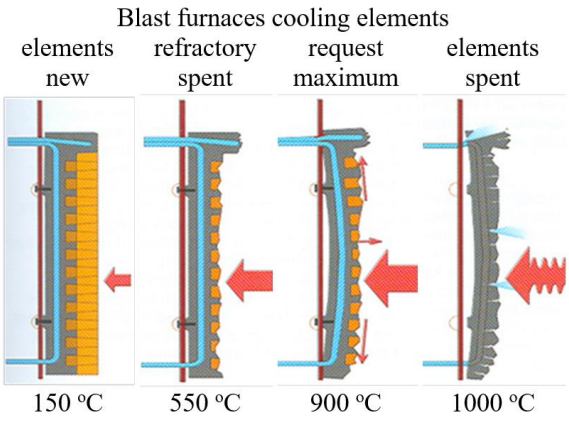

Fig. 3. *Blast furnaces cooling elements*

The temperature of the cooling (Table 2) element is considered critical when:

- at least one face warm temperature of an item ranges within the ranks R1, R2, R3, R4 > 150 °C for a period longer than 5 minutes;
- at least one face warm temperature of an item ranges within the ranks S5, S6 > 350 °C;
- at least one face warm temperature of an item ranges within S7 > 300 °C;
- at least one face warm temperature of an item ranges within the ranks S8, S9, S10, T11 > 400 °C for a period longer than 10 minutes.

Cooling water temperature is considered critical when:

- at least for one of the 28 temperatures (temperature measured at the exit of the row), the elements T11 is greater than 65 °C;
- return water temperature (before entering the heat exchanger) is greater than 55 °C.

Table 2.

Description	Row	Symbol	Material	Temperature	
				Alarm	Critical
Stak	11	T11	Cast iron	350	400
	10	S10	Cast iron	350	400
	9	S9	Cast iron	350	400
	8	S8	Cast iron	250	400
	7	S7	Steel	300	300
	6	S6	cast iron	300	350
	5	S5	cast iron	350	350
Hearth	4	R4	Copper	125	150
	3	R3	Copper	125	150
Bosh	2	R2	Copper	125	150
Belly	1	R1	Copper	125	150

This will create a mask that contain table with temperatures cooling elements. Background boxes will turn yellow when the temperature will exceed temperature alarm, the element will become red when

the element temperature will exceed the critical temperature. When exceeding the critical temperature, a similar table will count exceeding duration.

4. Case Study

When downloading material on an inclined plane from a certain height, there occur freely sloping angle cuttings depending on the nature and grain size of the material. Embankment angle is called the angle of natural embankment. When loading the furnace, where the flow conditions are different because the surface on which it falls is not right and is in motion, and lateral wall is lined at the mouth loading embankment angle; then the natural state changes. The angle cuttings from the furnace could be calculated with:

$$\operatorname{tg}\alpha = \operatorname{tg}\alpha_0 - K\frac{h}{R}$$

where:

- α = slope angle at the loading mouth;
- α_0 = angle natural embankment in free fall from a low height, degree;
- h = drop height, m;
- R = radius of the charge opening, m;
- K = coefficient, which depends on the conditions of fall, shape and material characteristics.

Travel position must consider, firstly, the gas flow diagram by section, and how loaded materials will settle will depend on different slope angle have (26 to 29º coke and 34-43º ores).

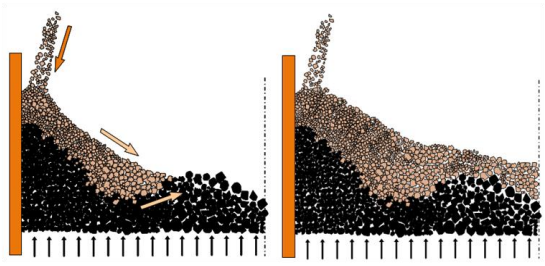

Fig. 4. *Particle size segregation (ore, coke)*

Peripheral circulation and the central one of the alignments is given by way of ore and coke layers in the charge opening, and that the gases always have the tendency to move against the wall of the furnace, where the hydraulic resistance of the column is lower. Whatever charging device would be used with simultaneous downloads (chargers bell) or successive round score (devices without bell), widely grain materials are subject to the phenomenon of segregation. As a result, larger pieces, particularly coke, tend to be thrown to the periphery and center, and small grain will settle forming a ridge, dense, somewhere between the center and the wall.

Distributions of gas above explain the tendency to move the peripheral and central. Setting the required gas to the center or the periphery can be done by distributing the mouth of charging layers to increase strength column, while increasing the efficiency of gas use. The main component of the cargo metal grit agglomerate is between 6-40 mm and the coke has a grain size ranging between 36-80 mm. When loading the furnace due to the graininess, broad sloping fabric takes place accompanied by the phenomenon of segregation.

The current load device with the second upper flap of the sealing bell is not able to distribute the charge material near the furnace wall and the gas distribution in the stack that is preferential to the wall. Heat losses are controlled. Charging device (Fig. 5) is not effective. Blast furnace productivity and low fuel consumption remain high.

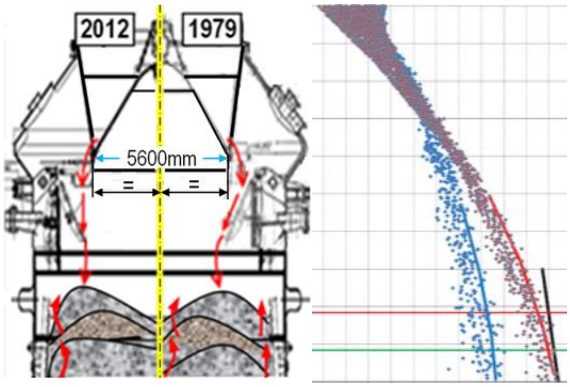

Fig. 5. *The distribution of the material at the mouth of charging*

Compared to other furnaces in operation, it shows that F5 draft report does not respect the usual great bell of diameter and neck diameter blast furnace.

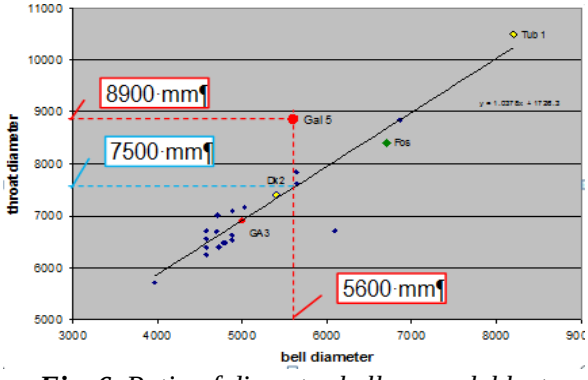

Fig. 6. *Ratio of diameter bell vs. neck blast furnace*

The following positions have no influence on the flow [1]:

- coke: pos. 2 to pos. 6;
- agglomerate: item 2 and item 7;
- pellets: pos. 3, pos. 5 and pos. 7.

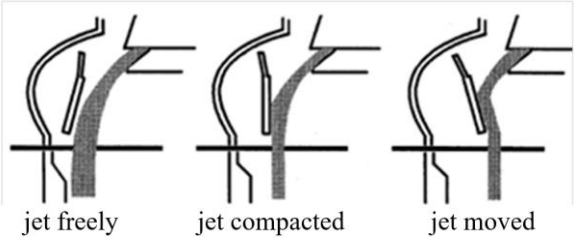

Fig. 7. *Armouring material influence on jet*

By convention were established:

- level "0" which is set at one meter below the bottom of the Jupe neck, adjustable in vertical position (position 2 adjustable neck);
- the "empty furnace" which is set at four meters below the bottom of the Jupe neck adjustable in vertical position (position 2 adjustable neck).

5. Obtained values

The specific consumption of coke is the second factor that depends on the productivity of the furnace and may vary within wide limits, depending on the nature of the cargo. The rate of coke has been reduced to start the furnace, the expected step 914 kg/t HM air blow at the beginning of the furnace was reduced to 354 kg/t HM.

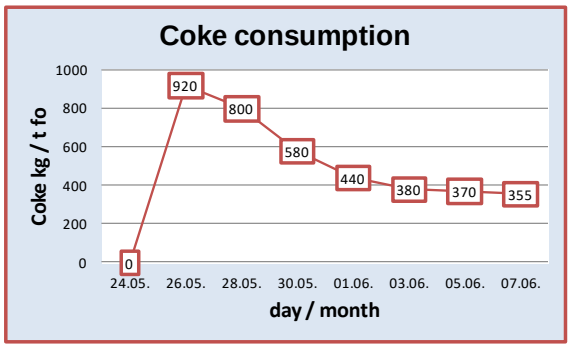

Fig. 8. *Specific consumption of coke*

Pulverized coal injection (PCI) is a process that involves blowing large volumes of fine coal dust in the furnace. This operation provides an additional source of carbon to accelerate the production of metallic iron, reducing the amount of coke, thereby decreases the consumption of coke / TFO and emissions into the atmosphere.

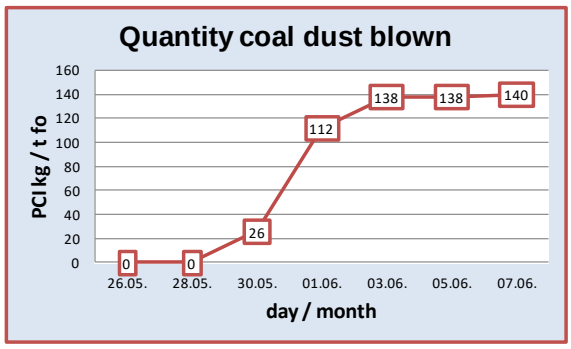

Fig. 9. *Coal dust injected*

What may be reduced is expressed by the speed at which iron in its oxides is released by reduction reactions. It is dependent on the nature of oxides:

- hardly reducible ores (magnetite Fe_3O_4);
- average reducible ores (hematite Fe_2O_3);
- average reducible ores (limonite $2Fe_2O_33H_2O$).

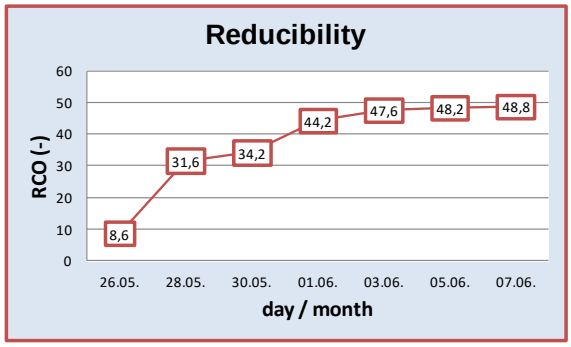

Fig. 10. *Reducibility*

The silicon content in iron, [Si] content developed in the first batch was great - max 8.023% and reached 1% to 6.5 days running. Average daily bath and metal fell from 5.493 at 1.014%, a rate of 0.746% daily decline.

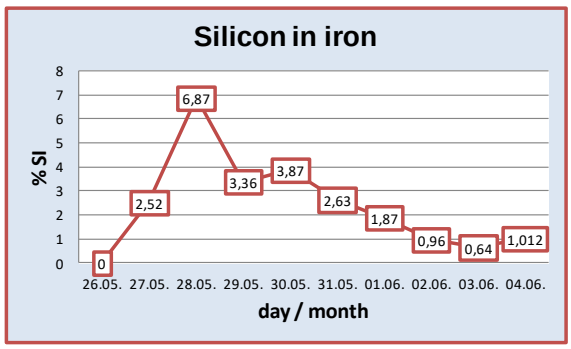

Fig. 11. *The silicon content in iron*

5. Conclusions

Blast furnace charge started from 23/05 to 25/04 (about 40 hours). Ignition and start was made with wind blowing through 12 holes. The first evacuation of pig iron was made on 26/05.

Using the skimmer began on 28/05 at 04:00. First delivery of BOF steel plant was done on 28/05 with [Si] content of 6.25. The furnace was restarted on 29/05 after an overhaul, with (32) nozzles opened.

PCI coal dust blowing began on 30/05 / at a rate of 26 kg / TFO, increasing the amount infused by up to approx. 140 kg/TFO.

The rate of coke charged to the furnace decreased from 914 kg/TFA, from start-up to a quantity of 354 kg/TFA over 8 days.

[SI] in the iron content was very high at a value of 8.023% max, but came to value of 1% at the end of the process.

The average temperature of the first batch of iron was 1438 °C, rising within 8 days until the furnace went into normal operating parameters, and the average temperature reached 1486 °C the next batch.

References

[1]. ***, *Documentation ArcelorMittal Steel Galaţi S.A.*, http://www.arcelormittal.sa.
[2]. Buzea O., *Îndrumător furnale - Partea III*, SIDEX.
[3]. Deică N., *Utilizarea rațională a produselor refractare*, Editura Tehnică, București, 1982.
[4]. *, *Documentation Paul Wurth*, http://www.paulwurth.com.
[5]. Dobrovici D., *Metalurgia fontei*, Editura Tehnică, Bucureşti, 1966.
[6]. Harting W. *et al.*, *Maßnahmen, die Produktivität der Hochöfen zu erhöhen*, Stahl und Eisen, Germania, no. 6, 2005.

THE ANNALS OF "DUNAREA DE JOS" UNIVERSITY OF GALATI
FASCICLE IX. METALLURGY AND MATERIALS SCIENCE
N°. 4 - 2016, ISSN 1453 – 083X

DESIGN OF A NEW TYPE OF GAS-DYNAMIC DISRUPTOR USED TO NEUTRALIZE IMPROVISED EXPLOSIVE DEVICES

Vasile BĂLAN[1], Marian BORDEI[2*]
[1]Tehnical Military Academy of Bucuresti
[2]"Dunarea de Jos" University of Galati, Romania
[*]Corresponding author
e-mail: mbordei@ugal.ro

ABSTRACT

The paper presents a type of recoilless disruptor developed according to the studies of two disruptors performance and shortcomings currently used DR2 and RICHMOND, respectively. In creating the new disruptor, there were kept some common elements of the two disruptors taken as models of operation (ex. dimensions from RICHMOND were used to design the new system of disruption).

KEYWORDS: disruptor, explosive device, neutralization

1. Introduction

The disruptors are gas-dynamics devices propelling jets using deflagration of colloidal powder.

The disruptors are explosive jet engines means, capable of being used to neutralize improvised explosive devices.

The gas-dynamic principle involves sending a payload (different agents of disruption) at a distance, using a gas pressure force resulting from the burning of a flinging load.

2. THOR - 1 disruptor: constructive considerations

The new disruptor, named THOR - 1 aims to remove certain shortcomings observed in the use of DR-2 and Richmond disruptors during the neutralization operations of some improvised explosive devices, namely:

- relatively heavy handling because of the mass of the entire system (stand-disruptor);
- inability to operate in certain areas and targets;
- the initiation of pyrotechnic elements component of some improvised explosive items by the disruption agent (electric detonating caps, etc.);
- the need to approach the suspect package to obtain a good efficiency;
- dusty remains unburned after the shooting.

This gas-dynamic system, the THOR – 1 disruptor, aims to meet the following demands to be able to use as disruption agents, different materials which cannot initiate pyrotechnic elements from the composition of an improvised explosive device;

- the pipe material can be made of duralumin due to the special physical and mechanical properties, such as resistance to high temperatures and much higher plasticity;
- simple construction and low weight;
- lack of recoil due to the reaction force that arises because of the leak backwards of a quantity of powder gases, through special slits;
- easy to use equipment with remote action means, the special type robots (R.O.V.);
- equipment relatively simple to use and can be quickly put in operation.

The above presented disruptors study revealed that a special importance in the neutralizing activity has the choice of disruption agent, based on the existing target, on the material characteristics (tire) in which the improvised explosive device exists. If d.e.i. exists in a metal tire (e.g. car body, pipe, thin-walled metal crates) it is necessary to use steel projectiles for their punching.

The use of these disruption agents involves taking more risks, which must be taken into account, such as:

- pyrotechnic intervention is usually done in urban areas; therefore, it must be remembered that during the drawing with metal bolts, this is propelled like a bullet in the gun, which can injure bystanders or cause property damage;
- scattering d.e.i debris is much higher. When one pulls on it directly with agents other than water, it

results a certain difficulty in gathering some post-neutralization samples.

To avoid the risks previously presented the new disruptor uses as agent of disruption, water, in various combinations. The THOR-1 disruptor is a modular equipment, recoilless, made of duralumin, specifically designed for the disruption of improvised explosive devices.

Duralumin was chosen because between the metals and non-ferrous alloys currently used in high-tech fields, aluminum and its alloys have the largest share due to their properties and characteristics, and especially because of the traditional techniques for hardening these alloys (based in particular on the alloying and hardening by cold plastic deformation).

3. THOR-1 disruptor design

The same as for the Richmond disruptor, the main feature of THOR-1 is completely recoilless operation using a water body for compensation ejected backwards to neutralize kickback. Due to this characteristic, the pipe together with the compensator and the assembly support do not require to have a great mass of the kickback compensation fact that led to the minimizing weight.

Armed and ready for operating, the disrupter with its support can be carried in one hand and weighs less than 5 kg.

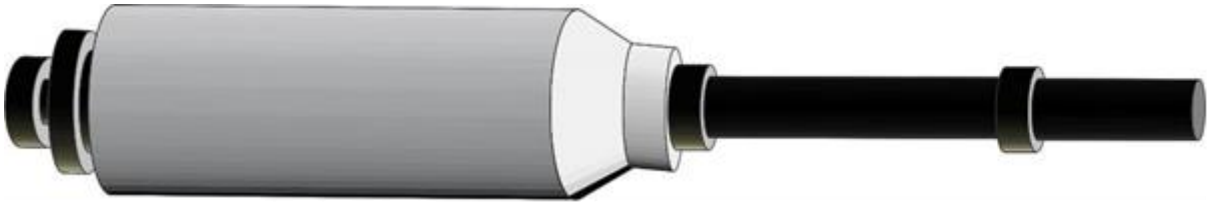

Fig. 1. *THOR -1 disruptor ensemble*

The THOR-1 disruptor is composed of ESA catch; pipe; lock mode, compensation shock; overall striker. The THOR-1 disruptor uses a volume of about 400 ml of water for compensation and is dimensioned to absorb the recoil when firing using the tube of 40 mm with the shock of 25 mm.

The 40 mm caliber barrel is screwed directly into the lock module and is used with the device attached to the muzzle - attenuator or shock. It is used in the configurations of disruption in proximity (Figure 2). The lock module is designed to accept 12.7 mm caliber cartridges (Figure 3).

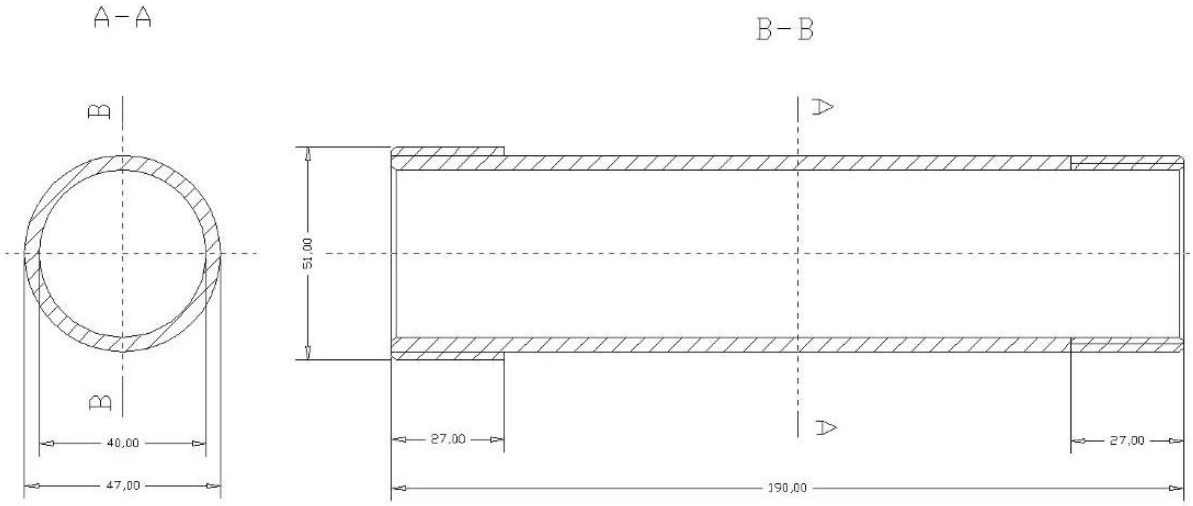

Fig. 2. *The barrel - calibre 40 mm*

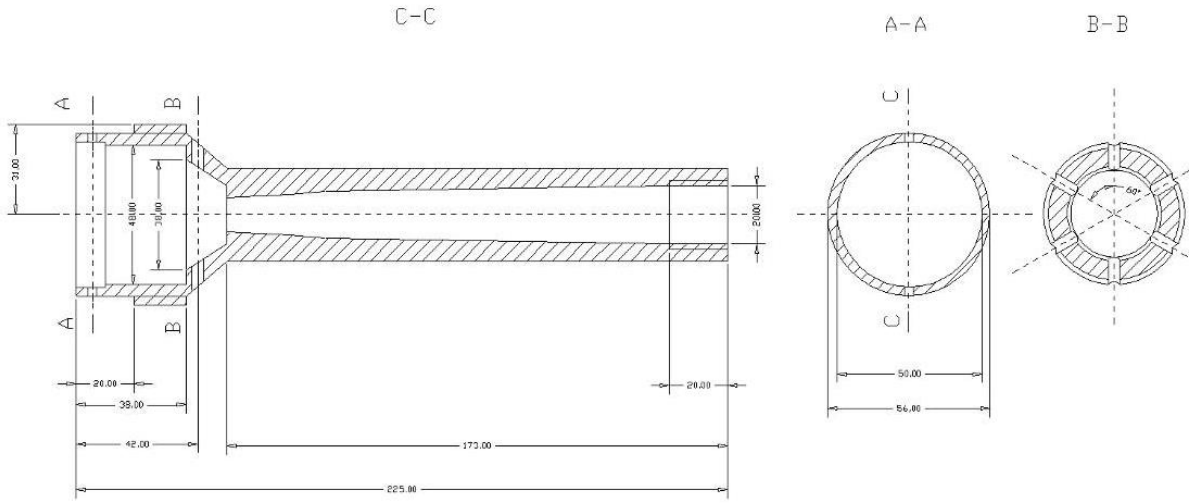

Fig. 3. *Disruptor module lock*

The THOR-1 disruptor uniqueness consists in particular, in the use of a shock with the diameter of 25 mm. Its use formats and speeds the water flow in order to maximize the power of penetration and thus generating a pressure of 1000 daN/cm^2.

It also eliminates the use of other elements, for example the slightly polyethylene plunger that Richmond uses. It is screwed directly into the 40 mm barrel horse (Figure 4).

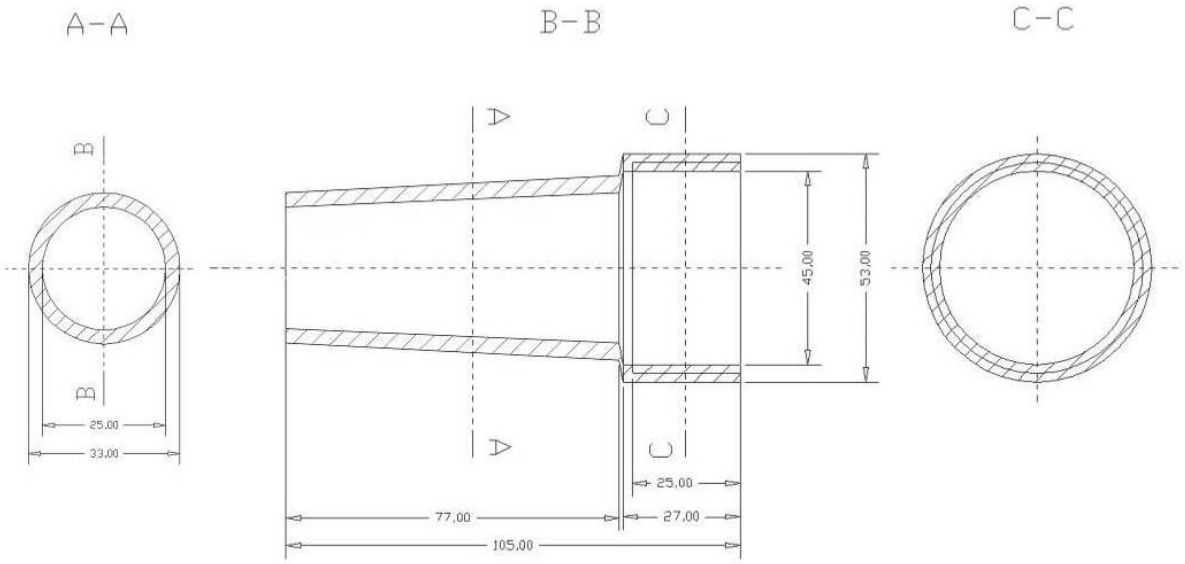

Fig. 4. *Disruptor shock*

The compensator functions to form a ring around the switch, the resulting cavity is used for filling with water (antifreeze solution) which forms the compensatory ballast necessary to recoil cancellation (Figure 5).

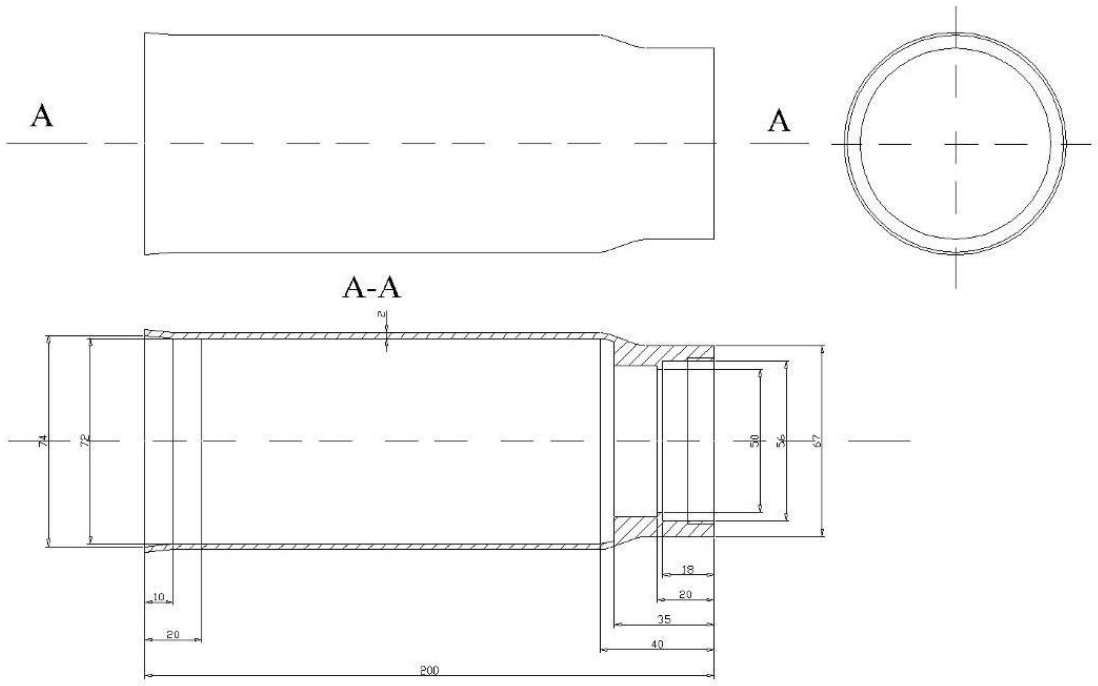

Fig. 5. *The compensator of the THOR-1 disruptor*

The striker assembly is designed to be used with 12.7 cartridges electrically initiated, provided with electric wires. The assembly is provided with a lip of extraction and a back oring which retains the catch sub-assembly in position when the hammer is removed (Figure 6).

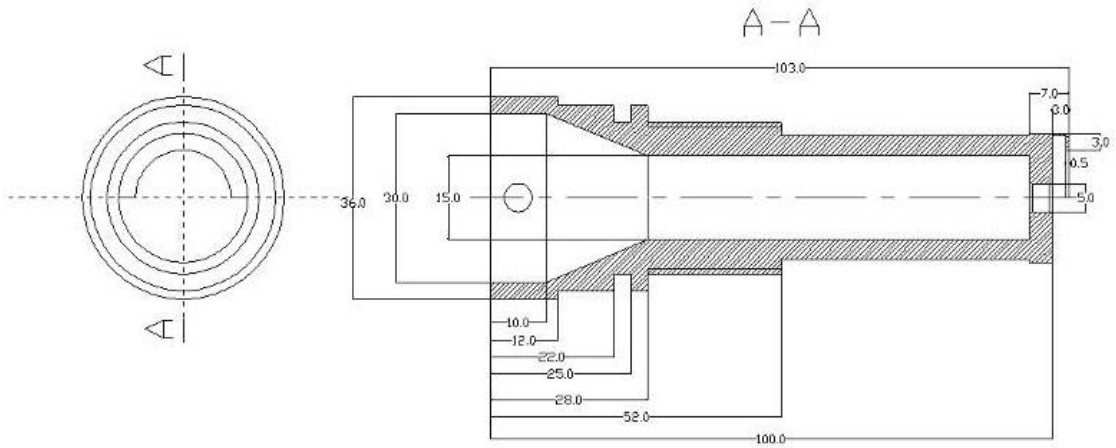

Fig. 6. *Thor-1 striker assembly*

The striker assembly is mounted behind the catching bolt that retains the ring piston, leaving out only the mass of the compensating water and the ring cover. It also has the role to minimize any damage caused by mass compensation which is discarded (Figure 7).

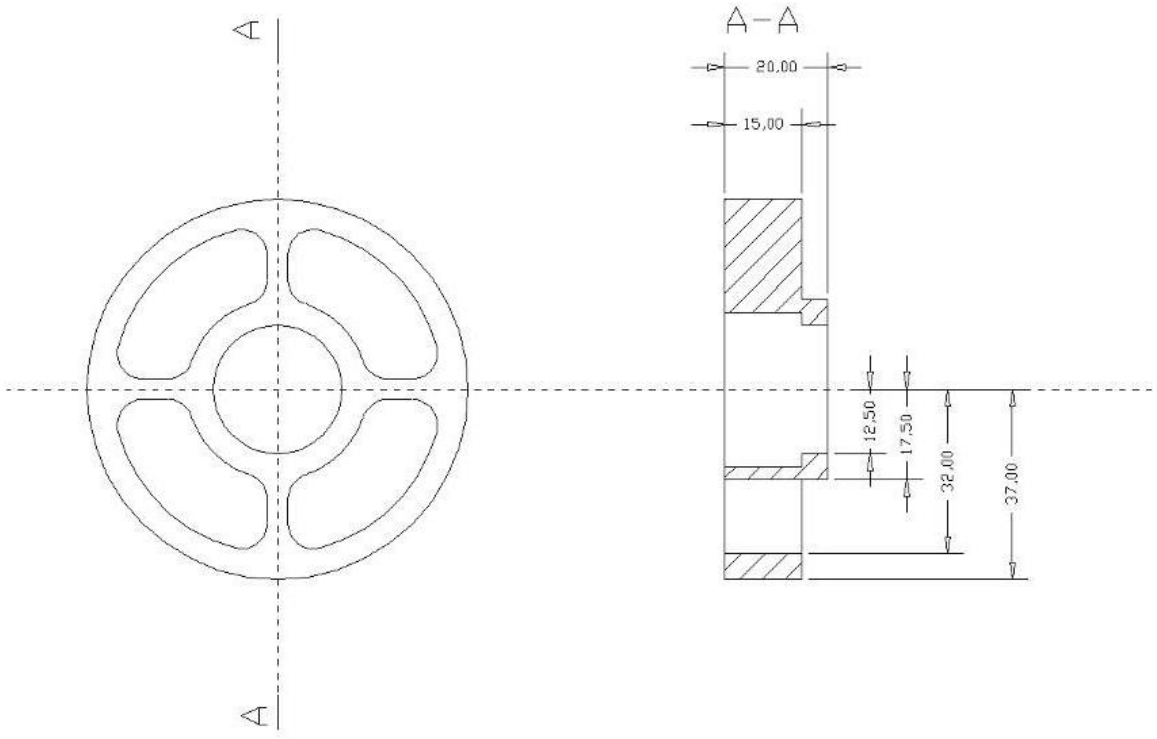

Fig. 7. *The catch subassembly*

Auxiliary elements:

Compensator cover - it aims to close in the compensator the quantity of water necessary to compensate the recoil (Figure 8).

The polyethylene piston role is to close the water in the compensator (Figure 9).

The closing cap serves to close the amount of water in the pipe of 40 mm at both ends (Figure 10).

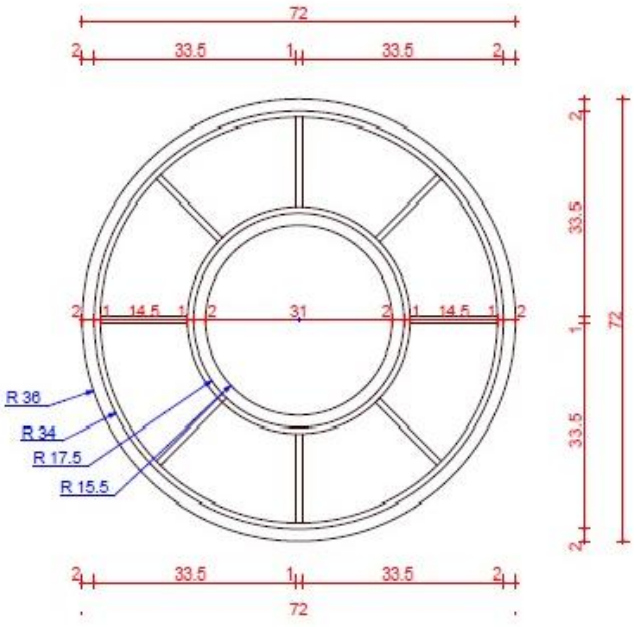

Fig. 8. *The compensator cover*

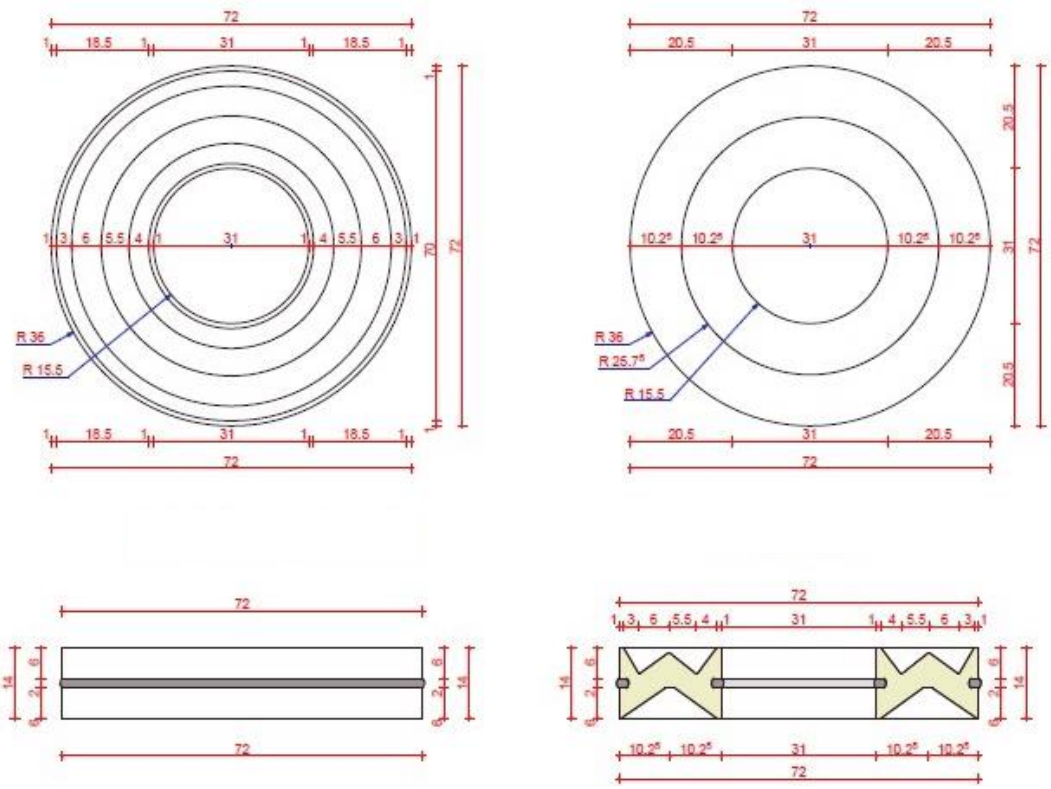

Fig. 9. *The polyethylene piston*

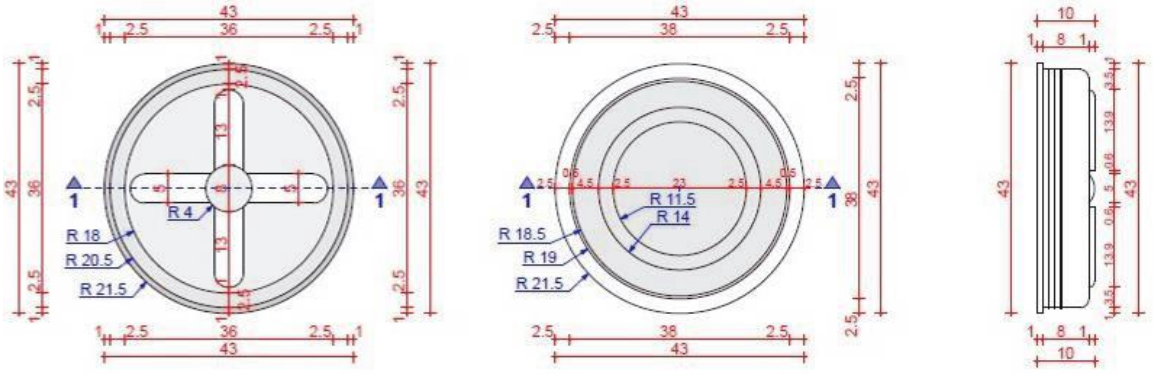

Fig. 10. *The closure cap*

4. Conclusions

- The THOR- disruptor 1 is a potent neutralization equipment, both for the values of the disruption speed agent and the energy of hitting the target;

- The duralumin construction facilitates the transport and handling, due to the very low weight;

- The simplicity of design facilitates rapid entry into operation and a minimal training for the pyrotechnics operators.

References

[1]. Bălan V., Bordei M., *Numerical Ballistic Phenomena*, The Annals of "Dunarea De Jos" University of Galati, Fascicle IX. Metallurgy and Materials Science, Special issue, p. 5-9, 2014.

[2]. Bălan V., Bordei M., *Numerical Ballistic Phenomena [part two]*, The Annals of "Dunarea De Jos" University of Galati, Fascicle IX. Metallurgy and Materials Science, p. 45-52, 1/2016.
[3]. Gingold R. A., Monaghan J. J., *Smoothed particle hydrodynamics-theory and application to non-spherical stars*, Mon Not R Astron Soc, vol. 181, p. 375-389, 1977.
[4]. Gingold R. A., Monaghan J. J., *Kernel estimates as a basis for general particle method in hydrodynamics*, J Comput Phys, vol. 46, p. 429-453, 1982.
[5]. Monaghan J. J., *Particle methods for hydrodynamics*, Comput Phys Rep, vol. 3, p. 71-124, 1985.
[6]. Dyka C., Ingel R., *An approach for tension instability in smoothed particle hydrodynamics (sph)*, Computers and Structures, vol. 57 (4), p. 573-580, 1995.
[7]. Swegle J., Hicks D., Attaway S., *Smooth particle hydrodynamics stability analysis*, J. Comp. Phys., vol. 116, p. 123-134, 1995.
[8]. Johnson J., Beissel S., *Normalized smoothing functions for sph impact computations*, Computer Methods in Apllied Mechanics and Engineering, vol. 139, p. 347-373, 1996.
[9]. Liu W., Jun S., Zhang Y., *Reproducing kernel particle methods*, International Journal for Numerical Methods in Engineering, vol. 20, p. 1081-1106, 1995.
[10]. Liu M. B., Liu G. R., *Smoothed Particle Hydrodynamics (SPH): An Overview and Recent Developments*, Arch Comput Methods Eng, vol. 17, p. 25-76, 2010.
[11]. Trană E., *Solicitarea materialelor metalice în regim dinamic. Legi constitutive*, Editura Univers Ştiinţific, Bucureşti, 2007.

THE ANNALS OF "DUNAREA DE JOS" UNIVERSITY OF GALATI
FASCICLE IX. METALLURGY AND MATERIALS SCIENCE
N°. 4 - 2016, ISSN 1453 – 083X

ASSESSMENT OF THE INFLUENCE OF BREAKAGE STRENGTH ROCKS BY COX METHOD

Mihaela TODERAŞ, Ciprian DANCIU
University of Petroșani, Faculty of Mines, 20 Universitatii, Petrosani-332006, Romania
e-mail: toderasmihaela@yahoo.com, danciu_ciprian@yahoo.com

ABSTRACT

Analyzed according to the theory of continuous mechanics, medium rock massif is a natural environment difficult to know, so the forecasts referring to its behaviour are approximate and uncertain. Such an assertion becomes a certitude, even resulting from reality; consequences of the four fundamental features of massif are multiple and involve really difficult issues in mining field and generally, in the constructions field. The concept and the way to assess the stability of underground construction involves understanding its phenomenological evolution and doubtless the character of rocks behaviour in massif. Based on the principle scheme of rocks behaviour way to failure, we propose a statistical analysis method of results obtained by laboratory tests using Cox regression. This method offers the possibility to provide quantitatively and qualitatively the time when the breakage occurs. The method enables us to establish the link between a certain factor through which can forecast rock breakage and the ability to resist; the method can be developed and applied on a massif scale and also in the stability analysis of underground works.

KEYWORDS: strength, hazard, breakage, regression, salt, event, time

1. Introduction

Viewed as a whole, the rock has a complex and nonlinear behavior and often with manifestation of dilatancy phenomenon under the action loads. Assessment of rocks behavior under load to fracture involves determining the mechanical and deformation characteristics and establishing the characteristic points on stress - deformation curve. From the principal schema of rocks behavior to breakage, it is found the existence of five areas and four characteristics stress levels on σ - ε characteristics curves (see Figure 1) [17, 18]:

- **Ist area,** initial area of characteristic curves, starting from t = 0 when the applied stress increases from $\sigma = \sigma_0 = 0$ to a value $\sigma = 0.05\ \sigma_{rc}$; this latter stress defines actually the linearity limit of longitudinal (axial) deformations, $\sigma_{o\varepsilon l}$ on $\sigma - \varepsilon_l$ curves. Such area may be present or not, its existence depending on rock's porosity, initial fractures density and fractures geometry, this statement resulting from the interpretation of experimental data;
- **IInd area** starts for $\sigma > 0.05\sigma_{rc}$, a continuous decrease of the sample volume being registered (it is assumed that porosity was surpassed and all fractures were already closed), and the rock acting linearly – homogeneously – elastically. Such linear – elastic behaviour ends at certain σ value, when the linearity limit of longitudinal deformations is reached, this corresponds to $\sigma_{if} \cong (0.3 - 0.4)\sigma_{rc}$ from that begins the fracturing initiation, that is when fracturing propagation process starts to develop [17];
- **IIIrd area**, stable or controlled initiation of fracturing, represents the beginning of dilatancy $\sigma > \sigma_{if}$. In this area Toderaș (1999) considers that the dilatancy reflects the increasing of the axial fractures, such as parallel fractures to maximal applied load direction; that fracturing process, together with stresses $\sigma > \sigma_{if}$ do not lead to diminishing the rock's strength. So, we can appreciate that fortuitous stable axial structural faults are not dangerous, having not significant effects on failure strength of studied rock;
- **IVth area** becomes present for a stress level $\sigma > \sigma_{fd}$, fracturing – destruction stress, when global volumetric deformation ε_v equals zero ($\varepsilon_v = 0$). Unstable, uncontrolled fracturing starts simultaneously with dilatancy intensification. Generally, according to [5] there takes place levels ranging between $(0.70 - 0.90)\sigma_{rc}$. At this

level of stress, the longitudinal and transversal deformations will be far away from linearity. Sliding is the major mechanism acting when such longitudinal and cross-sectional deformations appear. Hallbouer mentioned that this area is characterized by strong and significant structural changes of the specimens and the density of micro-fracturing increases seven times. Actually, such a stress level detains a specific significance: it can be employed in assessment of long time strength of rocks [1, 17, 18]. Consequently, load increases over the fracturing – destruction stress value, $\sigma > \sigma_{fd}$, are inducing a temporary effect of deformation – hardening, which cannot be restored only through rheological and which leads to rock destruction, that cannot be tolerated under permanent load;

- **Vth area** is worldwide employed in failure strength evaluation at compressive charges and in assessing critical failure value of rock or starting point of post-critical behaviour area of rocks.

These four stress levels were identified on stress – deformation curves, figure 1, are: (1) σ_o overcoming the perpendicular on loads direction porosity and micro-fractures stress which we were assimilated to the settling stress (σ_{asez}); (2) fracturing starting stress σ_{if} assimilated by all researchers [1, 17] to the stress of dilatancy threshold σ_d^*; (3) fracturing – fragmentation stress σ_{fs} and (4) failure stress or fracture strength at uniaxial compression σ_{rc}.

Breakage stress of rock is a function of the conditions in which the test is carried out and therefore, it constitutes an inherent property of the rock in question [17, 18].

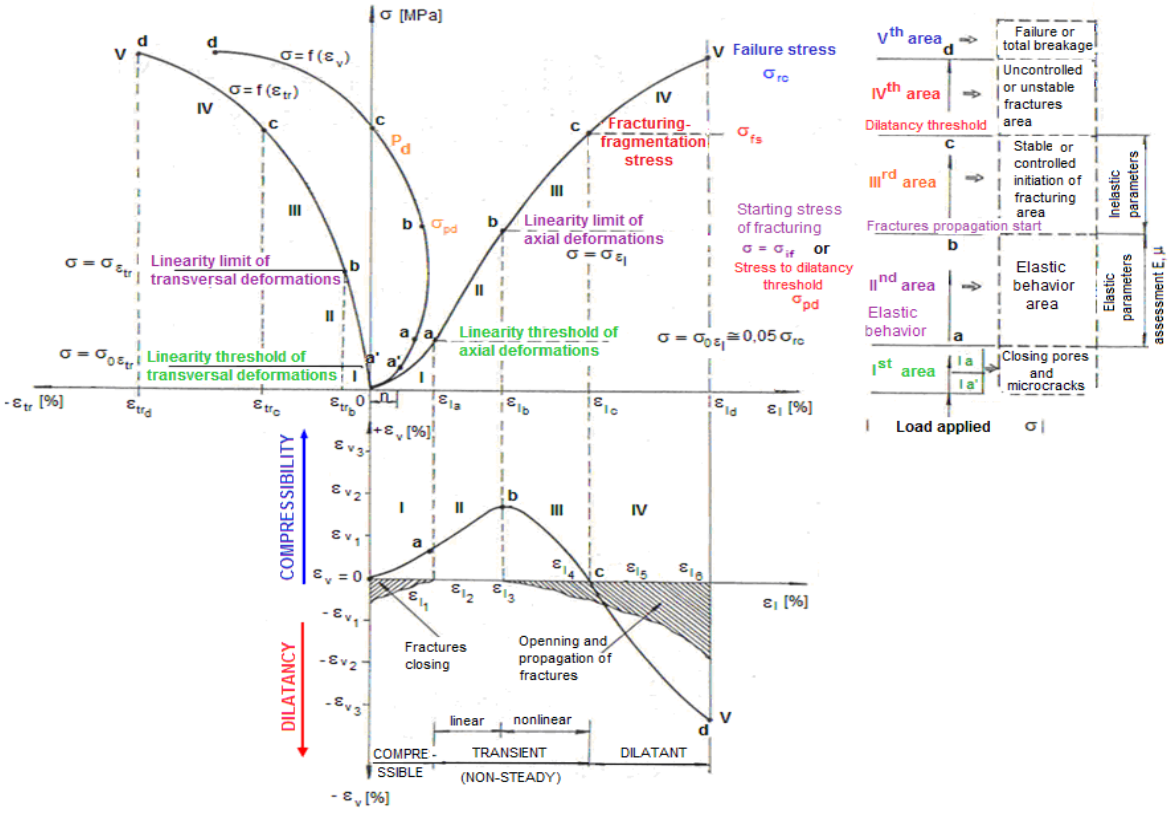

Fig. 1. *Nomogram for analysis – evaluation of rocks behaviour at deformation under uniaxial compressive load (after M. Toderaş, 1999)*

Only the stress levels σ_{if} and σ_{fs} are independent parameters of test conditions and specimen volume, and σ_{fs} stress can be considered as a true resistance of rock in the case of monoaxial compressive load, because the load above this stress level leads to destruction of the rock and that rock cannot tolerate it under a permanent load; σ_{if}, as a stress that in fact defines the dilatancy threshold.

2. Cox proportional hazards regression in the analysis of rocks breakage

Cox regression or of proportional hazard was developed for the first time in the medicine and biosciences [1-4, 11, 14], but it seems that it began to be applied on a fairly large scale in engineering, mainly in the study of rocks breakage time. This

regression is also called of "proportional hazard" since it is based on the assumption that if the hazard may vary over time, then the hazard functions' ratio remains constant, namely the two hazard functions are proportional to each other [6]. We consider that this method of probabilistic analysis can be developed and also applied in the stability - reliability analysis of underground workings. In the engineering field, Cox regression may show if and in what way a characteristic of an analyzed rock may influence the occurrence of breakage; if one of the rock characteristic parameters leads to the manifestation of breakage phenomenon, by Cox regression it can establish the action intensity of this parameter and the direction of its action; by means of this regression there is the possibility to determine the time until which the breakage occurred (the action of a parameter, in the sense that it can extend or reduce breakage time) [19].

Cox regression presents importance regarding the existence and the link between a factor that can predict the breakage of rock and the rock capacity to resist and not to break, in other words, the existence and importance of correlation between a prognostic factor and resistance capacity of rock (the holding time in that domain where might exist anytime the potential possibility of breakage). What is specific to Cox regression is the fact that the response variable is a time dependent event and therefore, can be applied of probabilistic analysis of occurrence of breakage rocks. Through such regression we can achieve a multivariate analysis, which involves determining the relative influences or effects of different causes (or factors) on a single event, namely the breaking rocks time.

The importance of effect that rock parameter or characteristic has on holding time to breakage can be highlighted by means of hazard ratio (or risk ratio) (HR), established on the basis of risk (hazard).

From the point of view of geo-mechanic, we will define the hazard as an instantaneous risk of a rock to register a pre-established event, even though until that moment it opposed the event occurrence; in our case, we are talking about instantaneous risk of rock breakage submitted to a load around breaking strength (here we speak specially about the IV^{th} on the nomogram for analysis – evaluation of rocks behaviour, where the cracking becomes unstable and uncontrolled and the dilatancy phenomenon intensifies too, Figure 1). The higher the hazard is, the higher the breakage risk is; but here we consider that other factors could also interfere here, and that could determine another event that could be produced (for example a growth of temperature or humidity, in case the analyzed sample is a salt one). Hazard ratio of a class or type of rock compared to another kind of rock represents the difference between hazards of two types of rocks, mathematically considered as subjects of study.

2.1. Analysis method of hazards

There are known different methods of analyzing the occurrence risk of breakage, but most often used one is analysis method or mode of breakage time distribution, respectively Kaplan – Meier method [19, 20]. By means of this analysis there can be obtained more regression by which can be expressed the relationship between continuous or multiple variables and time until the appearance of breakage. The term of hazard can be defined in different modes, for different situations that are studied. We tried to define this term from the viewpoint of potential possibility of occurrence of rocks breakage situated under the action of a certain level of stress.

In the field of rock mechanics and implicitly of geo-mechanics (considering the events at scale of massif and in order to analyze the stability of underground workings), the term of hazard or risk, phenomenon that can occur at any time, represents the potential risk of occurrence and development of rocks breakage (occurrence of pre-established event) in a very short period of time, for any material system and implicitly of rocks too, that had the capacity (or a sufficiently high resistance, a sufficiently internal cohesion) to oppose (or to resist) to the damage of internal structure until that time.

As compared to the definition of risk factor given for the first time by Barlow (1963), we also define this notion from the viewpoint of rock mechanics. We consider a range of time whose lower limit is different from zero (time sufficiently low where breakage can appear and big enough in which a rock sample can resist until breakage); than the coefficient of risk is defined as the probability per unit time of a considered interval in which a rock sample did not break under the action of load which it has undergone, but will break at the time *t* belonging to this range. In other words, the risk coefficient can be determined as the ratio of the number of defects per unit time from the interval considered and the average specimens of the same type of rock from which no breakage was recorded at the time value corresponding to the middle of pre-established time range.

The average value of time until the breakage of rock sample does not occur represents the time at which the function of cumulative strength is equal to 0.5; to note is that percentage of 50 % of the cumulative strength function does not always correspond with the point that represents the time until which half of rock samples did not record the occurrence of breakage.

The hazard (the risk) and the probability that material system resists and does not register breakage are two interrelated concepts, the correlation of these being complex; through this there is the possibility to establish one parameter using the other. If the risk is constant for the whole period of study, it seems that this one is independent of the length of time where the material system (the rock) had enough internal cohesion to withstand, namely to oppose of the applied effort.

If the risk is constant throughout the study, it means that the risk of breakage is independent of the length of time that material system, in our case the rock, had sufficient internal cohesion, namely to oppose to the applied effort. For example, in case of uniaxial compressive loads of rock samples, after the effort applied exceeded the threshold of dilatancy or the fracturing - fragmentation stress, a rock with lower strength would have the same risk of breakage manifestation as a rock of higher strength. In case of creep tests, a rock sample mentioned under load, on stress degree of $(0.7 – 0.85)\sigma_{rc}$, for a period of 10 days would present the same risk of breakage in the next immediately moment (in a very short time) like a rock sample that was mentioned under load at the same stress degree for a period of 30 days. But we cannot exclude the hypothesis where the risk of breakage occurrence and development increases with increasing of time in which the rock presents sufficient strength; authors' opinion is that, in such situations, it could be a similar process to work hardening of rock under load, namely hardening.

An approach as close to reality as possible regarding the constancy of hazard is to eliminate any possible assumption and determine this characteristic based on the results of the laboratory tests (or measurements in situ, if we analyze the situation of stability of rock contours around underground works); an assumption regarding this parameter would not be fair and would involve significant errors. Therefore, for a given type of rock it would be necessary that relative hazard be considered as a particular combination of the values of variables with significant weight at a certain moment of time. The relative hazard is defined as the ratio of hazard for combining those variables at a given time and the hazard for the same time of a hypothetical sample (ideal model) whose values are all equal to 0 for predictive variables [8-11, 16]. Such a phenomenon is known as "basic hazard" and it is a virtual notion, namely in case of rocks we could assume that such a sample would exist, but the "ideal" term in this situation will eliminate a number of parameters or factors (as variables) that have significant influence in the development and manifestation of breakage. Whereas the calculation errors of the probability of breakage and respectively of risk of breakage occurrence to be as small as possible, it should be analyzed each time at least 30 samples of the same rock type.

2.2. Cox's proportional hazard model

Cox's model expresses the function of instantaneous breakage risk of a rock, λ, depending on the time *t* and covariables $X_1, \ldots, X_n$, namely:

$$\lambda(t, X_1, \ldots, X_n) = \lambda_0(t) \exp\left(\sum_{i=1}^{n} \beta_i X_i\right) \quad (1)$$

For a rock sample, function $\lambda(t, X_1, \ldots, X_n)$ can correspond to the instantaneous risk of breakage at the moment t, knowing that at time t' < t breakage does not occur. The term $\lambda_0(t)$ is named *basic risk* (in fact is the same for all analyzed rock samples at a given time), it is time dependent and corresponds to instantaneous risk of breakage when all of covariables are null; what is important for us is the ratio of instantaneous risk of breakage of two samples of the same type of rock exposed to different risk factors. The second term on the right side of the relationship (1) is independent of time. From the relationship (1) results hypothesis of proportional risks, that in fact is an essential hypothesis of Cox's model. In other words, assuming two rock samples that differ only by a single covariable, either this X_k, this covariable taking the values 0 and 1 for the two specimens (0 for the first specimen and 1 for the second), then whatever time t, a rock specimen had an instantaneous risk of breakage $\exp(\beta_k)$ times higher compared to the other specimen considered; namely, for any time t, the risks ratio is independent of time; the term $\exp(\beta_k)$ cannot be interpreted as a relative risk.

Rocks breakage could be analyzed by means of two models: Cox's proportional hazard model and Cox's proportional hazard model with time dependent covariates. Cox's proportional hazard model assumes establishing the strength function of rock defined by probability:

$$S(t) = P\{T > t\} \quad (2)$$

where: t is generally the time; T is the time until breakage.

Distribution of strength duration is:

$$F(t) = 1 - S(t) \quad (3)$$

where: $f(t)=\frac{d}{dt}F(t)$ represents breakage rate of rock samples per unit of time.

From the point of view of mechanics rocks, we define the function of hazard as the risk of a rock to break away in a very short time *dt*, after a certain period of time T (assuming that until that moment the rock resisted); the function of hazard can be expressed according to the relationship:

$$\lambda(t)=P(t<T<t+dt)=\frac{f(t)\,dt}{S(t)}=-\frac{S'(t)\,dt}{S(t)} \quad (4)$$

Graphically, the strength curve of rock represents the cumulative strength curve with respect to time, and the derivative of strength curve will be the rate of occurrence of breakage in a short interval of time; this will be the hazard, namely a risk, and the ratio of hazards will be the relative risk. The hazard or risk can change in time, as meaning that it can increase or decrease, depending on certain factors (for example, the higher the time from appearance of cracks is, the higher the risk of breakage is).

Through regression or Cox model we can estimate the effect that in case of underground works, the applicability of consolidation method or improvement of rocks resistance characteristics on their contour, chosen in accordance with other independent variables (or factors) and so, we have the possibility to estimate the hazard (or the risk) of breakage or other event (or phenomenon) that would present interest, given their prognostic variables. In case that the analyzed rock samples (samples which were submitted to an improvement of the mechanical properties and the sample blank) are similar as regards the known variables that influence their strength capacity, the Cox model used for these variables will produce a more precise appraisal of the effect of increasing rock strength [19].

Proportional hazard model or Cox model is not based on any hypothesis regarding the distribution of strength, it is based on the assumption that the hazard is a function only of independent variables (predictive, covariates) $Z_1, Z_2, \ldots, Z_k$:

$$h(t; Z_1, Z_2,..., Z_k)=h_0(t)\cdot \exp(b_1\cdot Z_1+b_2\cdot Z_2+...+b_k\cdot Z_k) \quad (5)$$

That by applying the logarithm, becomes:

$$\ln\left(\frac{h(t; Z_1, Z_2,..., Z_k)}{h_0(t)}\right)=b_1\cdot Z_1+b_2\cdot Z_2+...+b_k\cdot Z_k \quad (6)$$

$$\Rightarrow \ln\left(\frac{h(t; Z_1, Z_2,..., Z_k)}{h_0(t)}\right)=\sum_{i=1}^{k} b_i\cdot Z_i$$

From this relationship it can be found that this is a semi-parametric model [7, 12]. The parameter h (t, Z) could be considered as a Weibull type density distribution, because [20]:

$$h(t, Z)=\lambda\cdot p\cdot t^{p-1} \quad (7)$$

where:

$$\lambda=\exp(b_1\cdot Z_1+b_2\cdot Z_2+...+b_k\cdot Z_k)$$
$$\text{or}\quad \lambda=\exp\left(\sum_{i=1}^{k} b_i\cdot Z_i\right) \quad (8)$$
$$h_0(t)=p\cdot t^{p-1}$$

$h_0(t)$ is named *basic hazard* and represents the hazard of a certain subject (specimen of rock) when all independent variables are equal to zero and, as it can be observed, it depends only on time t; the exponential refers only to $Z = (Z_1, Z_2, \ldots, Z_k)$ and also to variables Z_i that are independent of the time t (examples of variables that are time independent in the field of rock mechanics, would be: genesis of analyzed rock, rock sample weight; …). As shown in the scientific literature [8-10, 13, 15, 16], Cox's model is preferred to be used, since it appears that it would be one of the safest methods in many situations. The estimated hazards are positive, and if the term $h_0(t)$ cannot be specified, then it is possible to determine the hazard rate, HR, given by relation:

$$HR=\frac{h(t, Z^*)}{h(t, Z)} \quad (9)$$

where: $Z^*=(Z_1^*, Z_2^*, \ldots, Z_k^*)$ and Z = (Z_1, Z_2, …, Z_k).

To ease and simplify the interpretation [20], it is considered that HR ≥ 1, which means that:

$$h(t, Z^*)\geq h(t, Z) \quad (10)$$

It is considered Z* as a rock of Ist type (a population consisting of samples belonging to the Ist type of rock) having the higher risk of breakage (the hazard), respectively, Z representing a rock of IInd

type with lower risk of breakage (we can consider that for the II[nd] type it was applied a method of increasing rock strength). Taking into account the conditions:

- between $h_0(t)$ and log-liniar function of covariates, there must exist a multiplicative relationship, namely respecting the hypothesis of proportionality from the point of view of hazard;
- between hazard and independent variables there must exist a log-liniar relation, we obtain the hazard rate as being:

$$HR = \frac{h_0(t)\cdot \exp\left(\sum_{i=1}^{k}\beta_i \cdot Z_i^*\right)}{h_0(t)\cdot \exp\left(\sum_{i=1}^{k}\beta_i \cdot Z_i\right)} \qquad (11)$$

$$HR = \exp\left[\sum_{i=1}^{k}\beta_i \cdot \left(Z_i^* - Z_i\right)\right]$$

For example, if we consider the relation (6), we can use the predictive value of model by means of prognostic index (IP), defined as:

$$IP = b_1 \cdot Z_1 + b_2 \cdot Z_2 + ... + b_k \cdot Z_k$$
$$IP = \sum_{i=1}^{k} b_i \cdot Z_i \qquad (12)$$

Further, it can be established the function of strength or the function of maintaining the rock capacity to resist and not manifest the breakage:

$$S(t) = \exp\left[-H_0(t)\right]^{\exp(IP)} \qquad (13)$$

Where $H_0(t)$ represents cumulate basic hazard [6, 20] and is a variable of scale function.

3. Estimating coefficients

To establish the coefficients $\beta_i \mid_{i = 1, ..., k}$, the maximum probability method is applied; the likelihood of a representative group of a population is actually the probability to observe intuitively this group, namely it aims at its maximizing [8, 9, 11-13, 20]. In this aim, we will consider a group of independent data, whose notations are:

- X_i column vector of covariates of rock sample i (that could depend on the time);
- β column vector of β_i coefficients;
- $t_i \mid_{i = 1, ..., m}$ breakage times;
- d_i number of breakage at time t_i;
- D_i all breakages at time t_i;
- r_i number of rock samples with breakage risk at time t_i;
- R_i all samples with breakage risk at time t_i.

The probability that a sample will break at time t_i is:

$$p = \lambda_0(t_i)\exp\left(X_k^t\ \beta\right)dt \qquad (14)$$

At time t_i the probability of all samples belonging to D_i will be [6]:

$$p_{t_i} = \frac{\exp\left(\beta^t\right)^{\sum_{k\in D_i} X_k}}{\left[\sum_{l\in R_i}\exp\left(\beta^t\ X_l\right)\right]^{d_i}} \qquad (15)$$

Cox's probability function (partial) can be written as being [6]:

$$L(\beta) = \prod_{i=1}^{m}\frac{\exp\left(\beta^t\right)^{\sum_{k\in D_i} X_k}}{\left[\sum_{l\in R_i}\exp\left(\beta^t\ X_l\right)\right]^{d_i}} \qquad (16)$$

This is reduced to solve the equation (16), so as $L(\beta)$ is maximum; the value for which the function L reaches the maximum will represent the probability of the representative group considered.

4. Results and discussions

In the Laboratory of Geomechanics of the University of Petrosani it was studied a number of 37 salt cylindrical samples, having the fineness ratio $\lambda \cong 1.5$; the tests were conducted at monoaxial compression, following also time at which the breakage of salt samples was manifested (Figure 2). Taking into account the number of samples submitted to the tests, we chose a number of 18 salt samples for which we realized the statistical analysis of the influence of the rock strength on the breakage time. Analysis can be done either by t-test or using the ANOVA techniques [1, 2, 10, 13] or by dispersion analysis, respectively analysis of variance.

t-test is somehow limited because of realizing only a comparison of the differences between two groups. T-test is a method by means is only done comparing differences between two groups, so it is reduced just to those situations where there are only two ways of the independent variables; if applied, this method in case of more independent variables, then statistical errors or the error of the set of comparison increase each time when are applied for each of the possible pairs of two ways.

On the other hand, if we have a larger number of independent variable levels, then it is necessary to apply other techniques so that the effect of independent variable on the dependent once will be expressed by a higher degree of fineness [10], for example the ANOVA technique. To apply this technique, the first stage was to identify the possible method to be applied; available data are quantitative, thus the problem is reduced to the comparison of the averages of two populations (the time when the breakage occurs and the monoaxial compressive breaking strength of salt samples).

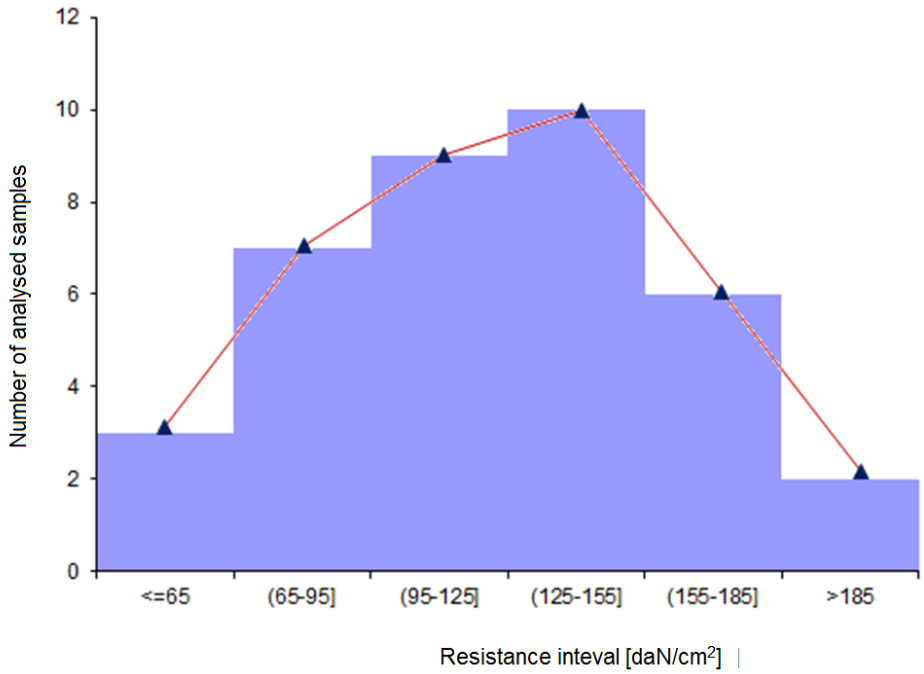

Fig. 2. *Histogram variation of compressive strength of analyzed salt specimens*

Table 1. *t-Test: Paired Two Sample for Means*

	Variable 1	*Variable 2*
Mean	159.4444	63.46035
Variance	21165.56	2935.414
Observations	18	18
Pearson Correlation	0.993908	
Hypothesized Mean Difference	0	
df	17	
t Stat	4.43462	
P(T<=t) one-tail	0.000182	
t Critical one-tail	1.739607	
P(T<=t) two-tail	0.000363	
t Critical two-tail	2.109816	

The fact that the analysis of these data proves that the two averages are different, means that we can apply the analysis of variance with one factor. The aim of the covariance analysis is to eliminate a number of external factors that cannot be identified, so that the effect of the independent variable can be clearly highlighted. Simple or unifactorial ANOVA analysis is a simple model considered to be a corresponding t-test for two independent specimens. Factorial ANOVA analysis is most often used, it is considered a more complex model and by this technique are tested the effects of several independent variables (or factors) on a dependent variable. In table 2 are presented the results obtained by statistical processing of experimental data, applying the ANOVA analysis of variance, simple or unifactorial (single factor), and in Table 3 are shown the results obtained by statistical processing applying the ANOVA factorial analysis of variance. In Table 2, in the area SUMMARY, are mentioned the data related to the two populations: number of units from each population, namely 18; the amount for each population; variance of population. It is observed that the smallest average and the highest dispersion were registered in terms of compressive breaking strength. In the area ANOVA from Table 2, is computed the statistics F for the unifactorial variance analysis, its value being 6.880762; in Table 3 the statistics F for variance factorial analysis is equal to $F_{calculat}$ = 4.716186729. Because $F_{calculat}$ = 6.880762 > F_{crit} = 4.130018, respectively $F_{calculat}$ = 4.716186729 > F_{crit} = 2.271893, it follows that we reject the null hypothesis H_0 and accept the alternative hypothesis H_1 as a true one. Therefore, it can be said with a probability of 95 % that the compressive strength of salt samples influence significantly time variation until their breaking occurs.

Table 2. *Summary output and ANOVA analysis Single Factor*

SUMMARY						
Groups	Count	Sum	Average	Variance		
Time until breakage	18	2870	159.4444	21162.56		
Compressive breakage strength	18	1142.286	63.46035	2935.414		
ANOVA						
Source of Variation	SS (sum of squares)	df	MS (mean square)	F	P-value	F crit
Between Groups	82916.5129	1	82916.51	6.880762	0.012949	4.130018
Within Groups	409716.4878	34	12050.48			
Total	492633.0007	35				

Table 3. *Summary output and ANOVA Two-Factor Without Replication*

Source of variation	SS	df	MS	F	P-value	F crit
Rows	338039.9476	17	19884.7028	4.716186729	0.001292	2.271893
Columns	82916.51289	1	82916.51289	19.66585881	0.000363	4.451322
Error	71676.54019	17	4216.26707			
Total	492633.0007	35				

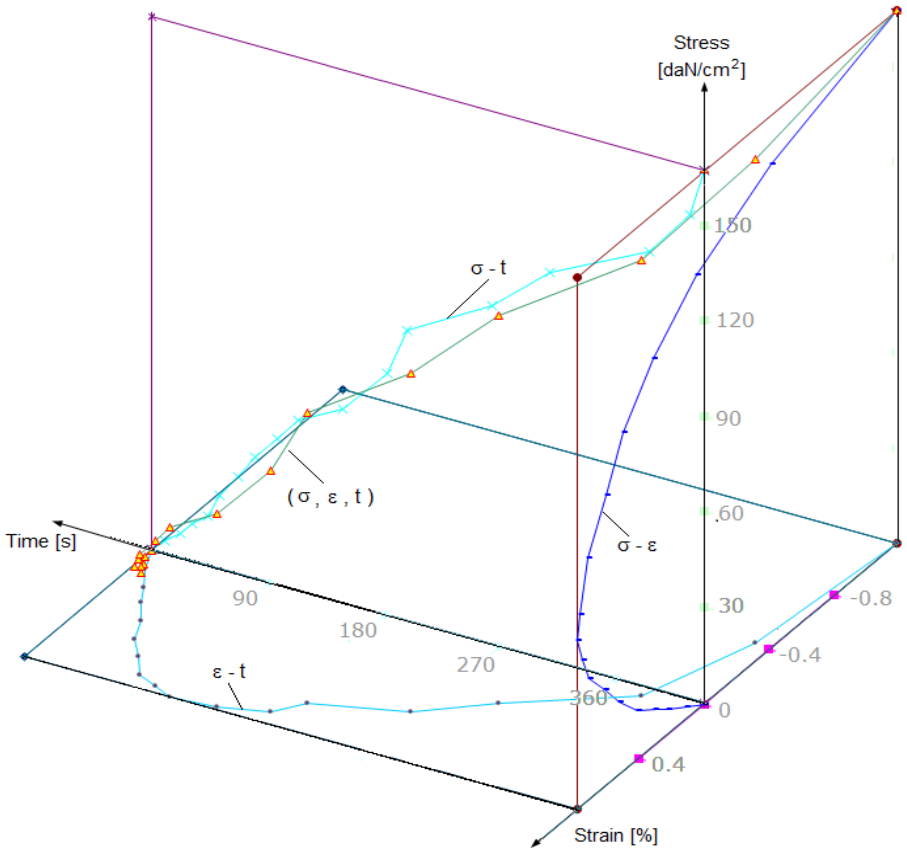

Fig. 3. *The curve of Cox's proportional hazard model*

For a confidence-associated range equal to 0.05 %, the hazard rate depends on the compressive breaking strength value of salt. Applying Cox's regression method, considering as interest variable the value of compressive strength and the other constant variables, for the Cox's regression the hazard rate shows that the variation of this characteristic value leads to the change of hazard rate. The calculus

showed a hazard rate HR = 3.01 > 1, which means that the decreasing compressive breaking strength leads to increased risk of occurrence of breakage and reduces the time of manifestation of this phenomenon (p-value = 0.1234). In Figure 3 is shown the Cox curve obtained from processing of experimental results.

5. Conclusions

Cracking changes significantly certain properties of rocks cracking (for example, permeability to fluids, damping of acoustic waves); other properties may be less affected by this phenomenon (density, the modules of elasticity for stress that maintain the cracks closed). The variation of volume during a mechanical testing is an effective indicator of cracking; for example, dilatancy and microcracking lead to a significant increase of permeability of rock salt and consequently, the initial tightness of intact salt is reduced. From the macroscopic point of view, cracking is characterized by dilatancy due to micro-cracking and relative displacements of grains and fragments, namely an increase of permeability, and also presenting sensitivity to the change of loading rate.

The method of the classical analysis of time in which a rock resists and breakage does not occur cannot be used if we want to analyze which is the simultaneous effect of several variables on the time where there is no possibility for breakage to occur. The multiple regression method cannot be used directly, because the variable describes time until breakage has not normal distribution, but an exponential distribution or Weibull type due to the fact that in any case there is a possibility that the breakage occurs; for this analysis of time resistance, we often do not have complete information. Therefore, in order to carry out such analysis, we suggested using a regressive method, as Cox's proportional hazad model; the same analysis can be also carried out on the basis of Cox's proportional hazard model with time – dependent covariants. By applying the Cox model or proportional hazards regression we have the possibility to predict the occurrence of relative risk (potential risk) of rocks breakage based on several variables, risk (hazard) which may have a different variation, either in the sense that it can increase over time either it may decrease; if at times there is no variable or factor leading to an evolution towards rock breakage, then the risk of breakage is lower. Cox method offers information regarding the effect of certain factors (variables) - extrinsic or intrinsic - on the time resistance of rock after adjusting the other independent variables; this method offers the possibility to assess the hazard or risk of rock breakage.

Salt presents a specific behavior under the effect of cracking phenomenon. Preexisting cracks or the ones caused by stresses could be developed and microscopically determine a change in volume, namely dilatancy; the cracking phenomena is irreversible. Dilatancy is a phenomenon that constitutes the effective indicator of the occurrence of cracking, leading to a significant increase of permeability of salt and consequently to the diminishment of its initial tightness; therefore, it can't be neglected in stability analysis of underground works executed in salt massive [18].

Through regression or Cox model we can estimate the effect that in case of underground works, the applicability of consolidation method or improvement of rocks resistance characteristics on their contour, chosen in accordance with other independent variables (or factors) and so, we have the possibility to estimate the hazard (or the risk) of breakage or other event (or phenomenon) that would present interest, given their prognostic variables. The higher the hazard is, the higher the risk of breakage is; other factors could also interfere here, and that could determine another event that could be produced (for example a growth of temperature or humidity, in case the analyzed sample is a salt one).

In horizontal plan (see Figure 3), the Cox curve projection expresses the strains variation corresponding to the breaking time of salt samples; the Cox curve projection in lateral plan expresses the strains variation corresponding to the appearance of breakage related to compressive strength. The results obtained by means of Cox proportional hazard model are in accordance with the nomogram for evaluation of behavior at deformation under load of rocks until the occurrence of breakage (see Figure 1) [17, 18].

References

[1]. Armitage P., Berry G., Matthews J. N. S., *Statistical Methods in Medical Research* (4th Edition), Oxford: Blackwell Science, 2001.
[2]. Armitage P., Berry G., *Statistical Methods in Medical Research* (3rd Edition), Blackwell, 1994.
[3]. Barlow W. E., *Robust variance estimation for the case-cohort design*. Biometrics., 50, p. 1064-1072, 1994.
[4]. Barlow W. E., Ichikawa L., Rosner D., Izumi S., *Analysis of case-cohort designs*, Journal of Clinical Epidemiology, 12, p. 1165-1172, 1999.
[5]. Bieniavski Z. T., *Mechanism of brittle fracture of rock*, Int. J. of Rock Mech. and Min. Sci., no. 4, 1967.
[6]. Cox D. R., *Partial Likelihood*, Biometrika, vol. 62, p. 269-276, 1975.
[7]. Dennis E. Hinkle, William Wiersma, Stephen G. Jurs, *Applied Statistics for the Behavioural Sciences*, Boston, Published by Houghton Mifflin (Academic), 3rd Edition, p. 706, ISBN 10: 0395675553, 1994.
[8]. Gorunescu F., Gorunescu M., *Analiza exploratorie şi procesarea datelor cu simulări în Matlab*, Editura Albastra.

[9]. Gorunescu F., Gorunescu M., *Modele regresive*, math.ucv.ro/~gorunescu/courses/EDA/curs2EDA.pdf.
[10]. Hinkle D. E., Wiersma W., Jurs S. G., *Applied statistics for the behavioral sciences* (3rd), Boston, USA, Houghton Mifflin Company, 1994.
[11]. Lin D. Y., *Cox Regression Analysis of Multivariate Failure Time Data: The Marginal Approach*, Statistics in Medicine, vol. 13, p. 2233-2247, 1994.
[12]. Keppel G., *Design and analysis: a researcher's handbook* (3rd ed.), Englewood Cliffs, USA: Prentice-Hall Inc, 1991.
[13]. Kleinbaum D. G. *et al.*, *Applied Regression Analysis and Other Multivariable Methods* (3rd Edition), Duxbury Press, 1998.
[14]. Radu I., Miclea M., Albu M., Nemeş S., Moldovan O., Szamoskozi Ş., *Metodologie psihologică şi analiza datelor*, Cluj-Napoca: Editura Sincron, 1993.
[15]. Schoenfeld D., *Partial Residuals for The Proportionnal Hazards Regression Model*, Biometrika, vol. 69, p. 239-241, 1982.
[16]. Spiekerman C. F., Lin D. Y., *Marginal Regression Models for Multivariate Failure Time Data*, Journal of the American Statistical Association, vol. 93, p. 1164-1175, 1998.
[17]. Toderas M., *Mecanica rocilor, pământurilor şi construcţii subterane*, Editura Universitas, Petroşani, ISBN 978-973-741-381-9, 1167 p., vol. I, ISBN 978-973-741-382-6, vol. II, ISBN 978-973-741-383-3, 2014.
[18]. Toderas M., *Cercetări şi rezultate în stabilitatea lucrărilor miniere subterane*, Editura Universitas, Petroşani, ISBN 978-973-741-486-1, 343 pages, 2016.
[19]. Toderaş M., Danciu C., *Analysis Possibilities of Rocks Breakage by Means of Proportional Hazard Regression*, 7th International Multidisciplinary Symposium „Sustainable Development through Quality and Innovation in Engineering and Research" SIMPRO 2016, Universitatea din Petroşani, p. 299-302. ISSN–L 1842-4449; ISSN 2344-4754, 2016.
[20]. Ying Z., Wei L. J., *The Kaplan-Meier Estimate for Dependent Failure Time Observations*, Journal of Multivariate Analysis, vol. 50, p. 17-29, 1994.

THE ANNALS OF "DUNAREA DE JOS" UNIVERSITY OF GALATI
FASCICLE IX. METALLURGY AND MATERIALS SCIENCE
N°. 4 - 2016, ISSN 1453 – 083X

STATIC AND DYNAMIC ANALYSIS OF STRESS AND DEFORMATIONS OF RĂSTOLIŢA DAM

Mihaela TODERAŞ[1], Ciprian DANCIU
University of Petrosani, Faculty of Mines, 20 Universitatii, Petrosani-332006, Romania
e-mail: toderasmihaela@yahoo.com, danciu_ciprian@yahoo.com

ABSTRACT

Large Dams are a particularly important case of seismic risk assessment. On the one hand, the dams themselves have a high value, having implications for the whole economy, through the production of electricity, water supply systems for irrigation and flood prevention etc. On the other hand, structural damage of a dam can lead to major disasters, the population exposure to effects caused by sudden floods. The situation in Romania is such that attention should be paid to the future safety of existing dams. The first reason is that these dams were designed and constructed on the basis of technical rules, which the majority are no longer in force; a second reason is the major climate changes in the last period, which have led to the accumulation of a large volume of water in increasingly large lakes. A third reason is, logically, the length of existing dams. In this paper is analysed the stress - deformation state that occurs in Răstolița dam body according to the type of rockfill; calculations were done for two cases, namely the completion of construction and, respectively, at the first filling of dam with water. The results show that after completion of construction, the maximum settlement is recorded in the central area of the dam, below the middle third; horizontal displacements of downstream prism are significantly higher compared to deformations of the upstream prism, in the area where the used material has a higher compressibility. Maximum principal normal stress registers some local distortions within acceptable limits; minimum principal normal stress presents important gradients in the contact zone downstream dam slope in the Ist stage with tuff-pyroclastic embankment layer and also in the first three layers of intercalated filling disposed near the slope. Stress increases due of hydrostatic pressure after the first filling does not lead to occurrence of stress concentrations in other zones than those reported at the completion of construction.

KEYWORDS: dam, static analysis, dynamic analysis, stress, deformations

1. Geological and geotechnical characteristics of dam emplacement

The dam was conceived as having 38 million m^3 available storage of water, which is done with a normal retention to the elevation 760 mdM, to minimum geometrical dimensions, to assure the hydroelectric power functionality of hydrotechnics schema. The solution proposed for Răstoliţa dam was to realize an impounding with normal retention level at 720 mdM, imposed by elevation and hydraulic load conditions of the adduction - energetic tap at elevation 700 mdM [9]. In order to optimize through the constructive solutions and investment parameters, the achievement in stages of Răstoliţa dam was provided; in the first stage, this was achieved with normal retention to elevation 720 mdM. To create the conditions of achieving the storage reservoir of the stipulated parameters, namely the retention level to the elevation 760 mdM, all parts afferent to the dam were sized according to the resistance and hydraulic criteria corresponding to the dam with normal retention (NNR) to the 760 mdM elevation. The dam is under construction on Răstoliţa river, right tributary of Mures, in the area of Topliţa – Deda clough. The constructive solution of Răstoliţa dam is rockfill dam with reinforced concrete apron (lutting wall) [1-3]. Data concerning the geology and hydrogeology of the studied area have highlighted that the rocks of Răstoliţa dam emplacement are composed of volcanic

agglomerates (pyroclastics) and of volcanic ashes, where, locally, it intercalates hard cracked andesite and sometimes altered. There were analysed the rocks intercepted by drillings F2 and F4 (see Figure 1), rocks consisting of pyroclastics appearance microconglomeratic, about 87 % of samples, volcanic ash cemented, about 7 % and andesites in a percentage 6 % [9].

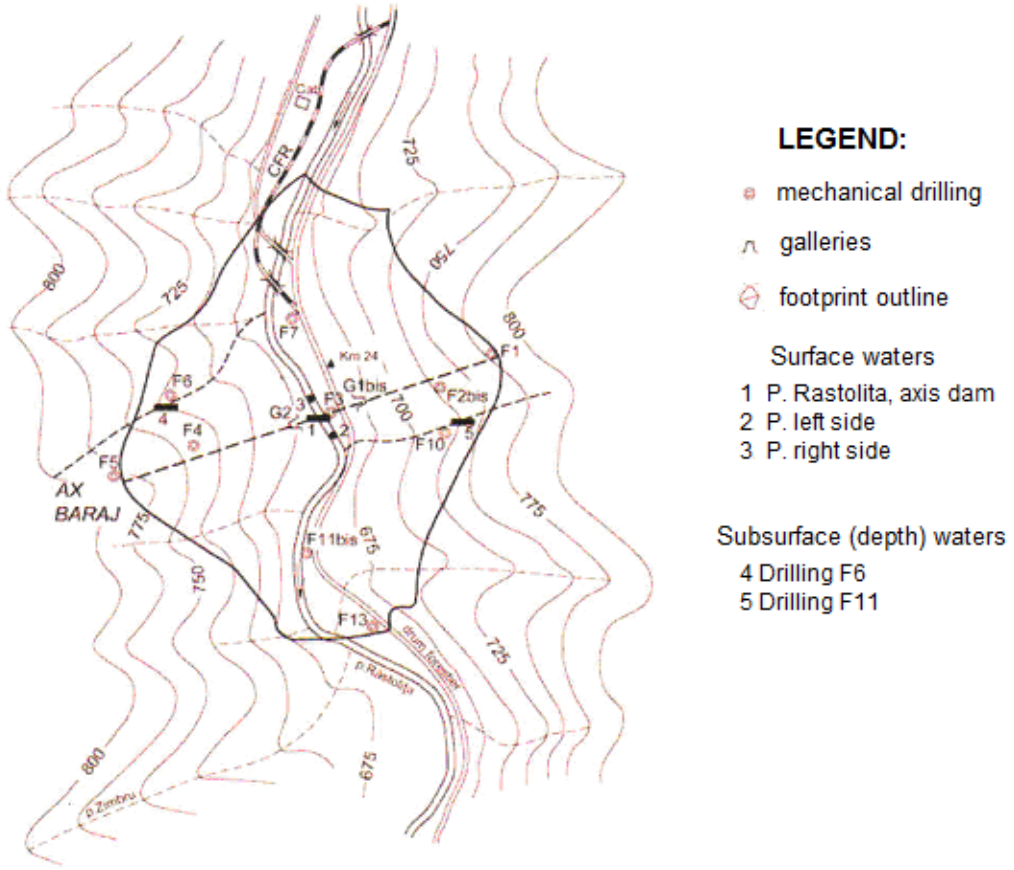

Fig. 1. *Map of drillings of rock' sampling*

Compared to the studied samples from drillings F3 and F7, where the percentage of rocks types mentioned above were 70 %, 12 % and 18 %, in drilling F2 have been identified pyroclastics areas that were more altered with a reddish rusty colour, cracked and damaged. The number of processed and studied samples and specimen from F2 and F4 drillings were:

a) drilling F2, from 2 m to 47.3 m; 26 samples; 73 specimens;

b) drilling F4, from 7.3 m to 21.2 m; 9 samples; 21 specimens.

Laboratory tests consisted in determining the following geotechnical characteristics: apparent specific density, porosity, absorption of water at normal pressures and temperatures, compressive breakage strength, shear breakage strength, velocity propagation of sonic waves, static and dynamic modulus of elasticity, dynamic Poisson's coefficient.

For all laboratory tests, samples provided from drillings have been processed by core drilling machine equipped with diamond disc and water cooling system. The shape and size of specimens were those indicated by standards, namely, there were carried out cubic samples with a side dimension of 5 cm, respectively, prismatic samples with dimensions of 4 x 4 x 16 cm, respecting the test methodology according to standards. The values of physical – mechanical and elastic characteristics are shown in Table 1. The values obtained show that the rocks provided from drillings F2 and F4 of Răstoliţa footprint dam, left side and right one, have similar characteristics with rocks intercepted by drillings F3 and F7, dam - bottom footprint, drawing in ranges of variation shown in Table 1, where between brackets are given the values obtained in stage I of research, drillings F3 and F7.

By analysing these values, it is noted a wide range of variation of characteristics established in

laboratory, especially for pyroclastics and volcanic ashes, which cannot be correctly separated as kind of petrographic types. In very different percentages in same pyroclastic sample occur fragments of andesite (as number and size) relating to cementing material composed of volcanic ash. Moreover, for samples resulted from cores extracted from F2 drilling also appear altered pyroclastics areas, identified between 2.00 m and 20.00 m which contributes to diminishing of mechanical characteristic values.

Table 1. *Variation range of geotechnical characteristics of rocks from Răstoliţa dam area*

No	Geotechnical characteristic		Rock and variation range of characteristic		
			Pyroclastic	Volcanic ashes	Andesite
1.	Specific density, g/cm^3		2.73 – 2.76 (2.72)	2.73 (2.70)	2.81 (2.80)
2.	Apparent specific density, g/cm^3		1.58 – 2.66 (1.90 – 2.40)	1.76 – 2.01 (1.53 – 1.99)	2.20 – 2.48 (2.3 – 2.73)
3.	Porosity, %		13.0 – 34.0 (11.0 – 30.0)	27.5 – 28.5 (26.0 – 40.0)	12.5 – 16.2 (3.0 – 10.0)
4.	Absorption of water at normal pressures and temperatures, %		5.4 – 21.5 (2.2 – 13.7)	- (3.65)	1.5 (0.8 – 5.2)
5.	Compressive breakage strength of rocks in natural state, daN/cm^2		27 – 220 (50 – 300)	89 – 155 (100 – 150)	280 (300 – 1170)
6.	Shear parameters	φ, grade	13 – 42 (15 – 43)	40 (10 – 40)	- (17 – 34)
		C, daN/cm^2	14.9 – 49.3 (4.2 – 50.0)	12.2 (16 – 30)	- (170 – 265)
7.	Longitudinal velocity of sonic wave, m/s		1700 – 4100 (1,300 – 3,600)	2,200 – 2,600 (1,600 – 2,500)	4,400 – 4,700 (2700 – 4,400)
8.	Static modulus of elasticity, daN/cm^2		57,000 – 12,4000 (33,000 – 190,000)	5,500 – 39,600 (-)	51,0000 (447,000 – 640,000)
9.	Shock strength, daN/cm^2		(6 – 12)	(-)	(-)

2. Răstoliţa dam characteristics

Răstoliţa dam is under construction, on the river with the same name, right affluent of Mureş River, in the area of Topliţa – Deda Clough. The solution proposed and approved for achieving this dam is of rockfill, with reinforced concrete apron; the characteristics of dam are presented in Table 2.

Dam body is made of rolled rockfill in layers of 1 m. In cross profile of transversal type, from upstream to downstream, the following zones were adopted:

1.B. – *rockfill protection layer* made in the upstream face of protection prism;

2.B. – *dusty – clayey material* in upstream prism, with the role to prevent the infiltrations by any accidents to the joint fireplace – concrete apron, in the most loaded region of dam;

1.A. – *reinforced concrete apron*. Reinforced concrete apron designed for Răstoliţa dam is a reinforced concrete element of variable thickness between 0.30 m to crest of wave and 0.50 m to the lowest level of concrete apron, namely to 662.00 mdM. On the dam height, the thickness variation of concrete apron is linear:

$$t = 0.30 + K\,H \quad [m] \qquad (1)$$

Table 2. *Main characteristics of Răstoliţa dam*

Crest of wave level (mdM)	Large dam (crest of wave at 765 mdM)	Dam – IInd stage (crest of wave at 725 mdM)
Maximum height, m	103	63
Crest of wave length, m	320	240
Total volume of dam, m^3	3400,000	895,000
Ist type rockfills - andesite, m^3	1580,000	795,000
Support layer concrete apron, m^3	87,000	37,000
Transition layer, m^3	104,000	34,000
Other zones (upstream prism, downstream protection), m^3	129,000	29,000

Where: t is the concrete apron thickness; K = 0.002; H – depth measured from the maximum water level, that in case of Răstoliţa dam is 103 m (H = 765 – 662 = 103 m).

Between reinforced concrete apron and rockfill prism are provided two zones, namely:

2.A. *Support layer of concrete apron*: crushed material graded Φ = 0 – 70 mm, and the coefficient of permeability K = 10^{-3} – 10^{-4} cm/s. The role of this zone is:

a) to ensure uniform and resistant support of reinforced concrete apron;

b) to avoid deviations from the theoretical profile of reinforced concrete apron;

c) by controlled distribution of sizes, it ensures a semi-permeable barrier that prevents the important infiltrations, even in case of preferential leak paths in cracks of concrete or defects joint sealing of reinforced concrete apron.

Composition of zone ensures the workability on layer.

3.A. *Transition layer from crushed material* graded Φ = 0 – 300 mm, and the coefficient of permeability K = 10^{-2} cm/s. Zone 3A works as an inverse filter between zone 2A and rockfill and also has the role to ensure free drainage of eventual water infiltrated by zone 2A.

3.B. *Quarry rockfill type I (andesite)* deposited in layers of 1 m.

Faces of wall slopes of resistance prisms are established based on verifying calculations through stability, deformations and stresses, having the following values:

Upstream	1:1.4 until level 1:2.5 until thalweg from 600 mdM and until thalweg situated at approximatively level of 622.00 (the prism is carried out after constructing dam concrete apron)
Downstream	1:1.7

Downstream face slope is a theoretical slope, without taking into account the access road that is carried out on the downstream face.

In order to achieve Răstoliţa dam, the followings have been considered:

- crest of wave level, 725 mdM
- NNR, 720 mdM
- V_{lake} = 6.5 mil. m^3
- $V_{embankment}$ = 889.176 m^3

In order to achieve the calculations, for the characteristics of component materials of embankment were used theoretical values shown in Table 3.

***Table 3**. Theoretical values of materials characteristics of embankment*

Material	Material characteristics				
	$E_s(x)$, [tf/m^2]	$Y_d(x)$, [tf/m^2]	μ(x)	Φ [degree]	C, [tf/m^2]
Support layer Φ = 0 – 70 mm, K = 10^{-3} – 10^{-4} cm/s	7,000	2.0	0.30	37.5	2.0
Transition layer Φ = 70 – 300 mm, K = 10^{-2} – 10^{-3} cm/s	5,000	2.0	0.30	37.5	2.0
Rockfill sorted drain	5,400	2.02	0.35	37.5	3.1
Rockfill type I (andesite)	5,400	2.02	0.35	37.5	3.1
Rockfill type II (pyroclastic)	3,000	1.72	0.30	33.5	4.4
Protection rockfill type	5,400	2.02	0.35	37.5	3.1
Dusty-clayey local material	1,900	1.46	0.40	9.0	11.2
Alluvium and altered pyroclastics (xx)	100,000	1.8	0.36	-	-
Unaltered pyroclastics (bedrock) (xx)	150,000	2.05	0.31	-	-

3. Limiting solutions of support deformations of concrete apron dam

Adopted solutions are considering limiting the deformations of concrete apron support to values that can be taken over by reinforced concrete element, Fig. 2 – Fig. 5. Essentially, dam deformations are shown out below.

Fig. 2. *Solution to achieve the dam concrete apron*

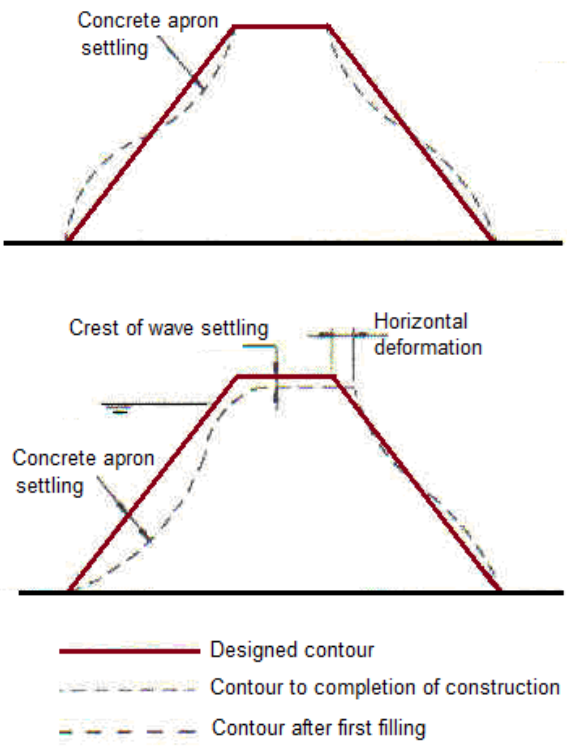

Fig. 3. *Diagrams of deformation for rockfill dam (according to Mori, 1999)*

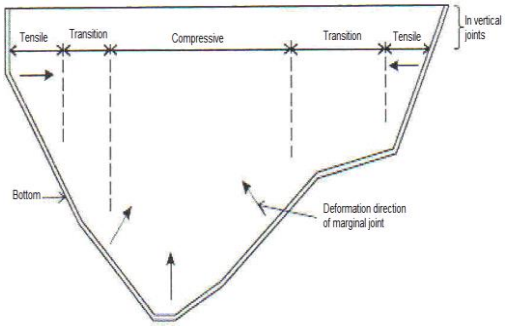

Fig. 4. *Upstream view of dam concrete apron: deformation directions and stresses types that appear*

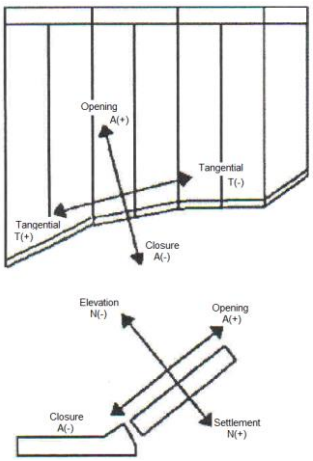

Fig. 5. *Deformation directions of marginal joint*

3.1. Static analysis of stresses and deformations

The existence of an important layer of tuff as lower quality rock from Albu rockfill quarry, which must be removed or used in a certain way, in order to enable its continuing exploitation, imposed the achievement of specific calculations of efforts and deformations, calculations to model the use of tuff in an appropriate zone of the dam body and the impact on the behavior at the first filling, namely the behavior in current exploitation [4-7]. Thus, it was modelled the use of tuff deposited in layers of 0.75 m thickness in the downstream prism of 3C zone of dam, intercalated with pyroclastic layers, operation that seeks a massif with better physical - mechanical characteristics than the weakest material, appropriate to the structure and stresses state from the area of deposit [6-8]. Analysis took into account the following:

- assessing horizontal and vertical movements during depositing the fillings layers from dam body at the end of construction and at the first filling of lake;
- assessing through static and dynamic stresses and deformations state in dam body;
- Establishing the maximum number of layers, its geometrical positioning and assessing stress and deformations state so that whole dam presents a good behavior without stress concentrations or the occurrence of plastic parts in all stages of analysis.

Stress and deformations state analysis in body dam was carried out by assuming nonlinear - elastic (hyperbolic) behavior of the material of dam body based on Duncan – Chang model, which admits elastic - plastic Mohr – Coulomb failure criterion. Hyperbolic characteristics obtained from triaxial tests both with determining of shear and Duncan - Chang parameters of volcanic tuffs were analysed by GEOTEC, the purpose of these determinations being motivated by the planning works of quarry on Albu creek which revealed layers of material with unexplored qualities until then have, namely volcanic tuff. Through the same study, were also supplied the basic static and dynamic geotechnical parameters of material from the rockfill quarry (Fig. 6).

Calibration of secant modulus for andesites and pyroclastics was made from curves analysis of vertical stresses - specific deformations by interpreting the measurements from DVT placed in the filling carried out at given time in dam footprint.

Peer values of stress – vertical specific deformation appropriate of fillings level allowed plotting stress - deformation curves for both prisms. In the first phase, secant modulus of rockfill resulted directly from plotted curves that have proved very low values due to the fact that calculated specific deformations include also deformations from creep; this is the consequence of slow execution and big breaks to achieve the fillings.

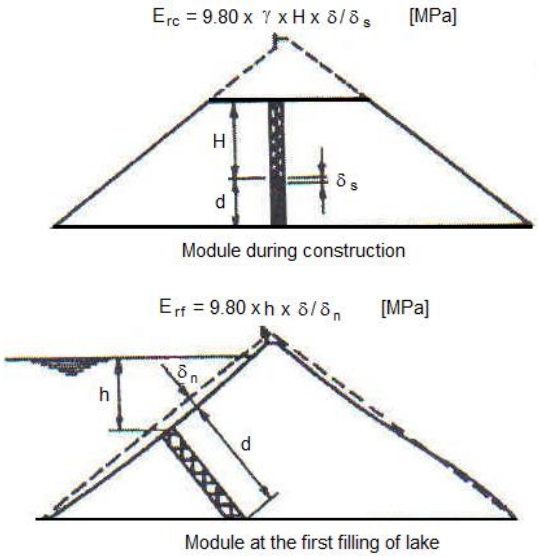

Fig. 6. *Rockfill modulus defining E_{rc} and E_{rf} (according to Fitzpatrick et al., 1985)*

Model calibration and the choice of final secant modulus were carried out admitting certain instantaneous specific deformations affected with (40 – 70 %) from measured total deformation; within a certain error, parametrical calculation have validated the adopted model (Table 4, Table 5, Fig. 7).

According to geotechnical study, all rockfill types (andesites, pyroclastics, volcanic tuff) are characterized by a wide range of variation of physical - mechanical characteristics; this is a reason why in calculations it was associated with a set of pessimistic values of basic geotechnical parameters (bulk density, angle of internal friction, static and dynamic Poisson's coefficient) and also Duncan – Chang parameters for volcanic tuff already established from geotechnical study developed by GEOTEC (Fig. 8).

Table 4. *Laboratory tests results*

σ [kN/m^2]	$\varepsilon_{instantaneous}$	E_{def} [kN/m^2]	ε x 1000
14.52	0.0002	72,600	0.20
29.05	0.0004	72,625	0.40
43.57	0.000575	75,774	0.575
56.02	0.000725	77,269	0.725
72.61	0.0009	80,678	0.90

Table 5. *Determining the initial tangent modulus of deformation - measured values of vertical settlement cells (CV)*

Plaque	Settlements Time [months] 0	7	10	h [m]	Deformations ε = Δh/h [mm]	$\varepsilon_{instantaneous}$ (absolute value)	ε x1000	$\gamma_{rockfill}$	Stress, σ [kN/m^2]	Deformation module E_d [kN/m^2]
CF	0	-13	-476							
P1	0	-10	-143	2.384	-0.004195	0.000419	0.419	20.30	48.395	115,374
P2	0	-10	-136	2.914	-0.003432	0.000515	0.515	20.30	59.154	114,917
P3	0	-9	-161	2.963	-0.003037	0.000456	0.456	20.30	60.149	132,016
P4	0	-16	-76	3.877	-0.004127	0.000619	0.619	20.30	78.703	127,138
P5	0	-19	-169	2.955	-0.00643	0.000964	0.964	20.30	59.986	62,194

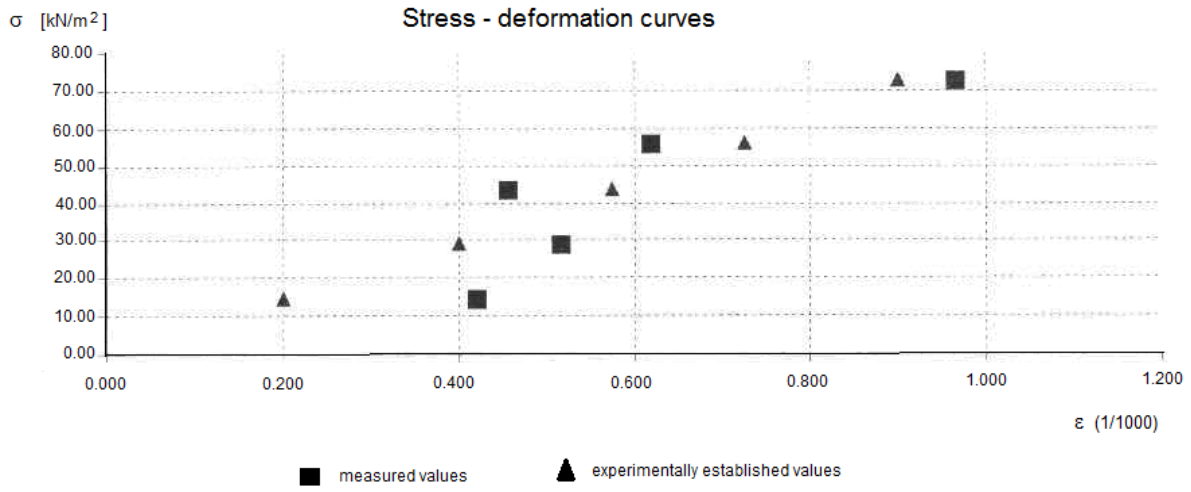

Fig. 7. *Stress – deformation curves*

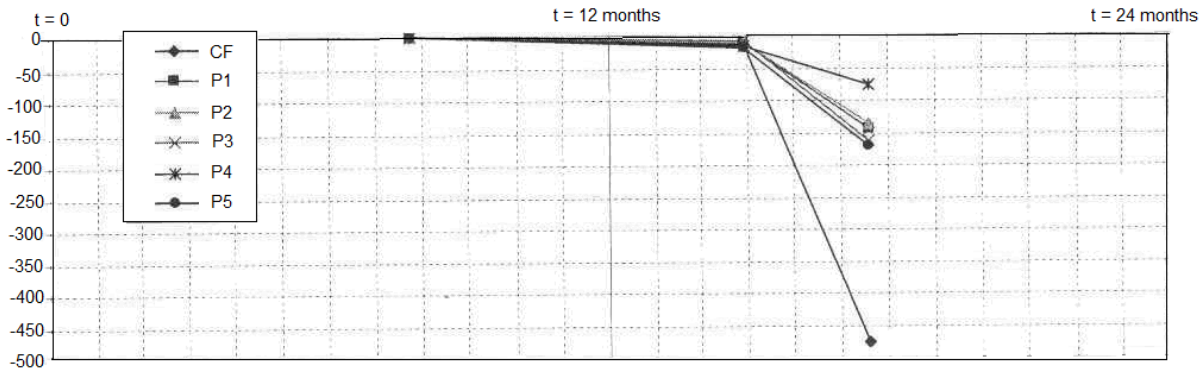

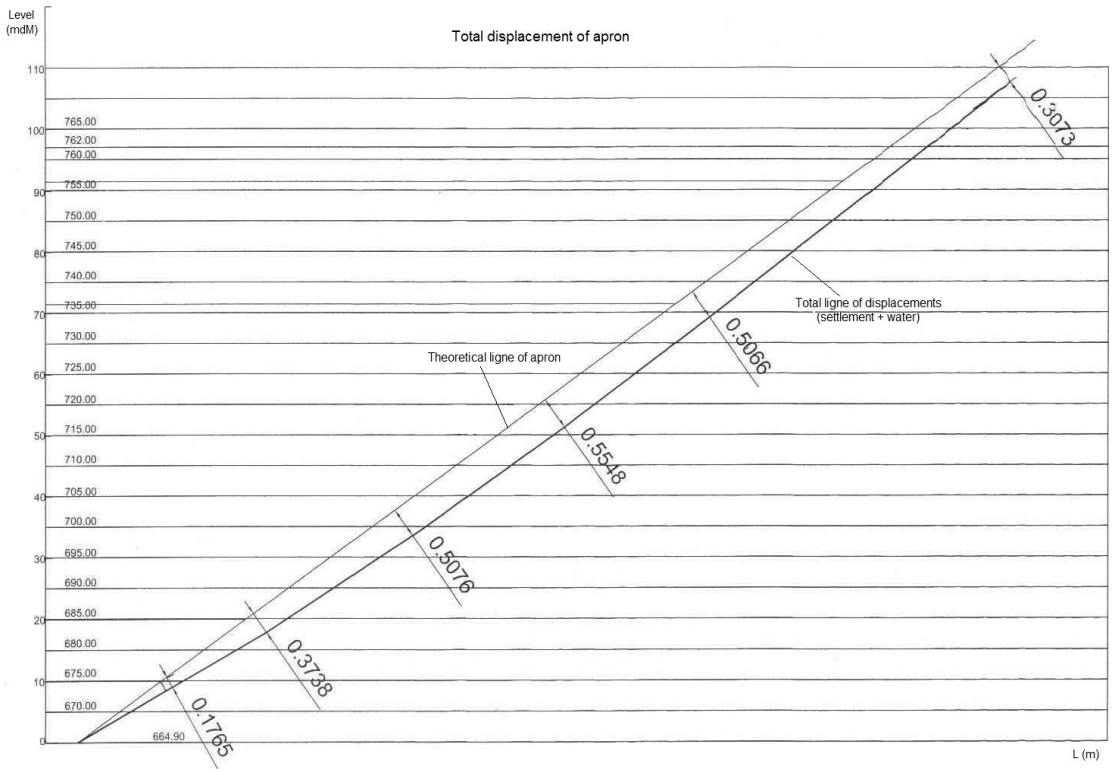

Fig. 8. *Measured settlements with CVT – fillings placed in the work and graphic of total displacement of concrete apron dam*

3.2. Obtained results

Calculus was carried out for two classical situations: completion of construction; first filling.

a) Completion of construction

Maximum settlements (- 1.07 m) are grouped in the centre of the dam, below tierce mean (H/3).

Horizontal displacements of upstream prism are in the range of values 0.09 – 0.30 m and also are arranged symmetrically in relation to those from downstream prism that are comprised in the range of values 0.10 – 0.48 m with a slight increase in relation to the upstream prism, in zone of material characterized by higher compressibility, namely tuff zone. Initial tangential elasticity modulus was significant through variations and gradients in the area of the contact surfaces between materials and along downstream face of dam from Ist stage. Distribution of elasticity modulus values (E_t) shows significant compression of material constitutes on volcanic tuff intercalated with pyroclastics. Maximum principal normal stress σ_1 (4 – 1,883 kN/m^2) is similar with σ_y, but with local distortions in accepted limits and without significant increases of equal stress lines, as a result of zoning of materials. Minimum principal normal stress of lateral confinement, σ_3 (1 – 858 kN/m^2), presents significant gradients in zone of contact downstream slope dam Ist stage – filling layer pyroclastic tuff and also in the first three layers of intercalated filling deposited near slope. The increases are not significant compared to the overall stress state of dam, but higher gradients in these areas may lead to diminishing the angle of internal friction with negative effects regarding the occurrence of local areas of instability. Shear tangential stress, τ_{xy} varies between -290 and 270 kN/m^2 and presents higher gradients through some discontinuities in downstream slope area of dam in Ist stage – filling layer of pyroclastic tuff.

b) First filling

From contribution of hydrostatic pressure maximum horizontal displacements – x direction – on upstream face of dam have the value of 0.34 m. From contribution of hydrostatic pressure maximum horizontal displacements – y direction – on upstream face of dam have the value of 0.19 m. Increases stress from hydrostatic pressure does not give rise to stresses concentrations in certain areas other than those signalled at the end of construction, maximum value of major principal normal stress being of 2,123 kN/m^2, respectively of 952 kN/m^2 for minor principal normal stress. Concreting works of concrete apron of Rastolita dam in first stage will begin after execution filling dam till 725 mdM level. Drawing works

comply with general lines from performed documentation, and upstream the concrete apron being delimited by marginal joint (RP) that is defined by bottom reference axis that passes through points P1 to P8. Concrete slabs are defined by the joints of concrete apron, marked by points from 1 to 56 to the side of the bottom and also from 2 to 19 on top of the plate corresponding of small dam (crest of wave of 725 mdM).

4. Conclusions

The rockfills used in order to achieve the dam must have imposed characteristics concerning on resistance (mechanical, shock resistance), not be brittle and be resistant to the chemical action of aggressive water.

Regardless the achieved compaction degree, the voids exist; therefore, it imposes an analysis of permeability. The presence of voids indicates that these fillings are permeable. Waterproofing is ensured by baffles or concrete apron on upstream face. Concrete apron must resist of occurring loads to water pressure.

Concrete slabs will be poured on a porous equalizer concrete which allows independent deformation of rockfill in relation to the screen, concrete apron being elastic but costly.

The price increase is also due to the used materials on marginal and vertical joints: copper foil, bituminous mastics Sika, and others. Mainly, the dam's stability in time, depends of the correct application of solution depends.

References

[1]. Clemets R. P., *Post-construction of rockfill dams*, Journal of Geotechnical Engineering, 110, p. 821-840, 1984.
[2]. Cooke J. B., *Progress in rockfill dams*, Journal of Geotechnical Engineering, 110, p. 1383-1414, 1984.
[3]. Cooke J. B., Sherard J. L., In Proceedings of the 2nd Symposium on Concrete Face Rockfill Dams: Design, Construction and Performance. Detroit, Mich, American Society of Civil Engineers (ASCE), New York, p. 1-658, October 1985.
[4]. Cooke J. B., Sherard J. L., *Concrete face rockfill dam: II Design*, Journal of Engineering, 112, p. 221-223, 1987.
[5]. Fitzpatrick M. D., Cole B. A., Kinstler F. L., Knoop B. P., *Design of concrete-faced rockfill dams*, In Proceedings of the Symposium on Concrete Face Rockfill Dams: Design, Construction and Performance. Detrit, Mich, Edited by J.B. Cooke and J.L. Sherard. American Society of Civil Engineers (ASCE), New York, p. 410-434, October 1985.
[6]. Freitas M. S. Jr., *Deformations and cracking in concrete face rockfill dams*, In Proceedings of the Symposium on 20 years for Chinese CFRD Construction. Yichang, p. 169-176, China, September 2005.
[7]. Moffat A. I. B., *Embankment dams and concepts of reservoir hazard analysis*, Reservoir Renovation. Proceedings of BNCOLD Conference, Manchester, paper 6.4, 1988.
[8]. Myoung-Soo Won, You-Seong Kim, *A case study on the post-construction deformation of concrete face rockfill dam*, Canadian Geotech Journal, p. 845-852, 2008.
[9]. *,** *Documentaţie tehnică şi geologică – Barajul Răstoliţa*.

THE ANNALS OF "DUNAREA DE JOS" UNIVERSITY OF GALATI
FASCICLE IX. METALLURGY AND MATERIALS SCIENCE
N°. 4 - 2016, ISSN 1453 – 083X

EXPERIMENTAL SHOOTING WITH THOR-1 DISRUPTOR: NEW TYPE OF GAS DEVICE USED TO NEUTRALIZE IMPROVISED EXPLOSIVE DEVICES

Vasile BĂLAN[1], Marian BORDEI[2*]
[1]Tehnical Military Academy of Bucuresti
[2]"Dunarea de Jos" University of Galati, Romania
[*]Corresponding author
e-mail: mbordei@ugal.ro

ABSTRACT

The paper presents experiments conducted with disruptor THOR-1, a new type of gas-dynamic device used to neutralize improvised explosive devices.

Disruptor THOR-1 [1] was designed and practically built as a gas-dynamic device that propels jets using colloidal particulate blast.

KEYWORDS: disruptor, explosive device, experimental, shooting

1. Experimental conditions

During experiments it was pursued, in particular, the qualitative verification of the jet behaviour of the disruption agent to the impact with various targets and the effect of the shock wave generation on the targets, characterized by modifying the cinematic properties of the target or of the elements resulting from it.

To determine the performance characteristics of disruptor THOR - 1, four tests were performed.

When choosing experimental tests, the following objectives were taken into consideration:

- the exact objective of each test;
- the propulsion device used - THOR 1 disruptor;
- the availability of existing materials;
- the availability of facilities, equipment and staff responsible for testing;
- the existence of control devices and appliances.

The equipment and materials used:

- the ultra-fast shooting video camera;
- the computer software necessary for image acquisition;
- power source;
- the neutralizing THOR 1 set;
- the disruption agent: water.

2. Experimental results

The experimental results are presented as follows.

TEST 1 NAME: the interaction study between jet and electric detonator

PURPOSE: To determine the effect of disrupting jet on the electrically blasting cap fastened on a wooden panel.

APPARATUS AND MATERIALS USED: JVC video camera; disruptor THOR-1; 12.7 mm pyrotechnic cartridge with 9.2 g of powder VUFL; disruption agent: water.

At the frontal collision between the water jet and the electrically blasting cap - the distance between the pipe and the cap being of 15 cm - it was observed deformation, not being detonated.

Loading data and results obtained:

Shooting no. 1-4	- electric cartridge - cal.12.7 mm - disruption agent: water - THOR disruptor -1 - the shooting was executed in very good conditions

TEST 2 NAME: The study of the interaction between the jet and an assembly consisting of an electric detonating cap inserted in an amount of 100 g plastic explosive;

PURPOSE: The determination of the effect of the disruptive jet on an assembly consisting of an electric detonating cap inserted in an amount of 100 grams of plastic explosives fixed on a 15 cm diameter pressed wood panel.

APPARATUS AND MATERIALS USED: JVC video camera; THOR-1 disruptor; 12.7 mm

pyrotechnic cartridge with 9.2 g of VUFL powder; disrupter agent: water.

At the frontal impact of the water jet with the electric detonating cap, the distance between the pipe and the cap was 10 cm. It was observed its deformation, not being detonated, fragments from the plastic explosive being scattered at approximately 2.80 m from the point of disruption.

The distance between the electrically detonating cap and the disruptor is about 15 cm

Disruptor ready for shooting

Electrically detonating cap deformed after disruption

Fig. 1. *The interaction between the jet and the electric detonator*

The electrically detonating cap assembly is placed in an amount of 100 grams of plastic explosive

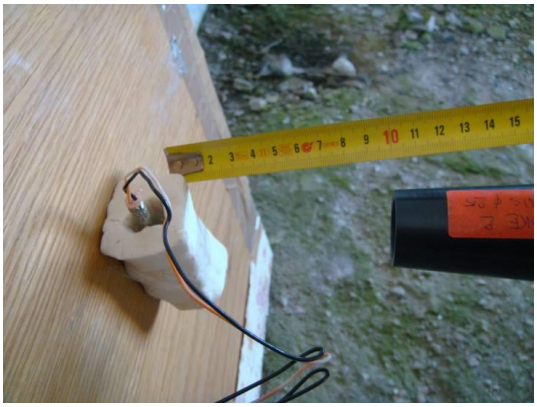

The distance between the electrically detonating cap inserted in an amount of 100 g plastic explosive and disrupter is about 10 cm

Disrupter ready for shooting

The effects of disruption on the pressed wood panel

The electrically detonating cap is deformed after the disruption

Fragment of plastic explosive resulting from disruption

The distance of approx. 280 cm at which fragments of plastic explosive were projected after disruption

Fig. 2. *The interaction between the jet and an assembly made up of an electric detonating cap inserted in a quantity of 100 g plastic explosive*

TEST NAME 3: the study of the interaction between the jet and an assembly consisting of an electric detonating cap inserted into a 100 g of TNT;

PURPOSE: to determine the effect of the disruptive jet on an assembly consisting of an electrically detonating cap inserted into a 100 g of TNT bin fixed to a 15 cm diameter pressed wood panel.

APPARATUS AND MATERIALS USED: JVC video camera; THOR-1 disruptor; 12.7 mm pyrotechnic cartridge with 9.2 g of VUFL powder; disrupter: water.

At the frontal impact of the water jet with electrically detonating cap, the distance between the pipe and the seam was 10 cm. It was observed its deformation, not being detonated, fragments of the TNT core being scattered at a distance of about 2.80 m from the disruption place.

The electrically detonating cap assembly is inserted into a 100 g of TNT body at a distance of 10 cm from the disruptor

Fragments of TNT resulting after disruption

Closure cap deformed after disruption

The distance of approx. 280 cm at which fragments of TNT were scattered after disruption

Fig. 3. *Interaction between the jet and an electrically detonating cap inserted into a 100 g of TNT*

TEST 4 NAME: the study of the interaction between the jet and an assembly consisting of a detonating wick with a length of 5 m (about 100 g for the pentrite).

PURPOSE: determination of the effect of the disruptive jet on a set consisting of a detonating wick with a length of 5 m fixed to a 15 cm diameter pressed wood panel.

APPARATUS AND MATERIALS USED: JVC video camera; THOR-1 disruptor; 12.7 mm pyrotechnical cartridge with 9.2 g of VUFL powder; disrupter agent: water.

At the front impact of the water jet with the detonating wick, the distance between the pipe and the wick being 10 cm, deformation was observed, not detonating.

Disrupter ready for shooting. The distance between the detonator wick and the disruptor is 10 cm

Compensating cover deformed after disruption

Fig. 4. *The interaction between the jet and a detonating wick with a length of 5 m*

4. Conclusions

Due to the lack of retraction, the device can be operated remotely: ROV (Remote Operated Vehicle);

To obtain the maximum effect, the disruptor should be placed as closely as possible to the improvised explosive devices potential but without touching it, the maximum distance being approx. 15 cm;

Attacking the improvised explosive devices to be neutralized potentially along the longest route increases the possibility of neutralization;

After the inspection of the improvised explosive devices with x-rays, its weakest point can be attacked, allowing the maximum energy to be transmitted in the improvised explosive devices mass

Only the liquid agent is used as a disrupter agent.

References

[1]. Bălan V., Bordei M., *Numerical Ballistic Phenomena*, The Annals of "Dunarea De Jos" University of Galati, Fascicle IX. Metallurgy and Materials Science, Special issue, p. 5-9, 2014.

[2]. Bălan V., Bordei M., *Numerical Ballistic Phenomena [part two]*, The Annals of "Dunarea De Jos" University of Galati, Fascicle IX. Metallurgy and Materials Science, vol. 1, p. 45-52, 2016.

[3]. Gingold R. A., Monaghan J. J., *Smoothed particle hydrodynamics-theory and application to non-spherical stars*, Mon Not R Astron Soc, vol. 181, p. 375-389, 1977.

[4]. Gingold R. A., Monaghan J. J., *Kernel estimates as a basis for general particle method in hydrodynamics*, J Comput Phys, vol. 46, p. 429-453, 1982.

[5]. Monaghan J. J., *Particle methods for hydrodynamics*, Comput Phys Rep, vol. 3, p. 71-124, 1985.

[6]. Dyka C., Ingel R., *An approach for tension instability in smoothed particle hydrodynamics (sph)*, Computers and Structures, vol. 57 (4), p. 573-580, 1995.

[7]. Swegle J., Hicks D., Attaway S., *Smooth particle hydrodynamics stability analysis*, J. Comp. Phys., vol. 116, p. 123-134, 1995.

[8]. Johnson J., Beissel S., *Normalized smoothing functions for sph impact computations*, Computer Methods in Apllied Mechanics and Engineering, vol. 139, p. 347-373, 1996.

[9]. Liu W., Jun S., Zhang Y., *Reproducing kernel particle methods*, International Journal for Numerical Methods in Engineering, vol. 20, p. 1081-1106, 1995.

[10]. Liu M. B., Liu G. R., *Smoothed Particle Hydrodynamics (SPH): An Overview and Recent Developments*, Arch Comput Methods Eng, vol. 17, p. 25-76, 2010.

[11]. Trană E., *Solicitarea materialelor metalice în regim dinamic. Legi constitutive*, Editura Univers Ştiinţific, Bucureşti, 2007.

THE ANNALS OF "DUNAREA DE JOS" UNIVERSITY OF GALATI
FASCICLE IX. METALLURGY AND MATERIALS SCIENCE
N°. 4 - 2016, ISSN 1453 – 083X

ASPECTS REGARDING THE TRACEABILITY IN TEMPERATURE MEASUREMENTS

Andreea-Diana MOROŞANU[1,a], Madalina Elena MILITARU[1,b], Gabriel Marius DUMITRU[2,a]

[1]EMTS Doctoral School, Industrial Engineering Department, University Polytechnic of Bucharest, Romania
[2]Faculty EMTS, Industrial Engineering Department, University Polytechnic of Bucharest, Romania
e-mail: andreeadianamorosanu@yahoo.com, militaruemadalina@yahoo.com, gmdumitru@yahoo.com

ABSTRACT

The traceability of national standards to a reference measurement is essential to correctly translate the information about customer preferences described in international standards as a prerequisite which exists for the design of goods that comply with the expected characteristics.

The traceability of national and reference measurement standards to the International System (S.I.) is achieved by: comparisons with the primary measurement standards of other countries and periodic calibration with respect to measurement standards of other international and national institutes of metrology, whose traceability to the SI is already proven and widely recognized internationally.

This paper discusses how traceability is possible or it is ensured in temperature measurements, by using measuring instruments that are traceable at International Temperature Scale of 1990 (ITS-90) [1].

KEYWORDS: temperature, traceability, measurements, management, standard

1. Introduction

The quality and development of products and services is dependent on accurate measurements.

The duty of Bureau International des Poids et Mesures (BIPM) [2] is to provide at global level uniformity of measurements and their traceability to the to the International System of Units (SI).

BIPM Key Comparison Database (KCDB) [3] supports the Mutual Recognition Arrangement of the CIPM (acronym CIPM MRA or in short MRA) [4].

The MRA was born from the desire to remove the unnecessary technical barriers. One example for such barrier is the requirement of traceability to a national metrology system.

MRA provides a system that allows customers and government to trust in calibration and measurement certificates of institutions from their country, institutions which participate in the MRA and this fact gives them the right to recognize those calibration certificates. This can be concluded in the expression "calibrated once, accepted everywhere".

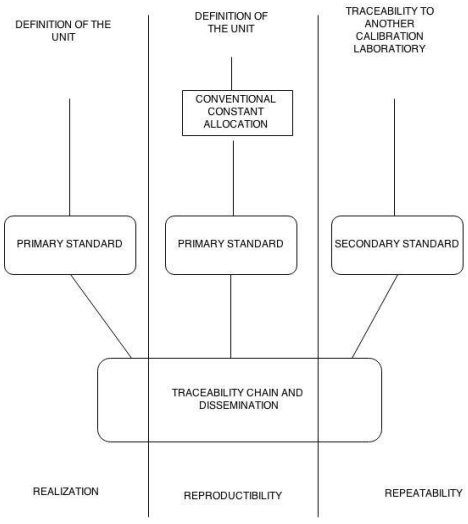

***Fig. 1.** Traceability scheme*

Traceability can be defined as "property of a measurement result whereby the result can be related to a reference through a documented unbroken chain of calibrations, each contributing to the measurement uncertainty" (2.41 VIM) [5].

The word *traceable* has a wide range of colloquial meanings, the most appropriate being 'able to be followed to the source' [6] (Figure 1).

The National Institute of Metrology (acronym INM) [7] maintains the Romania national standards for temperature.

Each country has similar national standards laboratories, which accomplish the same goal.

Traceability in temperature is supported by platinum resistance thermometers over a significant portion of temperature scale (ITS-90).

The fixed point is the most accurate instrument and it is realized by pure metals enclosed in a sealed, inert environment.

They work in conjunction with apparatus which surrounds them and provides the operational condition required for melting and freezing to obtain the reference plateau. The housing incorporates isothermal blocks with wells into which the probes are placed. Since fixed point temperatures are defined by physical laws, comparison of the test probe to a reference probe is not required.

Hierarchy of standards and temperature measuring instruments aim at achieving submission of temperature unit from the national standard and reference to working measuring instruments.

Scheme hierarchy of standards and temperature measuring instruments apply to the fundamental unit "thermodynamic temperature", symbol "T" which the SI unit is "Kelvin", symbol "K", that is equal in value to the "degree Celsius" symbol "C", SI unit of "Celsius temperature", symbol "t".

International Temperature Scale is a conventional scale, based on a series of fixed points, reproducible. The measuring instruments calibrated at these fixed points and the mathematical relationships, serve to establish interdependence of the indications of measuring and respectively temperature. Fixed points of definition are represented by reproducible equilibrium states (melting points, freezing points and triple points) of some high purity substance.

The ITS-90, which was designed so as the measured temperature in this scale to be a good approximation of thermodynamic temperature numerically corresponding. The relation between T_{90} and t_{90} is similar between T and t.

$$t_{90} = T_{90} - 273{,}15\ K \qquad (1)$$

Such a scale must satisfy three requirements:

- to be accurate and reproducible;
- to be carried out independently in all laboratories in the world with financial and time resources achievable;
- temperature values in this scale to be as close as possible with thermodynamic temperature values the best estimates made from suitability made when adopting scale.

ITS-90 it is based on:

- a set of fixed definition;
- interpolation methods specified between fixed points.

Table 1. *ITS-90 Fixed Points*

No.	Temperature		Substance[a]	Type[b]
	T_{90}lK	t_{90} °C	Ar	Triple
1	83,805 8	-189,344 2	Hg	Triple
2	234,315 6	- 38,834 4	H_2O	Triple
3	273,16	0,01	Ga	Melting
4	302,914 6	29,764 6	In	Freezing
5	429,748 5	156,598 5	Sn	Freezing
6	505,078	231,928	Zn	Freezing
7	692,677	419,527	Ar	Triple

[a] natural isotopic composition

[b] triple point- temperature at which the solid phases, liquid and gaseous are in equilibrium; freezing , melting point- temperature, at a pressure of 101 325 Pa, in the solid and liquid phases are in equilibrium

The purpose of this paper is to present how traceability of measurements is achieved in Temperature Laboratory of National Institute of Metrology (INM) by declaration of Calibration and measurement capabilities (CMCs), which are realized with international Key Comparison. For Romania, the CMC's are found in Appendix C from Key Comparison Database (KCDB) [3].

2. Experimental

In the hierarchy scheme for measuring temperature (Figure 2) it is represented the synthetic process of disseminating of temperature in the unit (-189.244 2 ... 660.323) ºC, the national standard / primary to working standards, to ensure metrological traceability of measurable results. Dissemination unit is based on the type of measuring instruments to be calibrated and their metrological quality resulting into different uncertainties measurement [8].

Transfer unit at the highest metrological level is carried out by sending the information directly from the primary standard directly to the working standard.

At INM, the temperature unit is transmitted from the primary / national standard to the fixed points of reference cells by comparing their direct values with cell components of / national standard through platinum resistance thermometers.

This procedure of unit dissemination, is the largely conserved of realisation temperature unit.

Calibration uncertainties values of fixed point cells in (-189.244 2 ... 660.323) ◦C presented in Hierarchy Scheme were confirmed and internationally recognized through EUROMET.T-K3 and EUROMET.T-K4 key comparisons.

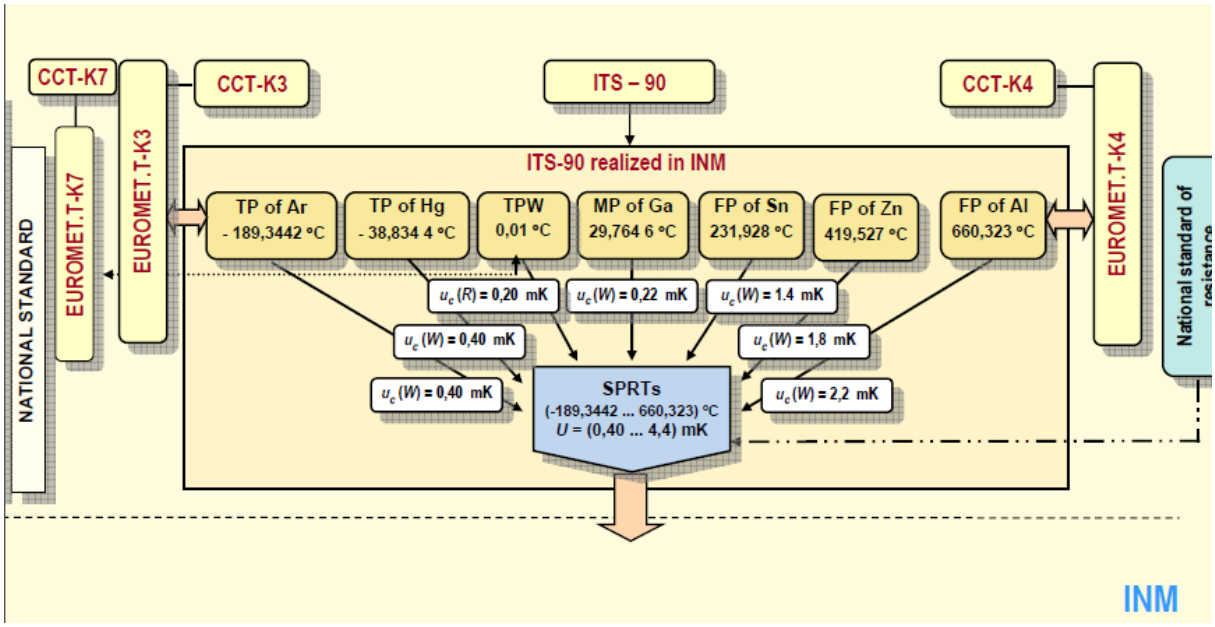

Fig. 2. *Hierarchy scheme of measuring temperature through Standard Precision Resistance Thermometer*

With respect to the next levels of accuracy, dissemination of national scale of temperature is performed by:

- direct measurement reference cells for fixed points;
- direct/indirect Comparison with reference standards.

2.1. Direct measurement reference cells for fixed points

A method is used to calibrate the standard thermometers resistance, S-type thermocouples and digital thermometers which are directly calibrated reference cells for fixed points.

For this method, we chose from the project "National standard characterisation of "Kelvin" unit of international temperature in the range (273.16 … 1 357.77) K" [9], the project is done annually for a better dissemination of temperature.

Primary standard of the temperature unit, within the range (-189.344 2 and 961.78) °C represents practical realisation of fixed point of ITS-90, associated with calibration of platinum resistance thermometers (acronym PRT)- interpolation instruments specified in ITS-90. The system used in the laboratory for achieving a fixed point and for platinum resistance thermometers calibration in relation to this reference is shown in Figure 3.

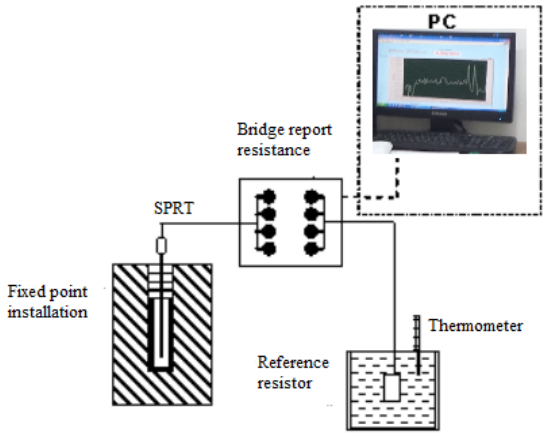

Fig. 3. *Realization of fixed points and platinum resistance thermometers calibration*

PRT is placed vertically upon the installation of materialisation fixed point. Its electrical resistance is measured with ASL F18 Automatic bridge ratio resistant. Bridge measuring the ratio of electric resistance is to be calibrated PRT and electrical resistance of reference resistor is held in a constant temperature bath. The bath temperature is monitored with a thermometer. The electrical resistance values of the reference resistor are corrected for temperature using the thermometer references.

Data provided by ASL F 18 Automatic bridge ratio are purchased and processed by a PC, using an IEEE 488 interface and LabVIEW programming environment (Figure 4).

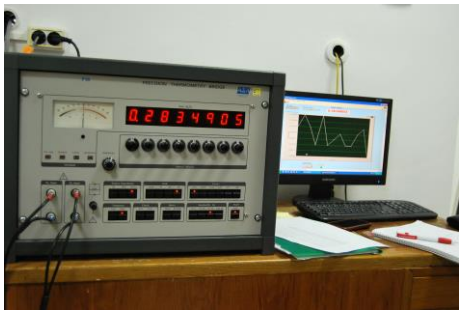

Fig. 4. *ASL F18 Automatic bridge ratio and monitored with LabVIEW programming environment*

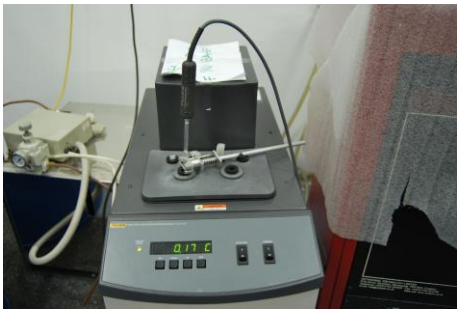

Fig. 5. *PRT calibration at triple point of water – TPW*

In Figure 6 we observe that at TPW calibration, the PRT is very stable and maximum fluctuations is within the range of 0.05 mK.

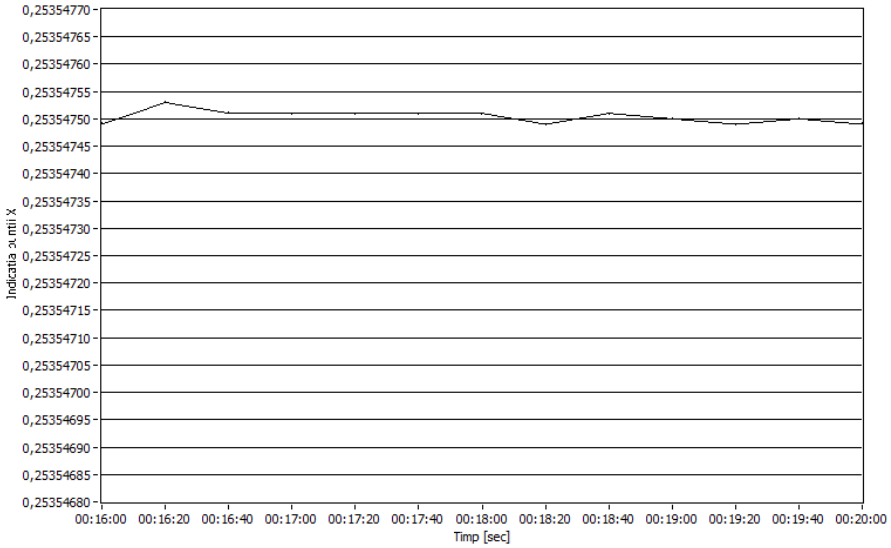

Fig. 6. *Outcome monitoring PRT in LabView at TPW for 4 minutes*

2.1 Direct / Indirect Comparison with reference standards

The method is used for calibrating platinum resistance thermometers, thermocouples, Liquid glass thermometers, digital thermometers, etc., direct or indirect comparison with reference standards in ovens and baths.

In Figure 7 we have a thermobalance with a temperature sensor which is calibrated at 3 specific points of temperature chosen by beneficiary.

It is known that balances are influenced by temperature. In this way, it is important to know what temperature has a huge influence on the sensor of thermobalance.

After calibration, the data from Table 2 was obtained.

Fig. 7. *Calibration thermobalance sensor at 15º, 20º and 30 ºC*

Table 2. *Data obtained from calibration thermobalance sensor at temperatures: 15º, 20º and 30 ºC*

Value/ºC				Uncertainty
Temperature set	**Indicated**	**True**	**Correction**	
15	14.9	14.92	-0.02	0.3
20	20.0	19.98	-0.02	
30	30.0	30.07	+0.07	

The current measurements measuring the true value are:

$$Tct = (Tind + C) \pm U\ (°C) \qquad (2)$$

where:

Tct = conventional true temperature;
Tind = indicated temperature;
C = correction;
U = expanded uncertainty.

If we apply the correction obtained in the Table, we will find the true temperature according to relation (2).

The uncertainty attributed is expanded uncertainty obtained by multiplying the standard uncertainty with coverage factor $k = 2$. The results are traceable according to the International System of Units. Traceability of measurement is achieved and maintained by international comparisons and calibration in agreement with SR EN ISO/CEI 17025:2005 [10].

3. Conclusions

Traceability can be achieved in practice, if we think that a substantial community effort is required.

To achieve traceability is necessary to follow the three main requirements for an international measurement system, such as:

- Primary physical standards are required to provide a unique definition of the measurement scales. All measurements should refer to the same SI unit.

- With temperature measurements, it is sometimes necessary to agree on a measurement protocol or to follow the same scale (for temperatures it is necessary to refer to ITS-90) in order to be able to make comparable measurements.

- Documentary standards are also used to define other protocols, some of which have a direct effect on measurements. These include standardized responses for platinum resistance thermometers and thermocouples, mechanical specifications for electrical instruments, etc.

Temperature measurements are not like many of the products that we buy. Given that a calibration or testing laboratory has followed documentary standards and calibrated its equipment, it must be demonstrated that it has conformed to the community expectation with respect to measurement standards and technical procedures.

Acknowledgment

The work has been funded by the Sectoral Operational Programme Human Resources Development 2007-2013 of the Ministry of European Funds through the Financial Agreement POSDRU/159/1.5/S/132397.

The work has also been funded by the Sectoral Operational Programme Human Resources Development 2007-2013 of the Ministry of European Funds through the Financial Agreement POSDRU/159/1.5/S/132395.

References

[1]. Preston-Thomas H., *The International Temperature of Scale of 1990 (ITS-90)*, Metrologia, vol. 27, p. 3-10, 1990.
[2]. ***, http://www.bipm.org/en/about-us/, accessed: 2015-05-18.
[3]. ***, http://kcdb.bipm.org/, accessed: 2015-05-18.
[4]. ***, http://www.bipm.org/en/cipm-mra/, accessed: 2015-05-18.
[4]. ***, *International Vocabulary of metrology*, *VIM*-(2007).
[5]. Nicholas J. V., White D. R., *Traceable Temperatures*, West Sussex, John Willey & Sons, p. 21-24, 2001.
[6]. ***, http://www.inm.ro/ro/?page=capability, accessed: 2015-05-18.
[7]. ***, http://www.temperature.ro/Sectiunea%205.6.1.htm, accessed: 2015-05-28.
[8]. Neagu M., Cicirlan E., Morosanu A. D., Dinu C., *National standard characterisation of "Kelvin" unit of international temperature in the range (273,16 … 1 357,77) K*, INM, 2013-2015.
[9]. ***, Standard SR EN ISO/CEI 17025:2005, *General requirements for the competence of testing and calibration laboratories.*

THE ANNALS OF "DUNAREA DE JOS" UNIVERSITY OF GALATI
FASCICLE IX. METALLURGY AND MATERIALS SCIENCE
Nº. 4 - 2016, ISSN 1453 – 083X

THE LEVEL OF NOISE POLLUTION IN UNIVERSITY CAMPUSES ADMINISTERED BY THE UNIVERSITY OF 1 DECEMBER 1918 IN ALBA IULIA

Elena MARICA
University of 1 December 1918 in Alba Iulia
e-mail: elenamarica93@yahoo.com

ABSTRACT

Sound pollution is becoming a major problem because of multiplying sources of noise. In this study, I will present the results of the noise measurements carried out in the four campuses of the 1 Decembrie 1918 University in Alba Iulia. Initially the noise level was measured at several points in the university campuses and the main sources of noise were identified. Finally, solutions have been sought to mitigate noise so that noise levels remain below the maximum allowable limits in order to create normal learning and resting conditions for students staying in these campuses.

KEYWORDS: noise pollution, noise level measurement

1. Introduction

Noise is derived from the Latin word "nausea" implying 'unwanted sound' or 'sound that is loud, unpleasant or unexpected' [1].

Sound pollution is a component of environmental pollution. Noise sources divide into 2 categories of natural noise sources and artificial sources of noise generated by people's activities.

Sound pollution is a threat to quality of life. It is more severe and widespread than before and will continue to grow in intensity due to population growth, industry development and road, air and rail traffic, thus becoming a major issue in all major cities in the world [2].

According to the World Health Organization, seven major effects of noise pollution were identified: Hearing Impairment, Interference with Spoken Communication, Sleep Disturbances, Cardiovascular Disturbances, Disturbances in Mental Health, Negative Social Behavior and Annoyance Reactions [3].

2. Materials and methods

We have measured the level of noise pollution in the four student dormitories administered by 1 Decembrie 1918 University in Alba Iulia.

For this project, we used a portable 2250 acoustic analyzer, Brüel & Kjær. This portable analyzer is the most widely used tool for noise measurements. It has several advantages compared to other measuring instruments: it is efficient, easy to handle, has a large memory, the data is saved on the inter card and can be transferred to the computer, it simultaneously measures several parameters like: LAF – the instantaneous 'A' frequency-weighted and 'F' time-weighted sound pressure level; LAFmax – the maximum 'A' frequency-weighted and 'F' time-weighted sound pressure level detected during a measurement; LAeq – the 'A' frequency-weighted equivalent continuous sound pressure level, that is, the average level representing the same energy as the measured fluctuating levels.

Fig. 1. *Campuses location*

Student hostels 1 and 2 are located on Vasile Alecsandri Street, and the 3 and 4 Suden Rooms are located on Vasile Goldiș Street. As can be seen in Figure 1, Campuses are numbered from C1 to C4.

I made noise measurements at two different times of the day, in the morning (between 08:30 - 10:00) and in the evening (between 20:00 and 22:00). Measurement time was 5 minutes, and this operation was repeated 2 times for greater accuracy of the results, then the average of the 2 results. The sonometer was seated at a height of 1.20 m.

3. Results and discussions

In the following Tables, the results of the values recorded during the measurements in the four campuses are presented.

In Figure 2 it can be seen the difference between the maximum admissible value and the noise level recorded on campus1.

Noise is produced by sources inside the campus, but also outside the campus. The main sources of noise inside the campus are: doors, parties, and secondary sources are: washing machine, students' dialogues, home appliances, audio devices. The main source of noise outside the campus is traffic, followed by various industrial activities taking place around campuses.

It can be seen from the tables that the noise level at one time exceeds the value of 50 dB, i.e. the maximum allowable limit. There are solutions to lessen the noise level so that the noise remains below the maximum allowable value over the longest period of time.

Table 1. *Values recorded in campus 1*

The selected point	Lecture hall		1st floor hallway		Outside the campus	
Time of day	**M**	**E**	**M**	**E**	**M**	**E**
LAeq	49.8	59.6	69.8	72.4	63.5	60.7
LAFmax	67.5	78.9	82.1	93.0	86.2	83.0
LAF90.0	40.6	45.2	50.1	56.0	48.7	47.4
Maximum admissible value	50	50	50	50	50	50

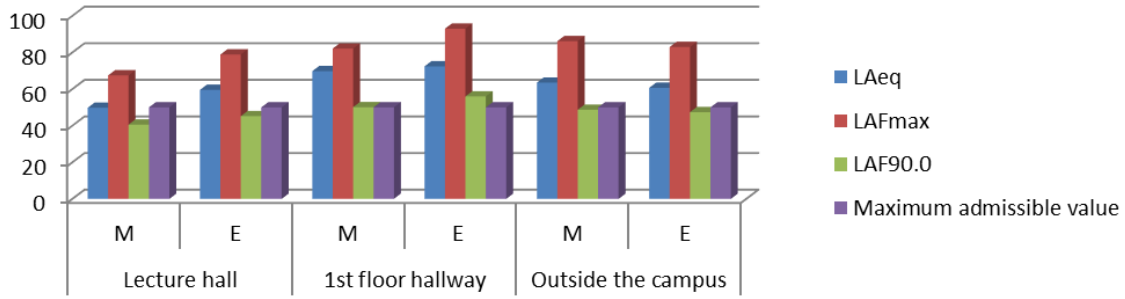

Fig. 2. *Values recorded in campus 1*

Table 2. *Values recorded in campus 2*

The selected point	Lecture hall		1st floor hallway		Kitchen		Outside the campus	
Time of day	**M**	**E**	**M**	**E**	**M**	**E**	**M**	**E**
LAeq	43.8	44.5	62.8	62.2	48.6	49.7	63.5	61.2
LAFmax	57.2	57.9	82.5	83.9	61.0	61.3	83.72	83.0
LAF90.0	39.9	40.1	45.8	46.6	45.9	46.8	45.7	46.8
Maximum admissible value	50	50	50	50	50	50	50	50

Table 3. *Values recorded in campus 3*

The selected point	Lecture hall		1st floor hallway		Kitchen		Outside the campus	
Time of day	**M**	**E**	**M**	**E**	**M**	**E**	**M**	E
LAeq	46.6	37.0	43.5	46.5	48.6	47.5	54.3	52.8
LAFmax	67.2	52.6	60.9	60.6	72	71.8	65.6	70.3
LAF90.0	34.3	30.2	36.8	41.6	40.0	42.2	47.1	45.0
Maximum admissible value	50	50	50	50	50	50	50	50

Table 4. *Values recorded in campus 4*

The selected point	Lecture hall		1st floor hallway		Kitchen		Outside the campus	
Time of day	**M**	E	**M**	E	**M**	E	**M**	E
LAeq	45.1	45.3	51.1	54.7	62.4	63.8	54.8	53.4
LAFmax	60.2	71.2	74.0	80.2	82.1	81.5	66.3	61.9
LAF90.0	34.1	33.1	40.3	43.9	46.9	49.2	44.0	44.9
Maximum admissible value	50	50	50	50	50	50	50	50

To reduce the noise on campuses, the following are proposed: weather-strips - to reduce the noise produced by the doors; regulation - to reduce the noise made by students; sound absorbing panels - to reduce noise on the propagation path., tree fences- to reduce the noise from outside the campus.

4. Conclusions

From the above we can conclude that in the 4 campus the noise level of 50 dB is overcome due to both external and internal sources.

The highest value recorded as a result of noise measurements was obtained in campus 1. The maximum admissible value by 43 dB was exceeded, the recorded value being 93 dB. The lowest value was obtained on campus 3. The sonometer recorded a value of 30.2 dB.

If we rank the campuses according to the recorded noise level, we will get the following ranking: campus 1 (the noisiest campus), campus 2, campus 4 and campus 3 (the least noisy campus).

By intervening with methods to combat noise pollution, the level of noise identified in student dormitories can be significantly diminished so that students are offered optimal study and rest conditions.

References

[1]. Narendra Singh, Davar S. C., *Noise Pollution-Sources, Effects and Control*, J. Hum. Ecol., 162, p. 181-187, 2004.
[2]. Lisa Goines, Louis Hagler, *Noise Pollution: A Modern Plague*, Southern Medical Journal, vol. 100, p. 287-294, 2007.
[3]. Berglund B., Lindvajl T., *Commuruty Noise*, Archives of the Center/or Sensory Research,2:1-195. This document is an updated version of the docwnent published by the World Health Organization in 1995.

THE ANNALS OF "DUNAREA DE JOS" UNIVERSITY OF GALATI
FASCICLE IX. METALLURGY AND MATERIALS SCIENCE
N°. 4 - 2016, ISSN 1453 – 083X

REDUCING THE SLUDGE QUANTITY PRODUCED FROM USED WATER PURIFICATION – A SOURCE OF PROFIT

Cornel SAVA, Iulia DRĂGAN, Ana Maria STROE, Luminița Cristina PIRĂU, Elena Maria PICĂ
Technical University, Cluj-Napoca, Romania
e-mail: sava.cornel47@yahoo.com

ABSTRACT

This paper has its origins in the analysis of a real situation met in the Water Purification Plant from Cluj-Napoca city. The produced dehydrated sludge is about 70 - 80 tonnes / 24 hours, with a density that allows for an equivalence of 1 tonne to 1 m³, 80,000 Kg or 80 m³, i.e. a huge amount and an impressive volume of material. This paper does not propose solutions to valorise or store the huge quantity of sludge, though the present solutions are quite inefficient. The stress is placed upon the sludge production sources, its transportation to the purification plants, the collection of the sludge in the purification plants and the dehydration methods that can be used. The analysis of these stages aims at identifying several measures that could lead to diminishing the amount of sludge produced after the purification of used and dehydrated water in the purification plants without affecting the quality of purified water. The measures identified are to be presented as measures that can be applied in the spirit of sustainable and efficient development. The business feature is given by the savings brought by the mitigation of the sludge amount to be stored and paid for in the ecological storage places in remote areas.

KEYWORDS: sludge, dehydration, reduction of amount, thickening, purification, expenses, profit

1. Introduction

The main source of sludge is the used water that reaches the purification plant through the sewers.

The types of materials reaching used water are:

- Toilet paper, a material that is dissolved in the toilet water, then reaches the purification plant and contributes to sludge formation;
- Small size food remains, thrown in the toilet;
- Naturally falling hair or hair coming from people who prefer to cut their hair in the bathroom;
- Debris, coming from dwelling repairs;
- Rests of sauerkraut or pickles, thrown in the sewers in spring;
- Leaves and vegetal rests from the autumn or spring garden and court cleaning;
- Cut and minced grass found after using the lawnmowers;
- Faeces from stock raising units;
- Metal and mud remains of industrial origin.

2. Experimental

2.1. An approximate calculation of the quantity of materials that normally should not reach the sewage system

Toilet paper:

Q_1 = n x q x z = 400,000 x 30 x 365 = 4,380,000 000 cm/year

4,380,000,000 cm: 200 cm = 21,900,000 toilet paper rolls per year

21,900,000 x 40 g = 876,000,000 g/year = 876 tonnes/year

where:

Q_1 = the overall amount of toilet paper reaching the system;
n = the number of inhabitants;
q_1 = the toilet paper consumption per one day;

z = the number of days used for the evaluation.

Debris and rests from the repairs of dwellings – get in the sewage system after tools and buckets used are cleaned and after intentionally throwing the debris in the toilet or directly in the street manhole:

Q_2 = n x q x z = 400,000 x 50 g x 365 = 7,300,000,000 g/year

Q_2 = 7,300 t/year

where:

Q_2 = the overall amount of debris thrown in the system in one year;
n = the number of inhabitants;
q_2 = the total amount of debris thrown by one inhabitant in the sewage system;
z = the number of days used for the evaluation.

Food remains (bread, rests, coffee grounds etc.) get in the kitchen sinks during dish washing or as they are intentionally thrown in the toilet:

Q_3 = q x n x z = 10 g x 400,000 x 365 = 1,460,000,000g = 1,460 t/year

where:

n = the number of inhabitants;
q_3 = the total amount of food remains thrown by one inhabitant in the sewage system;
z = the number of days used for the evaluation.

The figures do not represent very exact quantities because this phenomenon cannot be accurately measured and stopped.

In this paper, the authors intend to make an analysis of this phenomenon starting from the reality of several areas in Romania and to propose a coherent strategy to inform the population and to change the legislation so that the phenomenon could be eventually controlled.

The sludge produced after the purification of the used water remains after dehydration with a consistency of 20 - 25 % SU (Dry substance, including all the organic and inorganic substances found in the sludge at the moment of evaluation).

The volatile substances are those substances that define the organic content of used water.

The concentration of the activated sludge in the dry substance can vary in a wide range from 0,5 to 10 g/l, as commonly the activated sludge plants present a dry substance content of 1 - 4 g/l suspension. A good activated sludge (i.e. the sludge prepared to have a contribution in the biological purge of the used water) contains about 75% volatile substances.

The preparation of the sludge consists in populating it with bacteria that biologically decompose the compounds in the used water.

Bacteria can be grown in the purification plants or can be brought in activated sludge from other purification plants in use.

The calcination residue, that is what remains from the dry substance after burning in a kiln at a temperature of 600 - 800 °C, contains mineral salts and oxides of common elements from the used water which are also necessary for the growth of microorganisms.

In general, one can find: potassium (K), sodium (Na), magnesium (Mg), iron (Fe), aluminium (Al), chlorine (Cl), phosphorous (P) and other elements, in relation with the amount of water used. Among the elements the form the organic substance of the activated sludge, one can list: carbon (C), oxygen (O), hydrogen (H) and nitrogen (N).

The cellular components can take the following forms: proteins - about 60%, nucleic acids - approximately 15%, glucides/carbohydrates - 20% and lipids - 5%. Very well spread bacteria found in the activated sludge (Escherichia coli) contain between 3000 - 6000 types of molecules, of which half are small sized molecules (glucides, aminoacids, organic acids, phosphoric esters), while the rest contain 1500 - 3000 types of macromolecules (complex glucides, glucide precursors, complex lipids, proteins, ADN, ARN) [1-4].

This short description of the structures of the sludge wants to highlight the sludge content and to identify the materials in its composition.

2.2. Proposed business

A collaboration with all the companies that are concerned in the proper management of the sludge is proposed.

By presenting arguments based on measurements and filed observations, the companies could be convinced to invest in developing and promoting a strategy to inform and educate the population so that the amount of sludge from the purification plants could diminish by reducing the quantity of rests that are not allowed to be thrown in the sewage system.

Companies that could be concerned to promote this strategy:

- Producers of sludge and owners of purification plants, respectively.
- Agencies concerned with the environment protection.
- The administrations of the cities, towns and villages that possess drainage systems in their areas.

- The population that can be interested to find that the cost of 1 cubic meter of used water can be reduced.

2.3. Main benefits

The benefits from the application of this strategy can be quantified in the effect it could have upon the behaviour of the population relative to the collection of the used water and the further on expenses related to the purification of the used water. When the population is educated to properly use the very precious natural resource which is *water* facilitates the work of those concerned with water preparation, distribution, collection and significantly diminishes the costs related to this activity.

2.4. Defining the profit

Estimated costs:

a. Expenditures related to visiting the interested parties – 8,000 lei/year.

b. Expenditures to organise meeting to inform the population – 10,000lei/year.

c. Expenditures to print informative brochures and to produce educational films 100,000 lei/year

Financing sources:

The main financing source is provided by the interested parties: sludge producers and local authorities.

The project can also be funded by applying for a European financing, in the field of" Environment protection".

Estimated gains:

The finances found from diminishing the amount of dehydrated sludge amount.

A 20% reduction of the quantity of sludge produced in 24 hours means for the Purification plant of Cluj Napoca 16 tonnes/24 hours.

The cost paid to ecological dumps is about 250 lei/tonne.

E_{ec} = q x p = 16 x 250 = 4,000 lei/day = 1,460,000 lei/year

where:

E_{ec} = total saving.

q = sludge quantity not produced anymore, after implementing this strategy.

p = the cost paid to ecological dumps.

In this specific case, the profit is calculated by making the difference between the required investments to efficiently promote the strategy and the gains of the sludge producers.

The initiator and coordinator of this strategy can draw funding contracts with the interested parties, which are to be negotiated as a percentage of the profits of each company in this field.

3. Conclusions

The business proposed is mainly based upon the idea of contacting the interested parties, by informing them on the opportunity of running a study in this respect for each individual area and of convincing them to take part and finance such a project.

Acknowledgment

This paper has been completed due to the support of the Doctoral School within the Technical University of Cluj-Napoca, Romania.

References

[1]. Dumitru M., Răduţă C., Gameţ Eugenia, Damian Maria, Calciu I., Dumitru Elisabeta, Dancău H., *Cercetări pentru stabilirea sortimentului de culturi pretabile pe terenurile fertilizate cu nămol oraşenesc*, Lucrările CNSS Tulcea, p. 163-230, Bucureşti, nr. 28 E, 29 august-3 septembrie 1994.

[2]. Ionescu Gh. C., *Analiza factorilor de risc în funcţionarea staţiilor de epurare a apelor uzate*, Conferinţa Naţională cu participare Internaţională "*Instalaţii pentru construcţii şi confortul ambiental*" Editia a 17-a, Timişoara, 17-18 aprilie 2008.

[3]. Leonard I., Dumitru M., Nicoleta V., Motelică D. M., Veronica T., *Metodologie de utilizare a nămolului orăşenesc în agricultură*, Editura Solness, Timişoara, ISBN 978-973-729-107-3, 208, 2007.

[4]. ***, Directive 86/278/EEC, *Council directive on the protection of the environment, and in particular of the soil, when sewage sludge is used in agriculture*, Official Journal of the European Communities, 1986.

MANUSCRISELE, CĂRŢILE ŞI REVISTELE PENTRU SCHIMB, PRECUM ŞI ORICE CORESPONDENŢE SE VOR TRIMITE PE ADRESA:

MANUSCRIPTS, REVIEWS AND BOOKS FOR EXCHANGE COOPERATION, AS WELL AS ANY CORRESPONDANCE WILL BE MAILED TO:

LES MANUSCRIPTS, LES REVUES ET LES LIVRES POUR L'ECHANGE, TOUT AUSSI QUE LA CORRESPONDANCE SERONT ENVOYES A L'ADRESSE:

MANUSCKRIPTEN, ZIETSCHRITFTEN UND BUCHER FUR AUSTAUCH SOWIE DIE KORRESPONDENZ SID AN FOLGENDE ANSCHRIFT ZU SEDEN:

After the latest evaluation of the journals by the National Center for Science Policy and Scientometrics (**CENAPOSS**), in recognition of its quality and impact at national level, the journal will be included in the B^+ category, 215 code (http://cncsis.gov.ro/userfiles/file/CENAPOSS/Bplus_2011.pdf).

The journal is already indexed in:

SCIPIO-RO: http://www.scipio.ro/web/182206

EBSCO: http://www.ebscohost.com/titleLists/a9h-journals.pdf

Google Academic: https://scholar.google.ro

The papers published in this journal can be viewed on the website of "Dunarea de Jos" University of Galati, the Faculty of Engineering, web-page: http://www.fascicula9.ugal.ro.

Name and Address of Publisher:
Contact person: Elena MEREUȚĂ
Galati University Press - GUP
47 Domneasca St., 800008 - Galati, Romania
Phone: +40 336 130139, Fax: +40 236 461353
Email: gup@ugal.ro

Name and Address of Editor:
Prof. Dr. Eng. Marian BORDEI
Dunarea de Jos University of Galati, Faculty of Engineering
111 Domneasca St., 800201 - Galati, Romania
Phone: +40 336 130208
Phone/Fax: +40 336 130283
Email: mbordei@ugal.ro

AFFILIATED WITH:

- THE ROMANIAN SOCIETY FOR METALLURGY
- THE ROMANIAN SOCIETY FOR CHEMISTRY
- THE ROMANIAN SOCIETY FOR BIOMATERIALS
- THE ROMANIAN TECHNICAL FOUNDRY SOCIETY
- THE MATERIALS INFORMATION SOCIETY (ASM INTERNATIONAL)

Edited under the care of the FACULTY OF ENGINEERING

Annual subscription (4 issues per year)

Editing date: 15.12.2016
Number of issues: 200
Printed by Galati University Press (accredited by CNCSIS)
47 Domneasca Street, 800008, Galati, Romania